UCID--21362-Vol.3

DE90 006359

# Survey of Degradation Modes of Candidate Materials for High-Level Radioactive-Waste Disposal Containers

## Volume 3
## Localized Corrosion and Stress Corrosion Cracking of Austenitic Alloys

J. C. Farmer, R. A. Van Konynenburg, and R. D. McCright
Lawrence Livermore National Laboratory
Livermore, Calif.

D. B. Bullen
Science & Engineering Associates, Inc.
Pleasanton, Calif.

April 1988



LAWRENCE LIVERMORE NATIONAL LABORATORY
University of California • Livermore, California • 94550

# Contents

# List of Volumes of the Survey

This is Volume 3 of the report *Survey of Degradation Modes of Candidate Materials for High-Level Radioactive-Waste Disposal Containers*. The titles of all of the volumes are as follows:

Overview
Volume 1: Phase Stability
Volume 2: Oxidation and Corrosion
Volume 3: Localized Corrosion and Stress Corrosion Cracking of Austenitic Alloys
Volume 4: Stress Corrosion Cracking of Copper-Based Alloys
Volume 5: Localized Corrosion of Copper-Based Alloys
Volume 6: Effects of Hydrogen in Austenitic and Copper-Based Alloys
Volume 7: Weldability of Austenitic Alloys
Volume 8: Weldability of Copper-Based Alloys

# Acronyms

| | |
|---|---|
| AES | Auger electron spectroscopy |
| AISI | American Iron and Steel Institute |
| ASTM | American Society for Testing and Materials |
| BWR | boiling-water reactor |
| CDA | Copper Development Association |
| CEMS | conversion-electron Mossbauer spectroscopy |
| CERT | constant extension rate testing, or test |
| CF | corrosion fatigue |
| CI | CERT index |
| COD | crack opening displacement |
| CSR | constant strain rate |
| DO | dissolved oxygen |
| DOS | degree of sensitization |
| ECP | electrochemical potential |
| EOAE | electrolytic oxalic acid etch |
| EPR | electrochemical potentiokinetic reactivation |
| FS | furnace sensitization |
| HAZ | heat-affected zone |
| HVEM | high-voltage electron microscopy |
| IGSCC | intergranular stress corrosion cracking |
| LC | localized corrosion |
| MIC | microbiologically induced corrosion |
| NNWSI | Nevada Nuclear Waste Storage Investigations Project |
| OFHC | oxygen-free, high-conductivity |
| SA | solution annealing |
| SCC | stress corrosion cracking |
| SCE | saturated calomel electrode |
| SDR | slip dissolution-repassivation |
| SHE | standard hydrogen electrode |
| SP | shot peening |
| SSRT | slow strain rate testing, or test |
| TGC | transgranular cracking |
| TGSCC | transgranular stress corrosion cracking |
| UTS | ultimate tensile strength |
| XPS | x-ray photoelectron spectroscopy |
| YS | yield stress |

# Executive Summary

This volume compares the corrosion properties of three austenitic alloys. These materials are leading candidates for fabrication of the metal containers to be used in disposing of high-level radioactive waste at the prospective repository in Yucca Mountain, Nevada. The three austenitic alloys, Types 304L and 316L stainless steels and Alloy 825, are known for their good corrosion properties, their wide use in the marine, nuclear, and process industries, and their reasonable costs. The corrosion properties of copper alloys that are being considered are discussed in Vols. 4 and 5.

Disposal containers can undergo several forms of degradation during their lifetimes, including localized corrosion (LC) and stress corrosion cracking (SCC). SCC is a term used to describe service failures in engineering materials that occur by slow, environmentally induced crack propagation.

The selection of the candidate material that is adequate for repository conditions will be based on three tasks: a literature survey, corrosion testing, and predictions from models. Lawrence Livermore National Laboratory has responsibility for all three. This report is a survey of the literature on LC and on SCC.

Section 1 of this report is an introduction, and Sec. 2 provides a background on LC and SCC. Section 3 describes (1) the two forms of LC, which are crevice corrosion and pitting, (2) the role of pitting in initiating cracks, and (3) the propagation of cracks during SCC. Crevice corrosion occurs within crevices and other shielded areas on metal surfaces and consists of anodic dissolution of metal and undesirable halide reactions, in an accelerating process. The suppression of pH and the depletion of oxygen in crevices could enhance other forms of attack, such as pitting and SCC. The initiation of pitting depends on various conditions, such as chloride concentration, pH, and temperature. Models of initiation of pitting enable us to predict the effect of these conditions on critical pitting potential and on induction time, two quantities used to describe a metal's resistance to pitting and to measure the effects of heat treatment and welding on pitting. Modeling is also used to determine the rate of propagation of a growing pit.

Section 3 continues with a discussion of several models that describe the initiation of SCC by pitting. SCC can also be initiated by intergranular corrosion and slip dissolution. SCC begins at the critical potential, a quantity used to measure susceptibility to stress corrosion and to predict environmental conditions that lead to SCC. A discussion of the mechanisms of crack propagation concludes the section.

Section 4 introduces our review of the literature. Section 5 reviews the literature on pitting for the three austenitic candidates and for other alloys. Data are included on pitting potential, pit depth, and the effect of molybdenum.

Section 6 reviews the experimental data on SCC, and, to a lesser extent, the data on pitting and crevice corrosion. It begins by describing the three tests for SCC: (1) tests on statically loaded smooth samples, (2) tests on statically loaded precracked samples, and (3) tests using slowly strained samples. Much of the data for SCC in the literature comes from classic U-bend and beam experiments (statically loaded samples), and, recently, from slow strain rate testing (SSRT). A discussion then follows on the types of environments used to test for SCC and how environmental parameters influence the rate of crack growth. The effects of alloy composition, namely, nickel content, on SCC are discussed, and the role of carbon content in sensitization is examined. (Sensitization is increased susceptibility to attack following a thermal exposure that causes chromium carbide precipitation with consequent localized chromium depletion.) Various tests measuring the degree of sensitization are used to describe stress-corrosion susceptibility and crack growth rate. The role of grain-boundary segregation of impurities in austenitic alloys is also examined. The section concludes with a direct comparison of the SCC susceptibilities of the austenitic candidates.

Section 7 discusses two unusual environmental factors in the repository: high fluxes of gamma radiation, and microbiologically induced corrosion. Gamma radiation produces several reactive species in water as well as permanent changes in the oxide layer on the steel. Microbiologically induced corrosion cannot be totally ruled out, but the dry, radioactive environment of the containers would make it appear very unlikely.

The conclusions of the report are given in Sec. 8 and can be summarized as follows:

1. All austenitic candidates (Types 304L and 316L stainless steels and Alloy 825) demonstrate pitting and crevice corrosion in chloride-containing environments.

2. Alloy 825 has greater resistance to pitting and crevice corrosion than either Types 304L or 316L stainless steels.

3. SCC was not reported in the literature for Alloy 825. This does not mean that SCC could not occur in Alloy 825 under other circumstances.

4. On the basis of the data from the literature on susceptibility to SCC, the candidates are ranked as follows: Alloy 825 (best) > Type 316L > Type 304L (worst). Note that much of the data in this report is for solutions having higher ionic strengths than expected in the groundwater near the repository. However, these data are believed to be relevant since refluxing can concentrate water falling onto container surfaces.

5. Gamma irradiation enhances SCC of Types 304 and 316L stainless steels under some conditions. Alloy 825, however, shows no change in its resistance to SCC in the presence of gamma irradiation.

6. Though microbiologically induced (or influenced) corrosion and possible SCC have been observed for 300-series stainless steels, the nickel-based alloys such as Alloy 825 seem to be immune to such problems.

# Survey of Degradation Modes of Candidate Materials for High-Level Radioactive-Waste Disposal Containers

## Volume 3: Localized Corrosion and Stress Corrosion Cracking of Austenitic Alloys


## Abstract

Three iron- to nickel-based austenitic alloys (Types 304L and 316L stainless steels and Alloy 825) are being considered as candidate materials for the fabrication of high-level radioactive-waste containers. Waste will include fuel assemblies from reactors as well as high-level waste in borosilicate glass forms, and will be sent to the prospective repository at Yucca Mountain, Nevada.

The decay of radionuclides in the repository will result in the generation of substantial heat and in fluences of gamma radiation. Container materials may undergo any of several modes of degradation in this environment, including atmospheric oxidation; uniform aqueous phase corrosion; pitting; crevice corrosion; sensitization and intergranular stress corrosion cracking (IGSCC); and transgranular stress corrosion cracking (TGSCC). This report is an analysis of data relevant to the pitting, crevice corrosion, and stress corrosion cracking (SCC) of the three austenitic candidate alloys. The candidates are compared in terms of their susceptibilities to these forms of corrosion.

Although all three candidates have demonstrated pitting and crevice corrosion in chloride-containing environments, Alloy 825 has the greatest resistance to these types of localized corrosion (LC); such resistance is important because pits can penetrate the metal and serve as crack initiation sites. Both Types 304L and 316L stainless steels are susceptible to SCC in acidic chloride media. In contrast, SCC has not been documented in Alloy 825 under comparable conditions. Gamma radiation has been found to enhance SCC in Types 304 and 304L stainless steels, but it has no detectable effect on the resistance of Alloy 825 to SCC. Furthermore, while the effects of microbiologically induced corrosion have been observed for 300-series stainless steels, nickel-based alloys such as Alloy 825 seem to be immune to such problems.

This analysis indicates that the candidates should be ranked according to their resistance to LC and SCC as follows: Alloy 825 (best) > Type 316L > Type 304L (worst).


## 1. Introduction

Austenitic alloys and copper-based alloys are being considered as candidate materials for fabrication of the metal containers to be used in disposing of high-level radioactive waste at the Yucca Mountain site in Nevada. The austenitic materials are Types 304L and 316L stainless steels and Alloy 825 (Incoloy). These materials are leading candidates because of their good corrosion properties, their wide use in the marine, nuclear, and process industries, and their reasonable costs. There are also three copper-based candidate alloys, which are discussed in Vol. 2 of this report; these are CDA 102 (OFHC Cu), CDA 613 (Cu-7Al), and CDA 715 (Cu-30Ni).

The containers must maintain mechanical integrity for 50 yr and substantially complete

containment for 300 to 1000 yr [1, 2]. Radioactive decay of the stored waste results in substantial heat generation. Initially, many of the containers will rise to a peak temperature of about 250°C. After 100 yr, the temperature will drop to about 150°C and will continue dropping slowly. Containers with lower heat output and those located at the edge of the repository will have lower temperatures.

After emplacement, the container materials could undergo any of several modes of degradation, including atmospheric oxidation, general aqueous phase corrosion, and various forms of localized corrosion (LC). LC phenomena include crevice corrosion, pitting, intergranular stress corrosion cracking (IGSCC), and transgranular stress corrosion cracking (TGSCC).

After heat treatment at temperatures above 500°C, austenitic stainless steels may become unusually susceptible (sensitized) to IGSCC because of the precipitation of $Cr_{23}C_6$ particles at grain boundaries. The chromium-depleted region adjacent to the grain boundary serves as a vulnerable pathway for corrosive attack. Sensitization could be a serious problem in the heat-affected zone (HAZ) near welds. Corrosion phenomena can also be perturbed by the radiation field that exists in close proximity to the container. Radiolysis of salt-containing condensate films and air generates ionic, free radical, and molecular species that are not present under normal nonirradiated circumstances.

The Metal Barrier Selection and Testing Task of the Nevada Nuclear Waste Storage Investigations (NNWSI) Project has to select the candidate material with adequate performance under repository conditions. This selection will be based on a survey of the literature, corrosion testing at Lawrence Livermore National Laboratory and subcontractors, and predictions from models. The relevant literature on LC and stress corrosion cracking (SCC) in the three austenitic alloys is reviewed in this volume, and the candidates are ranked in order of their susceptibility to these modes of degradation. Over 1000 articles were reviewed for this volume, and of those, the most relevant [1–211] were selected for discussion. A detailed discussion on the methodology and extent of the literature search and on the selection of references can be found in the Overview.*

## 2. Background on LC and SCC

SCC is a term used to describe service failures in engineering materials that occur by environmentally induced crack propagation. The observed crack propagation is the result of the combined and synergistic interaction of mechanical stress and corrosion reactions.

Penetration rates at local sites of corrosive attack (LC) are far more serious threats to container life than rates due to uniform atmospheric and aqueous phase corrosion. Ionic and molecular species present in aqueous environments (water and moisture films) can serve as promoters, depolarizers, or inhibitors of LC and SCC in austenitic materials [3, 4]. For example, $F^-$, $Cl^-$, $Br^-$, and $S_2O_3^{2-}$ can induce localized breakdown of passive films, thereby initiating pit formation; such species are known as promoters. Unpublished results exist which indicate that $SO_4^{2-}$ may also serve as a promoter.

Frequently, stress corrosion cracks initiate at pits. Anodic dissolution at the bases of pits and at crack tips can be enhanced by a number of depolarizers, including $O_2$, $H^+$, $Fe^{3+}$, $Cu^{2+}$, and $Hg^{2+}$. The cathodic reduction of depolarizers on surfaces outside of crevices, pits, and cracks can galvanically couple with anodic dissolution and oxidation processes that occur inside pits. In contrast to $Cl^-$, ions such as $NO_3^-$, $I^-$, and acetate are known inhibitors of pitting and SCC of austenitic stainless steels. These inhibitors compete with halide ions for adsorption sites on the metal oxide film and base metal. In alkaline media, $OH^-$, $H^+$, and $PO_4^{3-}$ can serve as promoter, depolarizer, and buffer, respectively.

In addition to corrosive attack, mechanical stress is required for SCC. The stresses required are small, usually below the macroscopic yield stress, and are tensile in nature. The stresses can be externally applied, but residual stresses often

* J. C. Farmer, R. D. McCright, J. N. Kass, *Survey of Degradation Modes of Candidate Materials for High-Level Radioactive-Waste Disposal Containers, Overview*, Lawrence Livermore National Laboratory, Livermore, California, UCID-21362 Overview (1988).

cause SCC failures. One frequent misconception is that SCC is the result of stress concentration at corrosion-generated surface flaws (as quantified by the stress intensity factor, $K$), and that when a critical value of stress concentration, $K_{crit}$, is reached, mechanical fracture results. Although stress concentration does occur at such flaws, it does not in fact exceed the critical value required to cause mechanical fracture of the material in an inert environment ($K_{SCC} < K_{crit}$).

# 3. Mechanisms of LC and SCC

## 3.1 Crevice Corrosion

Intense LC frequently occurs within crevices and other shielded areas on metal surfaces exposed to corrosives. After placement of the containers in the repository, crevices will form at points where the container is supported. Furthermore, natural deposits of sand, dirt, corrosion products, and other solids can form crevices.

During uniform aqueous phase corrosion, the cathodic reduction of dissolved oxygen and the anodic dissolution of metal cations are galvanically coupled and proceed at rates that are independent of position on exposed metal surfaces. In contrast, oxygen reduction on metal surfaces in crevices eventually ceases because of the lack of this reactant. Oxygen becomes depleted in such recesses, and mass transport rates (diffusion-limited) are insufficient to replenish it. Consequently, the only process that occurs at an appreciable rate within the crevice is the anodic dissolution of metal. This tends to produce an excess of positive charge in the crevice solution ($M^{z+}$), which is necessarily balanced by the migration of halide ions, such as $Cl^-$, into the recess. The increased concentration of metal halide in the crevice results in undesirable, localized chemistry.

$$MCl + H_2O \rightarrow MOH(prec.) + HCl \qquad (1)$$

The halide salt hydrolizes in water to form a precipitate and free acid. Repassivation in the high-chloride, low-pH environment found in crevices is virtually impossible. The anodic dissolution of most metals is accelerated in such environments.

In addition to the large differences in concentration that exist inside and outside of crevices, there are large differences in current density. Oxygen reduction continues at relatively low current densities on all passivated (oxide-covered) metal surfaces outside of the crevice. This large overall cathodic current must be balanced by the anodic dissolution current on metal surfaces inside the crevice. Given the small active area within crevices, corresponding current densities are typically very large. Therefore, local penetration rates within crevices also tend to be very large (far greater than on unobscured surfaces).

## 3.2 Nucleation of Pits

It is important to understand the dependence of pitting on various environmental conditions such as chloride concentration, pH, and temperature. Models of pitting phenomena fall into two broad classes: initiation and propagation. Pit-initiation models enable us to predict the effects of environment on quantities such as the critical pitting potential and induction time [5, 6]. Once a pit is initiated, it is necessary to calculate the rate of propagation (penetration). Models like the one presented by Pickering and Frankenthal enable us to calculate pH depression inside the growing pit, the concentration of other species inside the pit, and the rate of propagation [7]. The application of stochastic probability theory may make it possible to account for observed variances in critical pitting potential. Furthermore, the rate of pitting can be determined from logarithmic plots of survival probability as a function of time [8].

Okada assumes that pit initiation on a stainless steel begins with formation of a hemispherical halide nucleus on the passive oxide film [5, 6]. If the nucleus is stable and grows continuously, it will eventually breach the protective oxide. After dissolution of the metal halide, the underlying metal is exposed and undergoes rapid corrosive attack. This mechanism is illustrated in Fig. 1. The following reactions are assumed to occur at the interface between the halide nucleus and the passive oxide:

$$M^{z+}(oxide) + zX^-(halide) \rightarrow MX_z(halide) \qquad (2)$$

$$O^{2-}(oxide) + 2H^+(halide) \rightarrow H_2O(halide) \qquad (3)$$

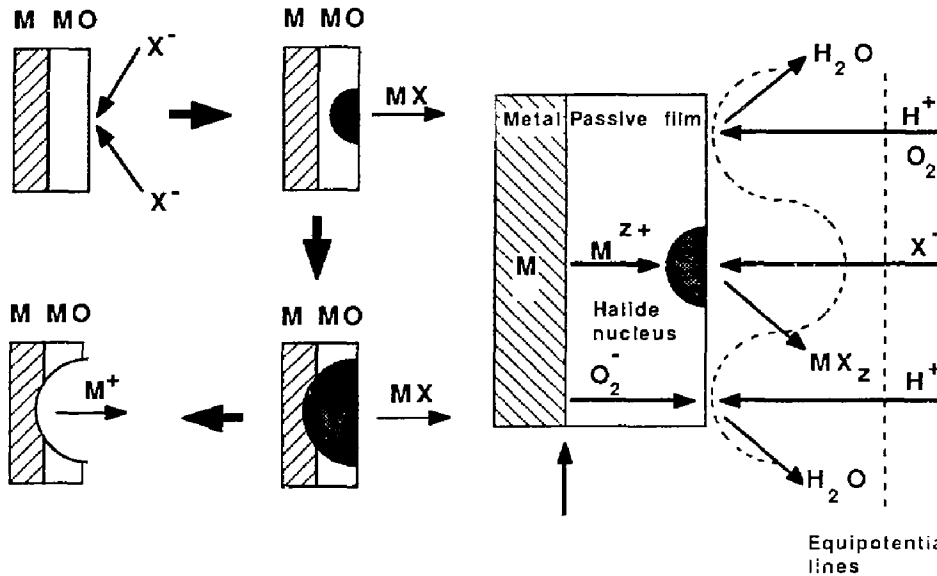


Figure 1. Stages of pit initiation on stainless steel as proposed by Okada [5, 6].

At the interface between the metal halide and the solution, these reactions are assumed:

$$M^{z+}(\text{halide}) \rightarrow M^{z+}(\text{solution}) \quad (4)$$

$$X^{-}(\text{halide}) \rightarrow X^{-}(\text{solution}) \quad (5)$$

Okada has used two independent approaches to derive the same expressions for the critical pitting potential, $E_c$, the induction time, $\tau$, and the critical size for a stable halide nucleus, $r^*$. Note that the critical pitting potential is a linear function of the logarithm of the halide ion concentration, $\ln[X^-]$.

$$E_c = \text{constant} - (RT/F)\ln[X^-] \quad (6a)$$

where $R$ is the universal gas constant, $T$ is the absolute temperature, and $F$ is Faraday's constant. This relationship between the critical pitting potential and halide ion concentration is consistent with the experimental results of several different research groups [9-11]. For example, variations of the pitting potential for Type 316 stainless steel in cellulose bleach solutions at 50°C have been correlated with chloride concentration and pH, as shown in Fig. 2 and Eq. (6a) [11]. Note that the pitting potential calculated by Eq. (6b) has the units of mV, SCE.

$$E_c = 2570 - 5.81T + 0.07T \cdot \text{pH} - 0.49T \log[Cl^-] \quad (6b)$$

The induction time is a function of both the halide ion concentration and the electrochemical potential, $E$.

$$\ln \tau = \text{constant} - 2n \ln[X^-] - (2FE/RT) \quad (7)$$

where $n$ is the valence of the metal cation. Note that Eq. (7) implies that the induction time increases exponentially as the chloride concentration decreases.

As noted above, Okada has used two independent approaches to derive these expressions for the critical pitting potential and the induction time for pit initiation. The first approach begins with the general evolution criterion proposed by Glansdorff and Prigogine for irreversible thermodynamics [Okada, Ref. 5]. The second approach assumes that small, localized anodic perturbations in the electrochemical potential are sufficient to nucleate patches of metal halide on the

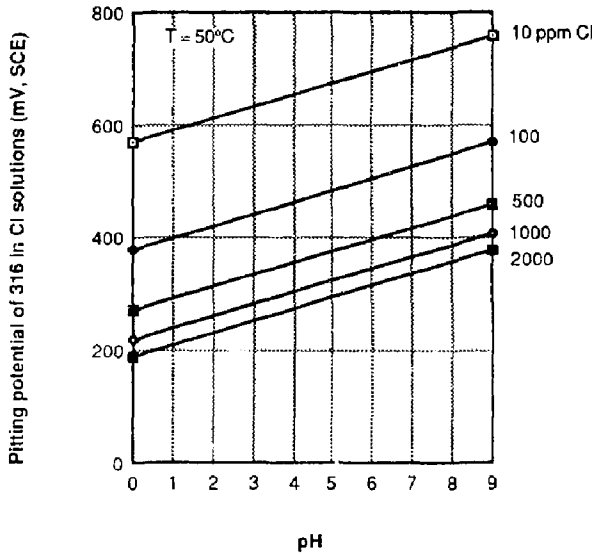


Figure 2. Variation of the pitting potential of Type 316 stainless steel with chloride concentration, pH, and temperature, in cellulose bleach solutions at 50°C [11].

oxide film [6]. At relatively anodic potentials, the halide is more stable than the oxide. Other models of pit initiation exist, such as the point defect model [12].

Pits can also nucleate at inclusions in the alloy surface. In 1980, Manning et al. published a study which determined the effect of sulfide inclusion morphology and composition, matrix, and environmental variables such as pH, temperature, and NaCl concentration on pit-initiation resistance [13]. Pitting corrosion tests were performed on Types 304L, 316, and 316L stainless steels. The sulfide-inclusion morphology was altered with high-temperature heat treatments.

Manning et al. conducted tests on as-received samples (10% cold worked), samples heat-treated at 1300°C for 8 hr and water-quenched, and samples annealed at 1050°C for 5 to 7 min and water-quenched. The annealing treatment at 1050°C did not change the grain size or the sulfide-inclusion morphology of the as-received material. However, the high-temperature heat treatment (1300°C) resulted in substantial grain growth and spheroidization of sulfide stringers. In the as-received condition, the length of sulfide inclusion/metal interface per unit area of microstructure ($L_{A\text{-}Me/S}$) was 26 mm/mm$^2$, which was almost identical to the value obtained for annealed material. In contrast, the value of $L_{A\text{-}Me/S}$ decreased to 15 mm/mm$^2$ after high-temperature heat treatment. Potentiodynamic pitting tests of heat-treated samples were performed at a potential sweep rate of 100 mV/hr in 1*N* NaCl (pH 4, 22°C).

In comparing pitting resistance to that of other heat treatments of Type 304L or other 300-series stainless steels in which pit initiation occurs at metal/sulfide interfaces, the value of $L_{A\text{-}Me/S}$ is not the critical factor. The matrix composition as well as the composition of the sulfide inclusions are the primary factors determining the relative resistance to pit initiation of these alloys.

Figure 3 illustrates the importance of sulfide-inclusion morphology on pitting potential, a measure of a material's tendency to pit. As-received and annealed Type 316L stainless steels have pitting potentials much more cathodic than those of Type 304L, even though the molybdenum content of Type 316L is higher than that of Type 304L. As will be discussed, molybdenum additions usually

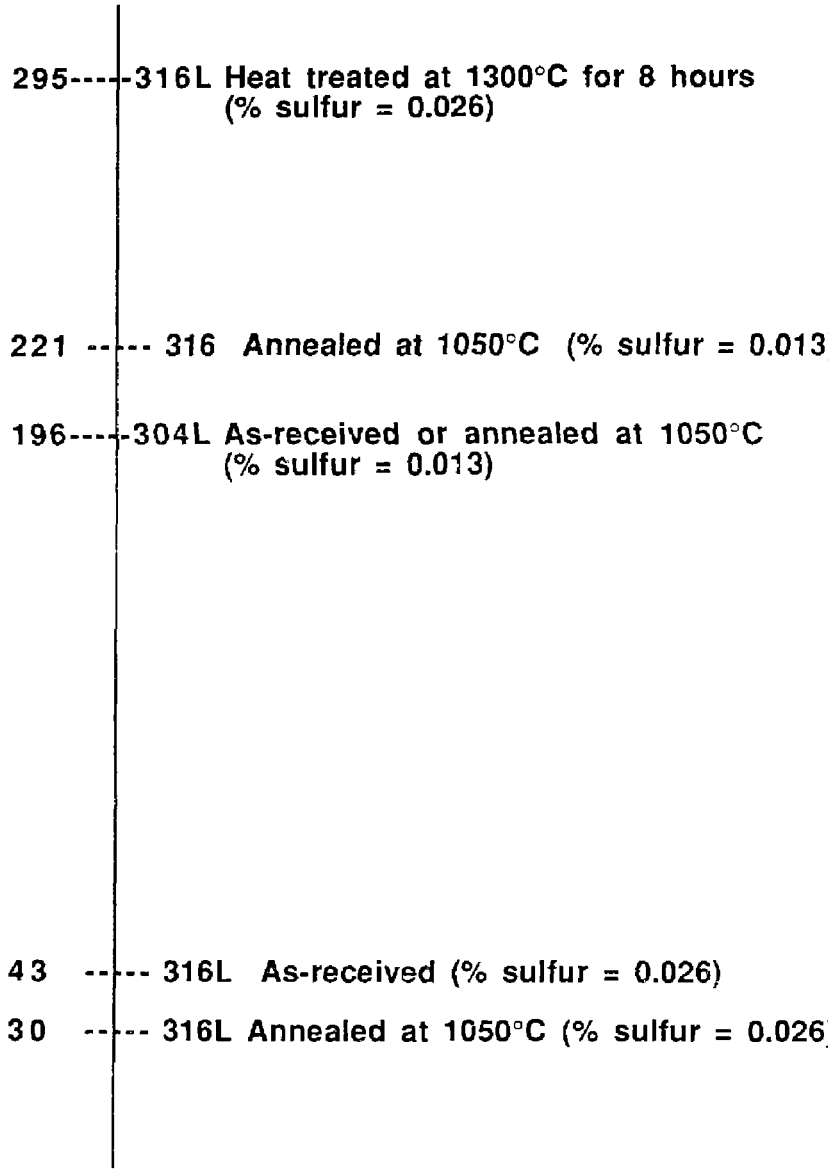


Figure 3. Potential scale in mV vs SCE, denoting the pitting potentials (1*N* NaCl, pH 4, 22°C) of several single-phase alloys with different heat treatments [13].

enhance resistance to pitting. However, in this case, the pitting resistance of the alloy having high molybdenum content is actually lower because of the presence of sulfide inclusions that have a higher content of sulfur. Note that as-received and heat-treated Type 316L specimens have twice as much sulfur as the Type 304L specimens. Type 316 stainless steel annealed at 1050°C and having the same sulfur content as Type 304L exhibits more resistance to pitting (higher pitting potential) because of its greater molybdenum content. Pitting resistances of high-sulfur (0.026%) Type 316L can be restored by heat treatment at 1300°C, which alters sulfide-inclusion morphology. Note that the annealed Type 316 and as-received and annealed Type 304L had essentially the same $L_{A\text{-}Me/S}$ values ($L_{A\text{-}Me/S}$ = 26.6 $mm/mm^2$ for 304L).

Manning et al. also performed tests on as-received single-phase and as-welded duplex Type 304L stainless steel as a function of environmental variables. The temperatures studied were 8, 22, 50, and 90°C. The NaCl concentrations used were 0.1, 0.5, and 1*N*. By adding HCl or NaOH, the pH was controlled at a value in the range of pH 2 to 12. The data in Figs. 4 and 5 show that a linear relationship exists between the pitting potential and the logarithm of the NaCl concentration. This result applies to single-phase and duplex alloys in solutions at pH 2 and 4 within a temperature

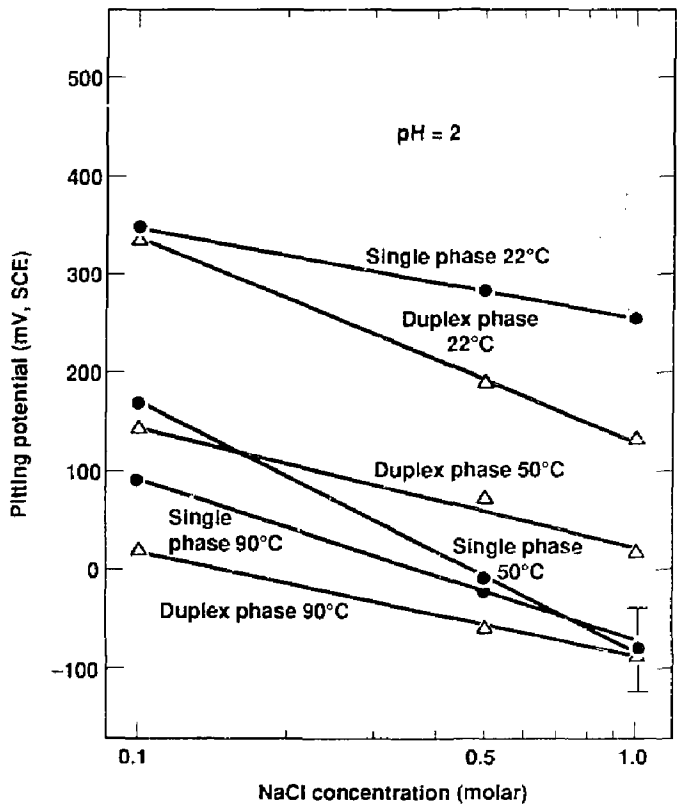


Figure 4. The pitting potential of Type 304L stainless steel has a linear relationship with the logarithm of the NaCl concentration at pH = 2 [13].

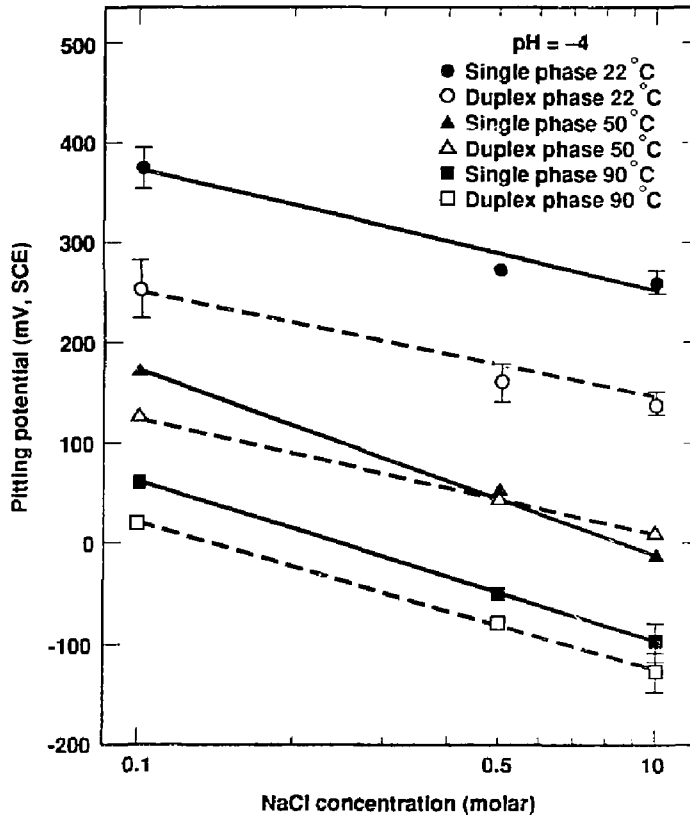


**Figure 5. Pitting potential of Type 304L stainless steel at pH = 4. As in Fig. 4, the relationship is linear.**

range of 22 to 90°C and is consistent with the expressions derived by Okada and the correlation given by Matamala [11].

The data in Fig. 6 show the effect of pH on pitting potential in 1*N* NaCl at various temperatures. For a pH value less than some critical value, the pitting potential is relatively independent of pH. For alkaline solutions, pitting resistance is improved at a pH value greater than 7 at 22°C, 9 at 50°C, and 10 at 90°C. At 22°C, the pitting resistance of the duplex alloy is inferior to that of the single-phase alloy below the transition-pH value. However, at higher temperatures, the two types of alloys behave in a similar manner. It may be noted that at 50°C, the single-phase alloy shows a statistically significant decrease in pitting resistance at pH 2. It has been suggested that the discontinuous change in pitting resistance at a high pH value may be attributed to preferential adsorption of $OH^-$ ions competing with $Cl^-$ ions. If this hypothesis is correct, the increase in transition pH with increasing temperature could be explained by less stable adsorption at high temperatures.

The effects of temperature on pitting potential in electrolytes with various concentrations of NaCl are shown in Fig. 7 (pH 4) and in Fig. 8 (pH 2). As the temperature is increased from 8 to 90°C, there is a continuous shift of pitting potential in the active direction at pH 4. At pH 2, however, a discontinuous decrease in pitting resistance of the single-phase alloy is observed in 0.5 and 1*N* NaCl at 50°C, and the pitting potential is approximately constant at 90°C. This behavior is

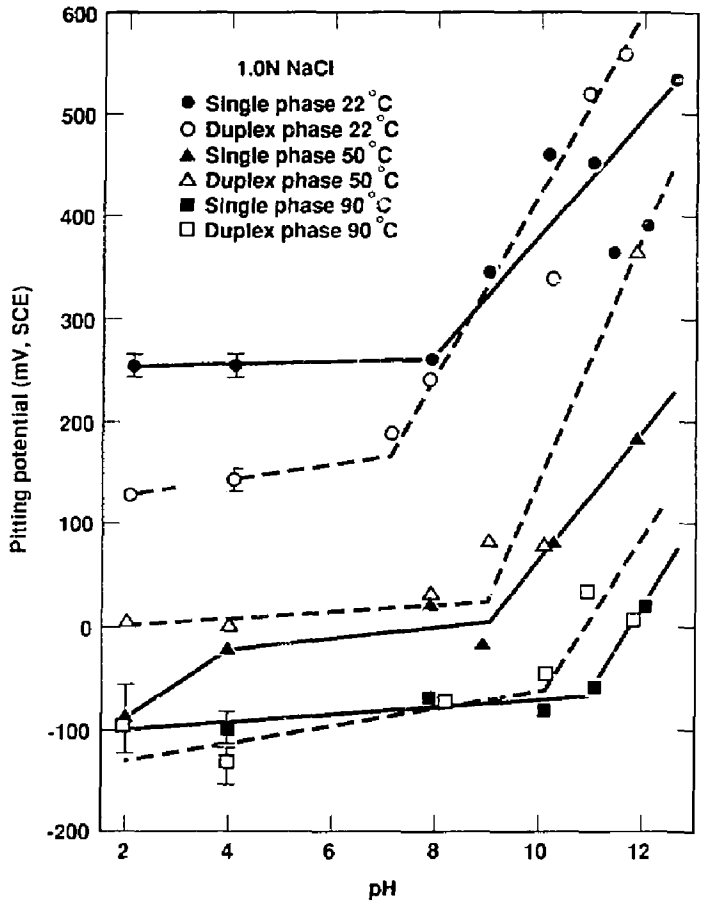


**Figure 6. Pitting potentials of single-phase and duplex Type 304L as a function of pH at several temperatures in 1*N* NaCl [13].**

associated with the dissolution kinetics of the sulfide inclusions (most susceptible site for pit initiation) as a function of environment. The duplex-alloy data in Figs. 3 through 7 show that acidification of the electrolyte from pH 4 to 2 does not significantly affect the pitting potential in the case where sulfide-dissolution kinetics do not play a role in the pit-initiation process.

In summary, Manning et al. drew the following conclusions:

(1) A rank order of resistance to pit initiation of the base materials examined is dependent upon sulfur content as well as molybdenum content. Type 316L stainless steel that had 0.026% sulfur and was heat-treated at 1300°C for 8 hr was most resistant to pitting, while the same material in the as-received and annealed condition was less resistant to pitting than as-received and annealed Type 304L having only 0.013% sulfur. Annealed Type 316 that had the same sulfur content as Type 304L was more resistant to pitting than Type 304L, primarily because of the relative differences in molybdenum content. All annealing was done at 1050°C.

(2) Sulfide-dissolution kinetics are presumed to control pit initiation of single-phase Type 304L stainless steel. The kinetics were influenced by the following variables: the method of

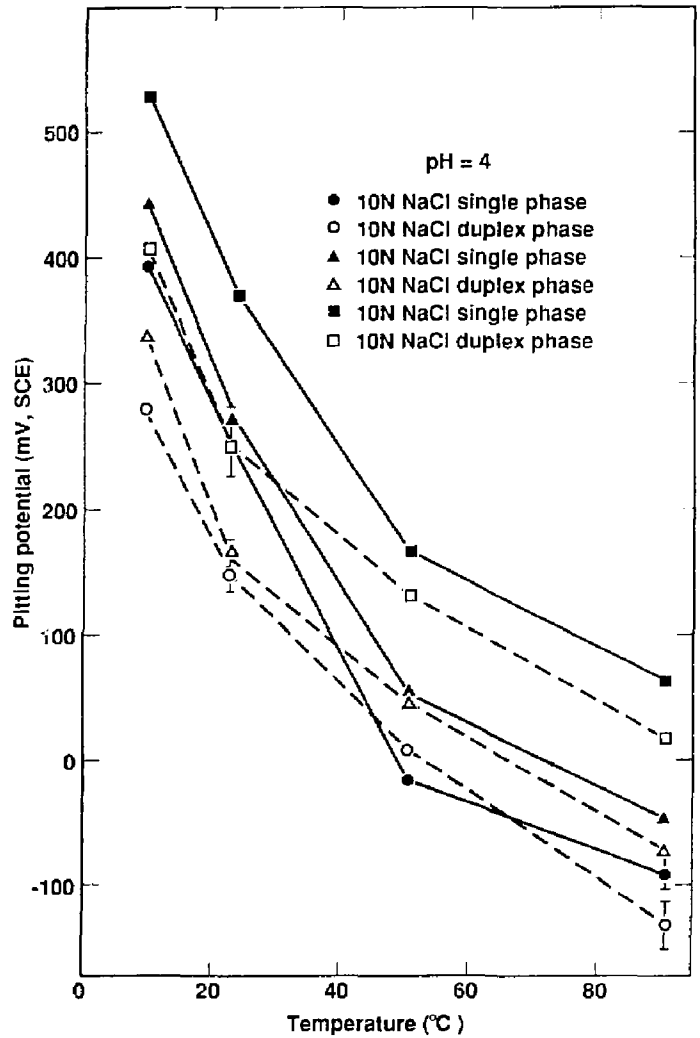


**Figure 7. Pitting potentials of single-phase and duplex Type 304 as a function of temperature in several NaCl concentrations with a constant pH of 4 [13].**

conducting the pit-initiation test, the morphology of the sulfide inclusions exposed to the electrolyte, and the composition and temperature of the bulk electrolyte. Sulfide-inclusion morphology was controlled by heat treatment.

(3) Dissolution begins at sulfide/metal interfaces when chloride ions are present and a potential is applied at which sulfide inclusions of a particularly susceptible composition are thermodynamically unstable. Acidification of the local electrolyte as well as concentration of chloride ions occur by migration. If geometrical conditions favor pit propagation, dissolution of the metal around the sulfide inclusion continues; if

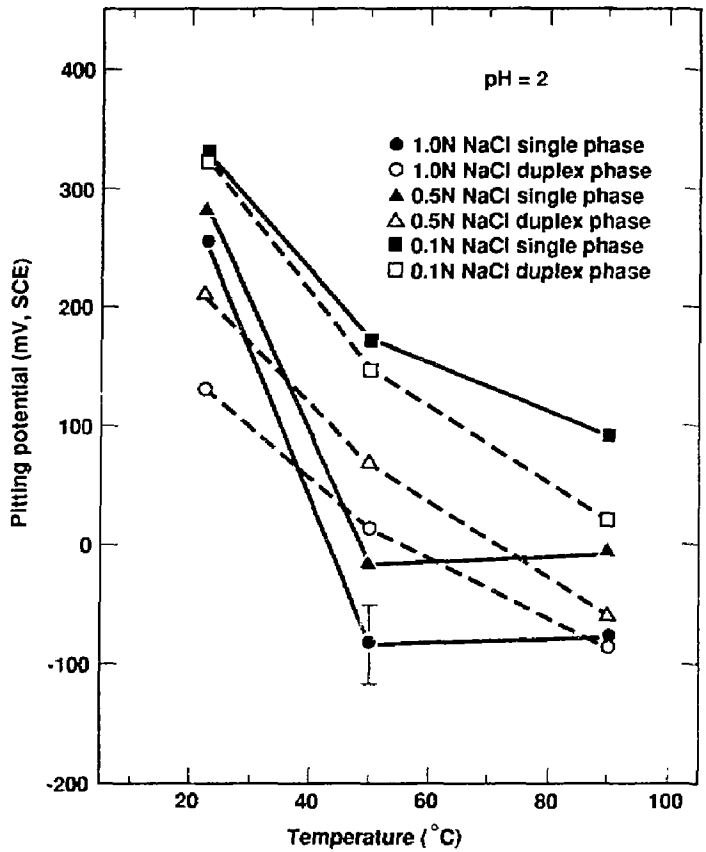


**Figure 8. Pitting potentials of single-phase and duplex Type 304L as a function of temperature in several NaCl concentrations with a constant pH of 2 [13].**

not, the pit repassivates. Initiation and repassivation events normally occur many times in pit embryos before pit propagation occurs.

(4) The method of conducting the pit-initiation tests was found to influence the time available for sulfide dissolution to occur at a given applied potential.

(5) Finally, in cases in which changes in sulfide inclusion morphology occur, such as in high-temperature (1300°C) heat treatment, other heat treatments of Type 304L, or other 300-series stainless steels, the $L_{A\text{-}Me/S}$ value is not the primary factor in determining pit-initiation resistance. The sulfide morphology and matrix compositions are the critical factors that determine the pit-initiation resistance.

## 3.3 Crack Initiation at Pits Having Critical Depth

Pits can serve as initiation sites for SCC. Though a well-developed model for the transition from pitting to SCC has not been developed, a model for the initiation of corrosion fatigue (CF) cracks at pits does exist. In the model discussed by Hagn [14], pits are regarded as half-elliptical surface cracks since they have tiny fissures at their bottoms. The following equation was derived from linear-elastic fracture mechanics for the stress-intensity threshold, $\Delta K_{th}$, required to initiate a fatigue crack at a corrosion pit.

$$\Delta K_{th} = \Delta\sigma(\pi a)^{1/2}F(a,c) \qquad (8)$$

where $\Delta\sigma$ is the alternating tensile stress, $a$ is the pit depth and major axis of the ellipse, $c$ is the minor axis of the ellipse, and $F(a,c)$ is a geometric factor calculated from $a$ and $c$. The exact expression for $F(a,c)$ is

$$F(a,c) = [1.13 - 0.07\sqrt{(a/c)}] + \sqrt{1 + 1.47(a/c)^{1.64}} \quad (9)$$

Equation (8) can be arranged to calculate the critical pit depth, $a_{th}$.

$$a_{th} = (1/\pi)(\Delta K_{th}/F(a,c)\Delta\sigma)^2 \quad (10)$$

This relationship is illustrated in Fig. 9. The curves shown represent various stress ratios ($R = \sigma_{min}/\sigma_{max}$) and aspect ratios ($a/c = 0.75$ or 1.35). Though this expression was discussed in

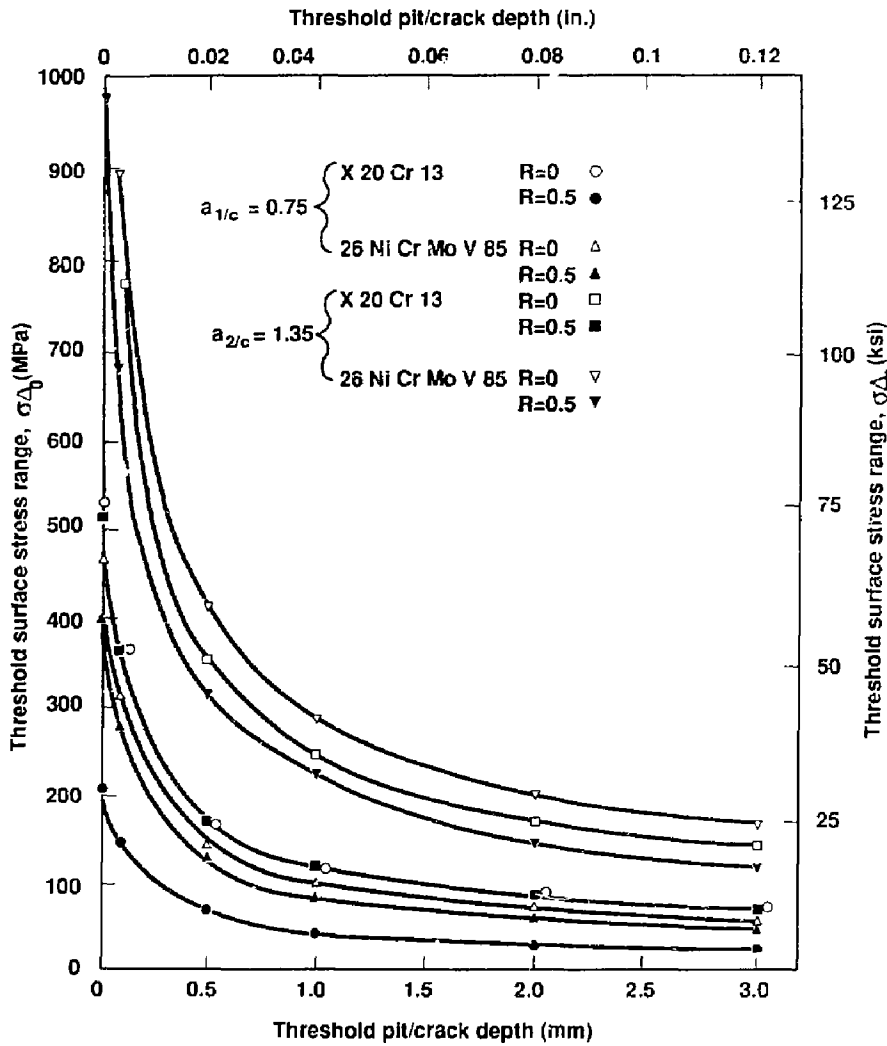


Figure 9. Relationship between stress amplitude and minimum depth of surface defects for 12% chromium steel and a 2.0% nickel-chromium-molybdenum-vanadium steel [14].

the context of CF, Hagn claims that it is also applicable to SCC. Others have used linear-elastic fracture mechanics to derive an expression for the time to initiate a crack, $t_{inc}$ [15].

$$t_{inc} = \frac{K_{ISCC}^2 \exp(-V_m/V_0)}{\pi B\left(\sigma^2 - \sigma_0^2\right)} \qquad (11)$$

where $K_{ISCC}$ is the stress-intensity threshold for initiation of SCC, $\sigma$ is the applied stress, $\sigma_0$ is the stress needed to close the crack, $B$ is a constant, $-V_m$ is the electrochemical potential of the sample, and $V_0$ is the reversible potential.

Stress corrosion crack initiation can also occur in the absence of pitting by intergranular corrosion or slip-dissolution processes. Intergranular-corrosion-initiated SCC requires that the local grain-boundary chemistry differ from the bulk chemistry. This condition occurs in sensitized austenitic stainless steels or with the segregation of impurities such as phosphorus, sulfur, or silicon in a variety of materials. Slip-dissolution-initiated SCC results from local corrosion at emerging slip planes and occurs primarily in low-stacking-fault materials. The processes of crack initiation and propagation by the slip-dissolution process are very similar.

## 3.4 Critical Potential for SCC Initiation in Sensitized Steels

According to Jones, the thermodynamic conditions for anodically assisted SCC are that dissolution or oxidation of the metal and its dissolution in the electrolyte must be thermodynamically possible and that a protective film, such as an oxide or salt, must be thermodynamically stable [16]. Critical potentials for SCC can be determined from linear polarization curves, and these potentials can be related to potential-pH stability diagrams (Pourbaix diagrams) because these diagrams describe the conditions at which film formation and metal oxidation will occur [17].

Figure 10 is a schematic of the relationship existing between electrode potential and current density for poorly passivating systems and strongly passivating systems. Potentials where severe cracking susceptibility is encountered in ductile alloys exposed to aqueous environments are designated [17]. Transgranular SCC (TGSCC) occurs in Fig. 10(a) because the material is in transition from active corrosion to passive film formation such that the simultaneous conditions for film formation on the crack walls and corrosion at the crack tip are met. A similar condition exists in Fig. 10(b), with the added factor that

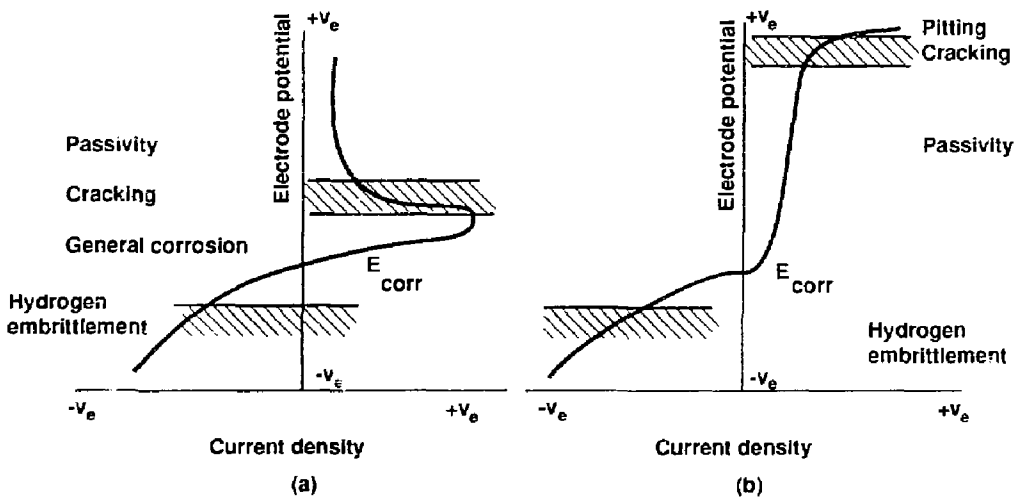


Figure 10. Electrode potential/current density relationship for (a) poorly passivating, and (b) strongly passivating systems, indicating, in the two cases, where severe cracking susceptibility in ductile-alloy/aqueous-environmental systems is commonly encountered [23].

these potentials are at or above the pitting potential, so that cracks can initiate by pitting.

Intergranular SCC (IGSCC) occurs over a wider range of potentials than those shown in Fig. 10(a) and (b) because chemical inhomogeneities at the grain boundary produce a different electrochemical response relative to the bulk material. Identification of critical potentials for SCC has led to the use of electrochemical methods for assessing stress corrosion susceptibility.

Cubicciotti and Ljungberg conducted tests that have shown that IGSCC does not occur in sensitized Type 304 stainless steel below $E_{IGSCC}$ [18]. Sensitization is defined as unusual susceptibility to IGSCC because of the precipitation of chromium carbides at grain boundaries. Such precipitation depletes the region adjacent to grain boundaries of chromium, leaving an active path for the propagation of intergranular corrosion cracks into the alloy. IGSCC can initiate at potentials, $E_{IGSCC}$, at which the protective film is destabilized. A correlation between $E_{IGSCC}$ and the stable phase containing chromium was found. Above $E_{IGSCC}$, the stable chromium-containing phase is $Cr_2O_3$. Below $E_{IGSCC}$, the stable phase is $FeCr_2O_4$. The interpretation of this correlation is that a surface oxide phase of $FeCr_2O_4$ is protective against IGSCC, while $Cr_2O_3$ is not.

The test environment described in ASTM G-36 [19] has been of sufficient interest to prompt studies of the passive film formed in the presence of $MgCl_2$. M. Da Cunha Belo et al. used activation analysis and Auger electron spectroscopy to study the relationship between the critical cracking potential for SCC of stainless steels and the chemical composition of the film formed in boiling 42% $MgCl_2$ [20]. This analytical study showed that the complex oxide of chromium and nickel, which is formed at potentials where the steel is susceptible to SCC, contains more chromium than nickel. Conversely, the oxide is richer in nickel than chromium if it develops at potentials at which the steel is protected. This finding is inconsistent with that of Cubicciotti and Ljungberg [18]. However, alloys with a higher nickel content, which may tend to form nickel-rich films, are more resistant to SCC. The effects of nickel content on SCC resistance are discussed in detail in Sec. 6.4.

Cragnolino has determined $E_{IGSCC}$ of sensitized Type 304 stainless steel at conditions simulating normal and faulty boiling-water reactor (BWR) environments [21]. He determined the effect of environmental variables such as temperature, pH, and solution composition on the value of $E_{IGSCC}$ and on crack propagation rate. The relevance of $E_{IGSCC}$ in predicting environmental conditions that lead to IGSCC is emphasized for both the current normal operating BWR environment and that modified by the injection of hydrogen. In this context, the significance of the corrosion potential of the material and the redox potential of the environment as affected by the composition of the aqueous system, in particular the concentration of reducible species, is briefly addressed. Experimental results indicate that IGSCC occurs only when $E_{corr} > E_{IGSCC}$.

TGSCC also can be prevented by maintaining the potential at a level below the critical potential. Mancia and Tamba used slow strain rate testing (SSRT) under potentiostatic control to determine the potential required for cathodic protection from TGSCC in neutral and acidic NaCl solutions [22].

## 3.5 Propagation of Cracks

Ford has published an excellent review of the SCC literature [23]. From his review, he has found that mechanisms for propagation fall into one of three general classes: (i) pre-existing active-path mechanisms, (ii) absorption-related mechanisms, and (iii) strain-assisted active-path mechanisms. In contrast, Jones classifies SCC mechanisms as either anodic or cathodic [16]. The most obvious anodic mechanism is that of simple active dissolution and removal of material from the crack tip. The most obvious cathodic mechanism is hydrogen evolution, absorption, diffusion, and embrittlement.

The breaking of the interatomic bonds at the crack tip occurs either by chemical solvation and dissolution or by mechanical fracture (ductile or brittle). Mechanical fracture includes normal fracture processes that are assumed to be stimulated or induced by one of the following interactions between the material and the environment: (i) adsorption of environmental species, (ii) surface reactions, (iii) reactions in the metal ahead of the crack tip, and (iv) surface films.

IGSCC is an example of a pre-existing active-path mechanism. Several thermodynamic models have been used to explain the role of alloy composition in sensitization of austenitic stainless steels, which leads to IGSCC [24]. The rate of

sensitization is limited by solid-state transport of chromium to grain boundaries, where $Cr_{23}C_6$ carbides form.

Failure caused by hydrogen embrittlement at a crack tip, which can result from electrochemical hydrogen evolution, is an example of an absorption-related mechanism [25].

Finally, TGSCC is an example of a strain-assisted active-path mechanism. In steels that have not been sensitized and in copper-based alloys, the most common mode of SCC failure is by TGSCC. In the case of TGSCC, it has been shown experimentally that the crack can proceed through the bulk material as a series of (passive) film rupture/repassivation steps [26]. Rupture of the passive film at the crack tip occurs after a period of "creep strain." When the strain in the passive film at the crack tip exceeds a critical value, the film ruptures. Then there is localized anodic dissolution of metal at the crack tip before repassivation. Temporary stress relaxation results from the crack widening. The rate of crack propagation depends on both the stress and the rates of dissolution and repassivation at the crack tip.

Dissolution and repassivation are both electrochemical processes; the rates of these processes are governed by heterogeneous reaction kinetics at the interface as well as by ion transport in the crack electrolyte [27, 28].

The limiting velocity $da/dt$ for a crack advancing under pure anodic dissolution is given by the following Faradaic relationship:

$$da/dt = i_a M/zpF \tag{12}$$

where $i_a$ is the anodic current density of a bare surface, $M$ is the atomic weight, z is the valence, $F$ is Faraday's constant, and $\rho$ is the material density. A number of factors can reduce the crack velocity below that given by Eq. (12). The most widely examined crack growth retardation process is that resulting from the crack tip being covered by a film for some fraction of time. A typical crack is illustrated in Fig. 11.

Nakayama and Takano have applied a slip dissolution-repassivation (SDR) model to SCC of Type 304 stainless steel in a boiling $MgCl_2$ solution [29]. They used SSRT to demonstrate that the SCC was dependent on strain rate, applied potential, and solution temperature. This behavior was qualitatively explained by considering both the formation rate of slip steps and the characteristics of their dissolution-repassivation. Furthermore, they used high-voltage electron microscopy (HVEM) to image crack tips and found that transgranular cracks propagate along active slip planes. Thus, they proved that the SDR mechanism is acceptable for describing the transgranular cracking (TGC) of Type 304 stainless steel in 42% $MgCl_2$ solution. An SDR model was developed which could quantitatively predict the crack propagation rate as a function of applied potential and slip-step formation rate.

Development of the SDR model begins with the expression for the dissolution current density, $i(t)$, at a crack tip for a single slip step. Note that $i(t)$ decays exponentially because of repassivation of the active surface at the crack tip.

$$i(t) = i^\circ \exp(-\beta t) \tag{13}$$

where $t$ is time, $i^\circ$ is the dissolution current density of the fresh surface at $t = 0$, and $\beta$ is the decay constant. Note that $i^\circ$ has been observed to increase and $\beta$ has been observed to decrease with potential. The time average of the dissolution current density is calculated as shown in Eq. (14):

$$\langle i \rangle = \int_0^{1/n_s} i(t)\, dt/(1/n_s) \tag{14}$$

$$\langle i \rangle = i^\circ/\beta n_s[1 - \exp(-\beta/n_s)] \tag{15}$$

where $n_s$ is the formation rate of slip steps. The crack propagation rate, $da/dt$, can then be calculated by an expression similar to Eq. (12):

$$da/dt = M \langle i \rangle/zF\rho \tag{16}$$

A more comprehensive model is presented by Andresen for the instantaneous crack growth rate, $da/dt$ [30]. His model assumes that crack advancement is due to the rupture of an anodic film at the base of the crack.

$$da/dt = (MQ_f\, d\varepsilon_{ct}/dt)/(zF\rho\varepsilon_f) \tag{17}$$

where $M$ is the atomic weight, $Q_f$ is the anodic (oxidation) charge density, $d\varepsilon_{ct}/dt$ is the crack tip strain rate, z is the valence, $\rho$ is the material density, $F$ is Faraday's constant, and $\varepsilon_{ct}$ is the oxide fracture strain. Though this concept was developed for TGSCC, a linear relationship also exists between $da/dt$ and $d\varepsilon_{ct}/dt$ [$\log(da/dt)$ vs $\log(d\varepsilon_{ct}/dt)$] for IGSCC, as illustrated in Fig. 12 [16]. The anodic processes associated with $Q_f$ are

$$M \rightarrow M^+ + e^- \tag{18}$$

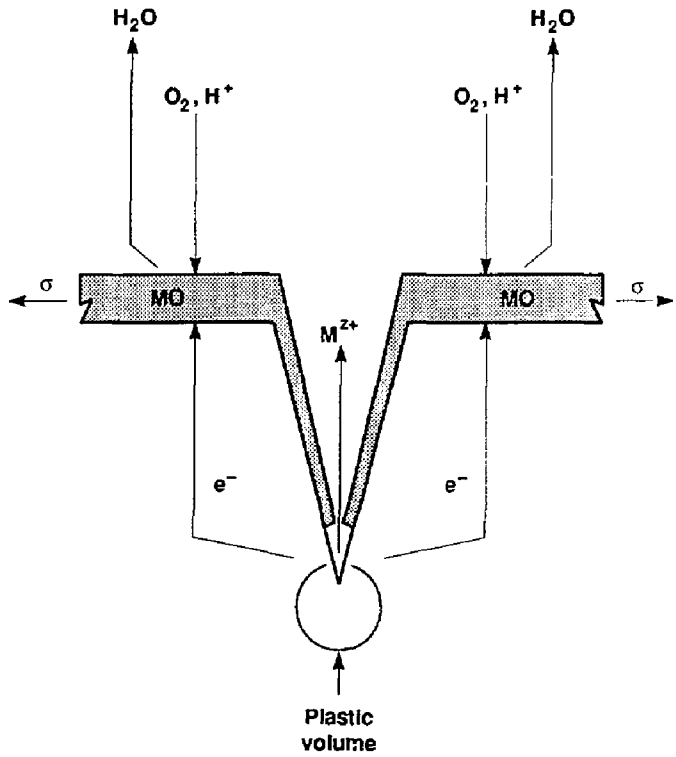


Figure 11. Illustration of propagation of a typical crack.

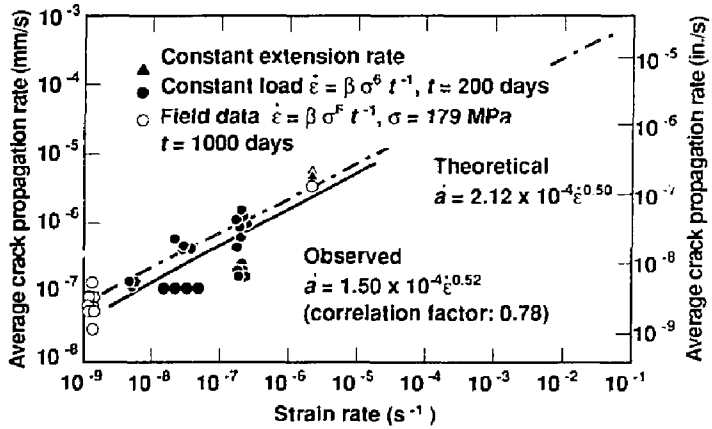


Figure 12. Comparison between observed and theoretical crack propagation rate/strain rate ($a/\varepsilon$) relationship for furnace-sensitized Type 304 stainless steel in water/0.2 ppm oxygen at 228°C (550°F) [16].

$$M + H_2O \rightarrow MO + H^+ + e^- \quad (19)$$

$$M^+ + H_2O \rightarrow MO + H^+ \quad (20)$$

Note that these equations represent generic reactions and are, therefore, not balanced. The generic oxide species, MO, could represent $Cr_2O_3$, $Cr(OH)_3$, $Cr(OH)_2$, $Fe_2O_3$, or $Fe_3O_4$. Galvanically coupled cathodic reactions include the reduction of oxygen and hydrogen ion:

$$O_2 + H_2 + e^- \rightarrow OH^- \quad (21)$$

$$O_2 + 4H^+ + 4e^- \rightarrow 2H_2O \quad (22)$$

$$2H^+ + e^- \rightarrow H_2 \quad (23)$$

Note that Maier and Galvele have used the straining metal electrode technique as an SCC test for Type 304 stainless steel in NaCl + $H_2SO_4$ solutions [31]. They concluded that a periodic film formation process (repassivation) does indeed occur during straining, which is consistent with the models of Nakayama and Takano [29] and Andresen [30]. Marshall and Burstein have studied the kinetics of the repassivation process on Types 304L and 316L in detail using a scratch technique [32]. They concluded that the repassivation rate is controlled by ion conduction through the growing oxide film under high electric field.

There are several possible rate limiting steps: (i) mass transport along the crack to the crack tip; (ii) reactions in the solution near the crack; (iii) surface adsorption at or near the crack tip; (iv) surface diffusion; (v) surface reactions; (vi) absorption into the bulk; (vii) bulk diffusion to the plastic zone ahead of the advancing crack; (viii) chemical reactions in the bulk; and (ix) the rate of interatomic bond rupture [16].

In order to determine the effect of repository conditions (electrolyte film concentration, temperature, etc.) on the rate of crack propagation, it is necessary to solve the transport equations for ion transport in the crack using the heterogeneous reaction rates at the interface as boundary conditions. Since there is a term for electromigration effects, Laplace's equation must also be solved [27, 28]. IGSCC propagation, when it occurs, can be modeled in a similar fashion. Figure 13 shows the relationship between the crack propagation rate, $da/dt$, and stress intensity, $K$, for different crack-tip strain rates, $d\varepsilon_{ct}/dt$. At slow strain rates and low stress intensity, $da/dt$ is controlled by film rupture and repassivation rates. As the stress intensity increases, $da/dt$ becomes limited by transport rates in the aqueous phase [23].

# 4. Data from the Literature on Pitting and SCC

Well over 1000 articles on pitting, crevice corrosion, and SCC of the candidates have been reviewed for this report. Of those articles, the most relevant (over 200) are discussed in this report. The information for Type 304 is abundant, whereas relatively little information exists for Alloy 825. Also, note that most tests have been conducted in boiling 42% $MgCl_2$, solutions of NaCl and $Na_2SO_4$, seawater, or hot pressurized water at 288°C. Despite the scarcity of information on the performance of Alloy 825, we were fortunate to find a few key articles which make direct comparisons of the SCC susceptibility of the austenitic candidates. One reference described comparison tests that were conducted in the presence of gamma radiation.

# 5. Experimental Data on Pitting

## 5.1 Pitting Potential

Hodgkiess and Rigas conducted a study of the corrosion resistance of several materials, including Type 316L stainless steel and Alloy 825, in seawater that had a pH ranging from 7.5 to 8.3 [33]. This investigation included long-term immersion tests and anodic-polarization experiments.

The results confirmed the susceptibility of Type 316L stainless steel to LC in aerated sea water at ambient temperatures, although its performance is improved by reducing the amount of dissolved oxygen in the environment. This

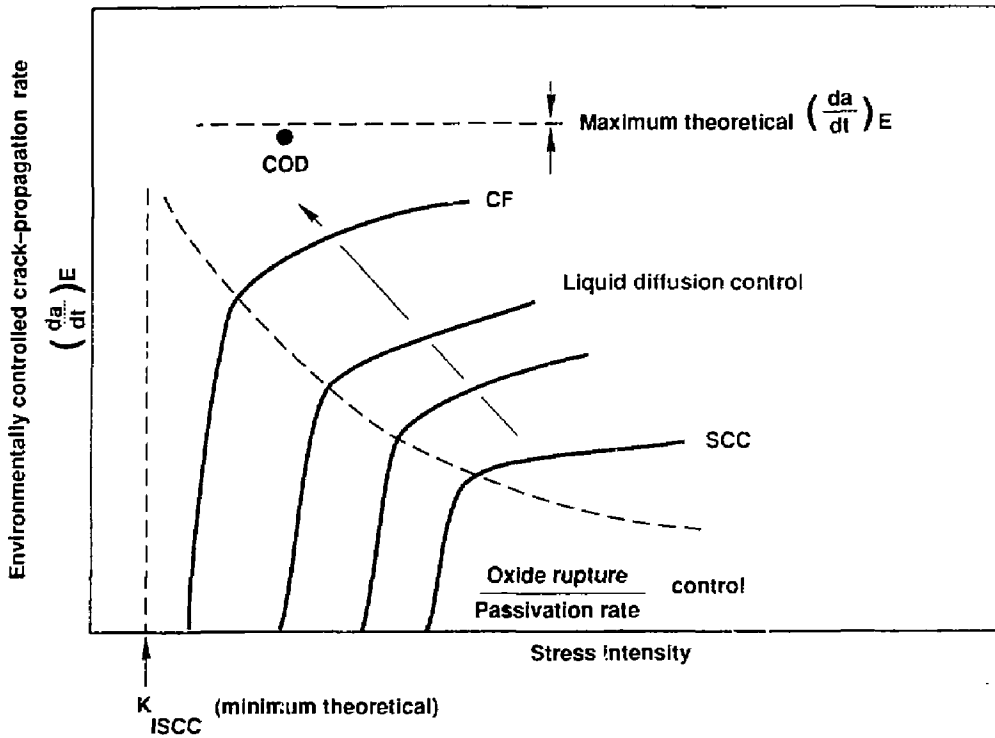


**Figure 13. Schematic variation of the crack propagation rate with stress intensity for different instantaneous crack tip strain rates. Note the smooth transition between SCC and corrosion fatigue (CF) regimes, associated with the different rate-determining processes [23]. COD, crack opening displacement.**

investigation also demonstrated the beneficial effect of increased chromium and molybdenum content on resistance to LC. Corrosion, pitting, and repassivation potentials for Type 316L stainless steel and Alloy 825 are given in Table 1 and are compared in Figs. 14 and 15.

The difference between the pitting potential, $E_c$, and the corrosion potential, $E_{corr}$, serves as a quantitative measure of the susceptibility of an alloy to pitting; the greater the difference, the greater the resistance to pitting. Similarly, the difference between the pitting potential and the repassivation potential, $E_p$, serves as a measure of the resistance of an alloy to crevice corrosion. These quantities are compared in Figs. 14 and 15. Though Alloy 825 and Type 316L are both

Table 1. Corrosion, pitting, and repassivation potentials in aerated seawater.

| Alloy | $T$ (°C) | $E_{corr}$ (mV) | $E_c$ (mV) | $E_p$ (mV) | Comment |
|---|---|---|---|---|---|
| 316L | 20 | −310 | 250 | 30 | Pits |
| | 60 | −180 | 30 | −160 | Deep pits and crevice corrosion |
| 825 | 20 | −240 | 1050 | 1030 | Shallow pits and crevice corrosion |
| | 60 | −280 | 230 | 0 | Pits and crevice corrosion |

Note: All potentials are relative to a saturated calomel electrode (SCE).

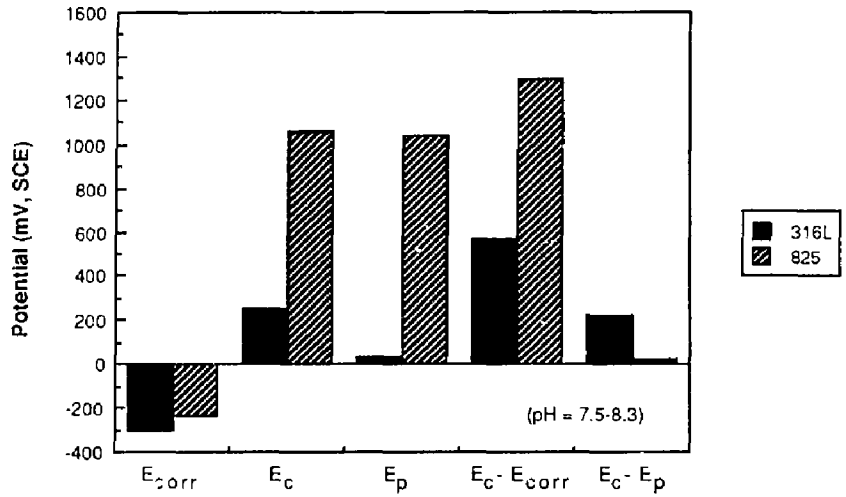


Figure 14. Corrosion potential ($E_{corr}$), pitting potential ($E_c$), and repassivation potential ($E_p$) for Type 316L stainless steel and Alloy 825 in aerated seawater at 20°C [33].

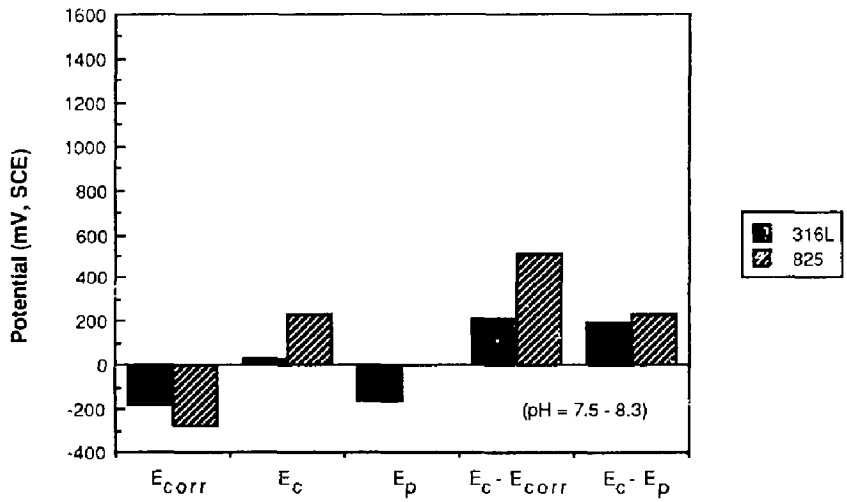


Figure 15. Corrosion potential ($E_{corr}$), pitting potential ($E_c$), and repassivation potential ($E_p$) for Type 316L stainless steel and Alloy 825 in aerated seawater at 60°C [33].

susceptible to pitting and crevice corrosion in seawater, Alloy 825 appears to be more resistant to pitting than Type 316L.

Scarberry et al. have used slow- and rapid-scan potentiodynamic techniques, scratch techniques, and immersion tests to study the pitting of Types 304 and 316 stainless steels, Alloy 825, and Alloy 625 (Inconel) in ocean water at approximately 80°C, nondeaerated and saturated with $SO_2$ [34]. Substitute ocean water was prepared for testing by ASTM Procedure D1141-52 (without heavy metals). Specimens for potentiodynamic tests were sanded with 120-grit aluminum oxide sandpaper and had surface areas of 7 to 10 $cm^2$, whereas specimens for constant-potential and scratch tests were sanded to 500-grit. Scan rates for slow- and rapid-scan potentiodynamic tests were 0.6 and 50 V/hr, respectively. Scratch tests were conducted with a silicon carbide stylus.

During the immersion tests, it was found that Type 316 stainless steel and Alloy 825 showed only incipient pitting. Alloy 625 was not attacked. Incipient pits are defined here as pinpoint areas of attack, without measurable depth, surrounded by a thin layer of corrosion product. In the $SO_2$-saturated substitute ocean water, Types 304 and 316 stainless steels immediately showed a high density of pits. The pits then grew together, producing a thick layer of black corrosion product. This was followed by severe general corrosion beneath the surface layer. Alloy 825 suffered severe pitting, but not general attack. Alloy 625 was not attacked.

Anodic curves determined by rapid-scan potentiodynamic tests for deaerated and $SO_2$-saturated substitute ocean water are shown in Figs. 16 and 17, respectively. The classical effect of increasing molybdenum content upon the width of the passive region is evident in Fig. 16. The curves generated during the rapid-scan tests illustrate the close proximity of the corrosion and pitting potentials of Types 304 and 316 stainless steels. From these results, it is concluded that these two 300-series stainless steels are likely to pit. In contrast, Alloy 825 would be expected to exhibit only marginal pitting behavior, whereas Alloy 625 would not be expected to pit.

Quantitative results of the potentiodynamic and scratch tests are summarized in Tables 2(a) and (b) for deaerated and $SO_2$-saturated substitute ocean water, respectively. Again, recall that the more positive the difference $E_c - E_{corr}$, the more resistant an alloy is to pitting. Negative numbers indicate that pitting occurs readily at the corrosion potential. Based upon this criterion, the ranking of the four alloys considered by Scarberry is: Type 304 (least resistant) < Type 316 < Alloy 825 < Alloy 625 (most resistant). This ranking is identical for both deaerated and $SO_2$ solutions and is consistent with results from the immersion tests. However, the $SO_2$-saturated solution was more aggressive than the deaerated solution. Alloy 625 was included since it is often used as a weld metal for Alloy 825. The data from Tables 2(a) and (b) are compared graphically in Figs. 18 through 21.

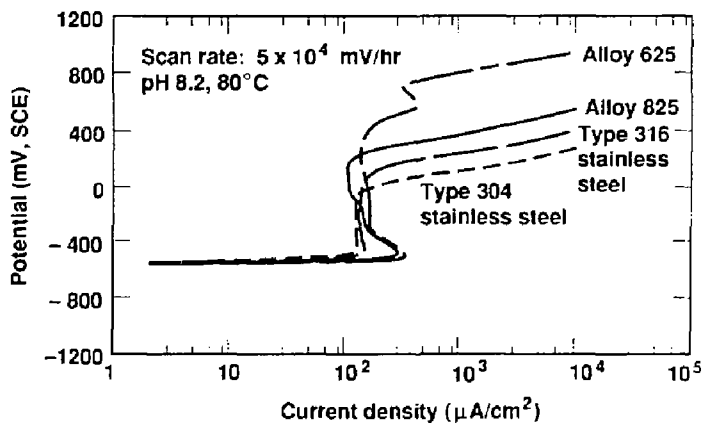


Figure 16. Anodic polarization curves for deaerated, substitute ocean water [34].

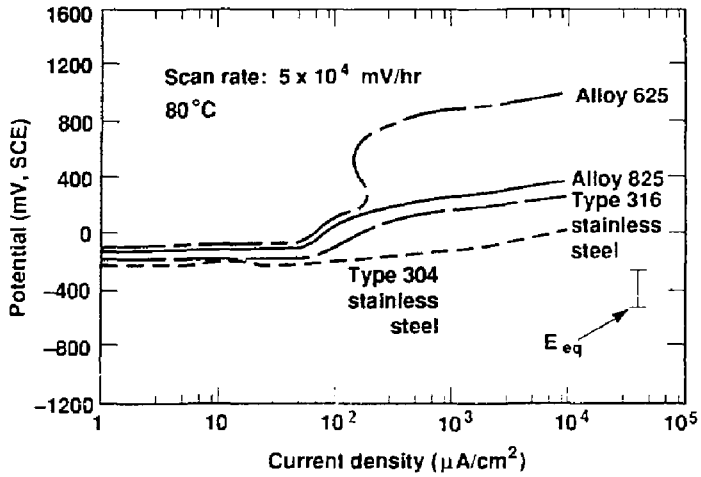


Figure 17. Anodic curves for $SO_2$-saturated, substitute ocean water [34].

Fratesi has made a statistical estimate of the pitting potential of Type 316L stainless steel in 3.5% NaCl [35]. Two types of experiments were performed, one series based upon a potentiodynamic technique with a scan rate of 10 mV/min and a second series based upon a potentiostatic scratch technique. Application of the statistical method to the results confirmed that for each set of tests, the scattering of the pitting-potential values could be related to the stochastic nature of the passive-film failure in a given medium. However, the notable differences in the pitting potentials obtained by the scratch method for the surface under potentiostatic polarization in aerated and deaerated solutions suggested that the mechanical damage of the passive film was more serious than that occurring spontaneously at the defective sites as a result of the medium's aggressiveness at the pitting potential. Results are summarized in Table 3.

Note the tremendous effect that deaeration of the 3.5% NaCl solution (similar to seawater) has on the resistance to pitting, quantified as the difference $E_c - E_{corr}$. Samples in aerated solutions are more likely to pit than samples in deaerated water, in large part because of the effect of oxygen on the corrosion potential, $E_{corr}$. These measurements indicate that Type 316L is more resistant to pitting than the Type 316 samples studied by Scarberry et al. However, as Fratesi points out, there is a large statistical variation in such measurements.

Manning et al. studied the effect of potential scan rate on the pitting potential determination of several high-performance alloys in a solution of 4% NaCl and 0.01M HCl at pH 2 and 70°C [13]. The materials investigated included Type 316 stainless steel (austenitic), Ferralium 255 alloy (duplex), 20Cb-3 and Haynes 20-Mod alloys (super stainless), Alloy 825, and Alloy G (Hastelloy G).

Rectangular test specimens were cut from a 0.64-cm plate and were 1.3 × 7 cm in dimension. The specimens were ground with 220-grit paper, degreased in boiling acetone, rinsed with deionized water, and immediately placed in the test cell.

Three types of pitting tests were employed in this particular study. The majority of the experiments were potentiodynamic pitting tests, which were initiated at –300 mV vs SCE (cathodic potential for all alloys examined) after a 2-min time period at the corrosion potential. The potential was scanned in the noble direction linearly with time at various rates, including 0.36, 0.72, 1, 5, 20 and 50 V/hr. Results for selected alloys at two scan rates that are roughly comparable to those used by Scarberry et al. are given in Table 4. Unfortunately, corrosion potentials are not given, so the difference $E_c - E_{corr}$ cannot be calculated.

Errors represent 95% confidence limits. From these data, it is concluded that Alloy 825 requires a more anodic potential for pitting than does Type 316 stainless steel. Galvanic coupling to a

Table 2(a). Corrosion and pitting potentials (mV, SCE) for deaerated substitute ocean water (80°C, pH 8.2).

| Alloy | Test | $E_c$ (mV) | $E_{corr}$ (mV) | $E_c - E_{corr}$ (mV) | Immersion test |
|---|---|---|---|---|---|
| 304 | FS | −300 | −53 to −115 | −247 to −185 | Pitted |
| 316 | FS | −185 | −30 to −8 | −155 to −177 | Heavy incipient pitting |
| 825 | FS | −40 | −42 to −35 | 2 to −5 | Incipient pitting |
| 625 | FS | 630 | −35 to −10 | 665 to 640 | No pitting |
| 304 | SS | −202 | −115 to −53 | −87 to −149 | Pitted |
| 316 | SS | −205 | −30 to −8 | −175 to −197 | Heavy incipient pitting |
| 825 | SS | 40 | −42 to −35 | 5 to −2 | Incipient pitting |
| 625 | SS | 260 | −35 to −10 | 225 to 250 | No pitting |
| 304 | ST | −70 | −115 to −53 | 45 to −17 | Pitted |
| 316 | ST | 0 | −30 to −8 | 30 to 8 | Heavy incipient pitting |
| 825 | ST | 260 | −42 to −35 | 218 to 225 | Incipient pitting |
| 625 | ST | None | −35 to −10 | None | No pitting |

Note: FS = fast scan; SS = slow scan; ST = scratch test.

Table 2(b). Corrosion and pitting potentials (mV, SCE) of substitute ocean water (80°C) that is saturated with $SO_2$.

| Alloy | Test | $E_c$ (mV) | $E_{corr}$ (mV) | $E_c - E_{corr}$ (mV) | Immersion test |
|---|---|---|---|---|---|
| 304 | FS | −130 | −80 to −10 | −50 to −120 | Pitted |
| 316 | FS | 10 | −140 to −80 | 150 to 90 | Pitted |
| 825 | FS | 40 | −100 to −60 | 140 to 100 | Pitted |
| 625 | FS | 620 | −30 to −10 | 630 to 650 | No pitting |
| 304 | SS | −268 | −80 to −10 | −148 to −258 | Pitted |
| 316 | SS | -60 | −140 to −80 | 20 to −80 | Pitted |
| 825 | SS | 70 | −100 to −60 | 170 to 110 | Pitted |
| 625 | SS | 440 | −30 to −10 | −410 to −430 | No pitting |
| 304 | ST | −230 | −80 to −10 | −150 to −220 | Pitted |
| 316 | ST | −130 | −140 to −80 | 10 to −50 | Pitted |
| 825 | ST | −130 | −100 to −60 | −30 to −70 | Pitted |
| 625 | ST | None | −30 to −10 | None | No pitting |

Note: FS = fast scan; SS = slow scan; ST = scratch test.

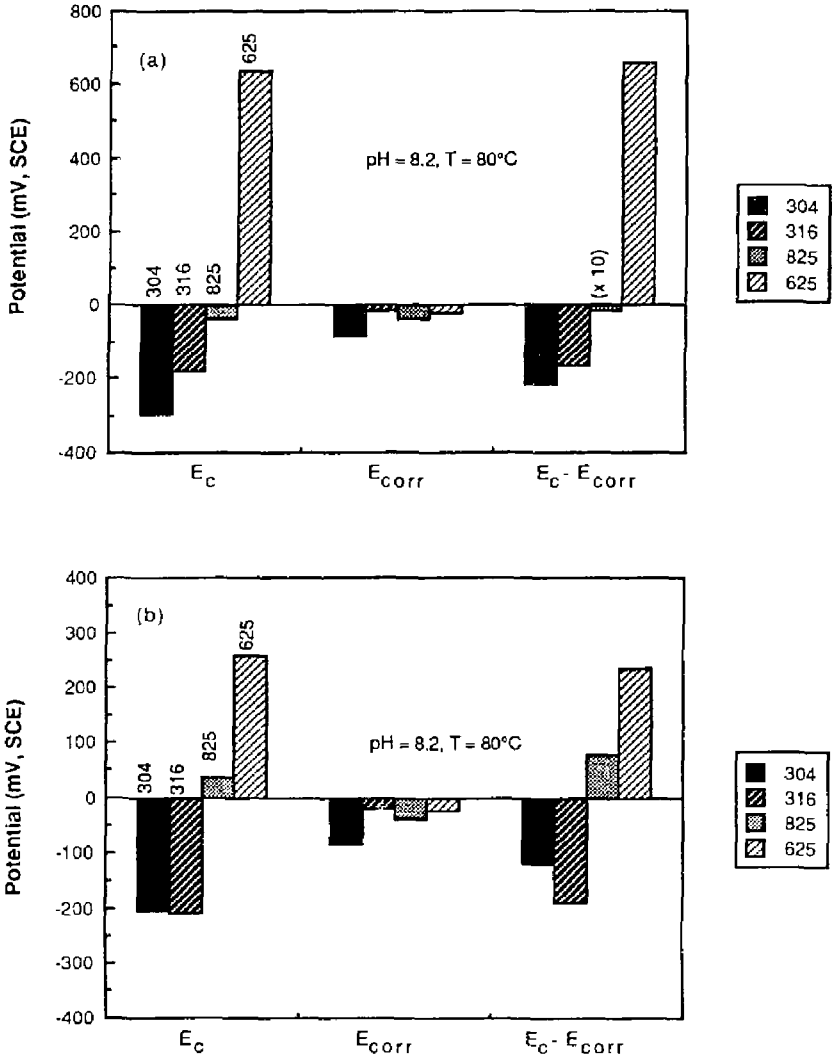


**Figure 18. Pitting potential ($E_c$) and corrosion potential ($E_{corr}$) of candidate materials for (a) fast, and (b) slow scan tests in deaerated substitute ocean water [34].**

noble metal or alloy would induce pitting in Type 316 more easily than in Alloy 825. Manning et al. also used electron microscopy and energy-dispersive x-ray spectroscopy to study points of pit initiation on the metal surface. Frequently, pits began at inclusions in the base metal. The compositions of the inclusions responsible for pit initiation in the various alloys are summarized in Table 5.

Pitting and the onset of concomitant SCC can be prevented by controlling the potential at a level cathodic of the pitting potential. Newman

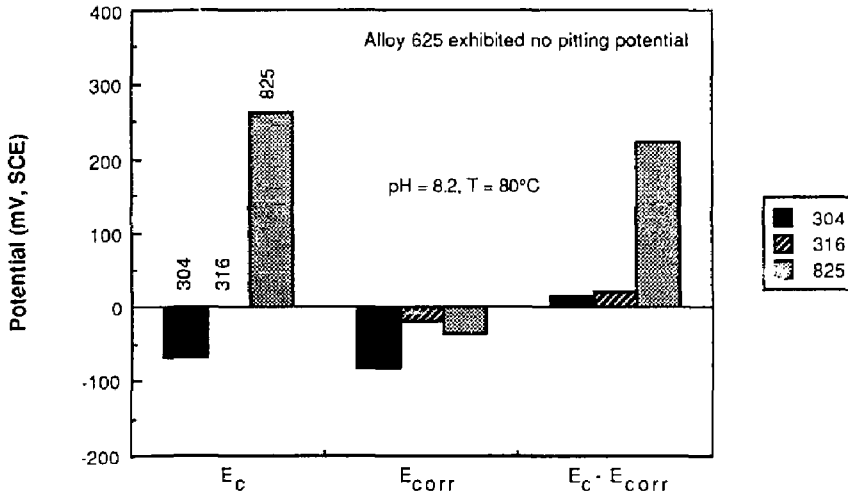


**Figure 19. Pitting potential ($E_c$), and corrosion potential ($E_{corr}$), of candidate materials for scratch tests [34].**

and Franz have studied this aspect of pitting extensively and have determined the protection potential for pitting, $E_{pp}$, for Type 304 stainless steel in 1*M* NaCl with 0.04 sodium thiosulfate added to stabilize pit growth [36]. They observed that instantaneous pit current varied roughly linearly with potential above –200 mV, SCE. Abrupt repassivation occurred at potentials less than or equal to $E_{pp}$ (–245 mV, SCE). Their measurements were consistent with other published results that they cited.

Mancia and Tamba have found that the conditions for the prevention and control of LC (pitting and SCC) of Type 304 stainless steels in chloride-containing water can be defined by means of diagrams of experimental electrode potential, *E*, vs NaCl concentration [37]. The validity of the diagrams was checked by means of long-term tests carried out under controlled conditions (in a laboratory loop and in neutral seawater) on precorroded and nonprecorroded specimens provided with crevice geometry. The prevention of SCC was studied by means of slow strain rate tests (SSRTs) performed either at the free corrosion potential or at an imposed potential. The existence was established of a range of potentials within which LC propagation is stopped by a deactivation mechanism while the free surface of the stainless steel remains passive; this type of protection is termed "cathanodic."

## 5.2 Pit Depths

As will be evident from subsequent discussion, SCC can begin at pits once the pits have penetrated the base metal sufficiently. Therefore, a correlation exists between SCC initiation and pit depth. Lichti et al. conducted a test program to assess the SCC and pitting corrosion of several engineering alloys, including Types 304 and 316L stainless steels, Alloy 825, Alloy 625, and Alloy C-276 (Hastelloy) [38].

In the work of Lichti et al., heated U-bends (100°C) were exposed to a drip solution of geothermal condensate with 30 to 70 ppm chloride. The test was intended to simulate running conditions on the outside of a hot off-gas discharge pipe located within a natural-draft cooling

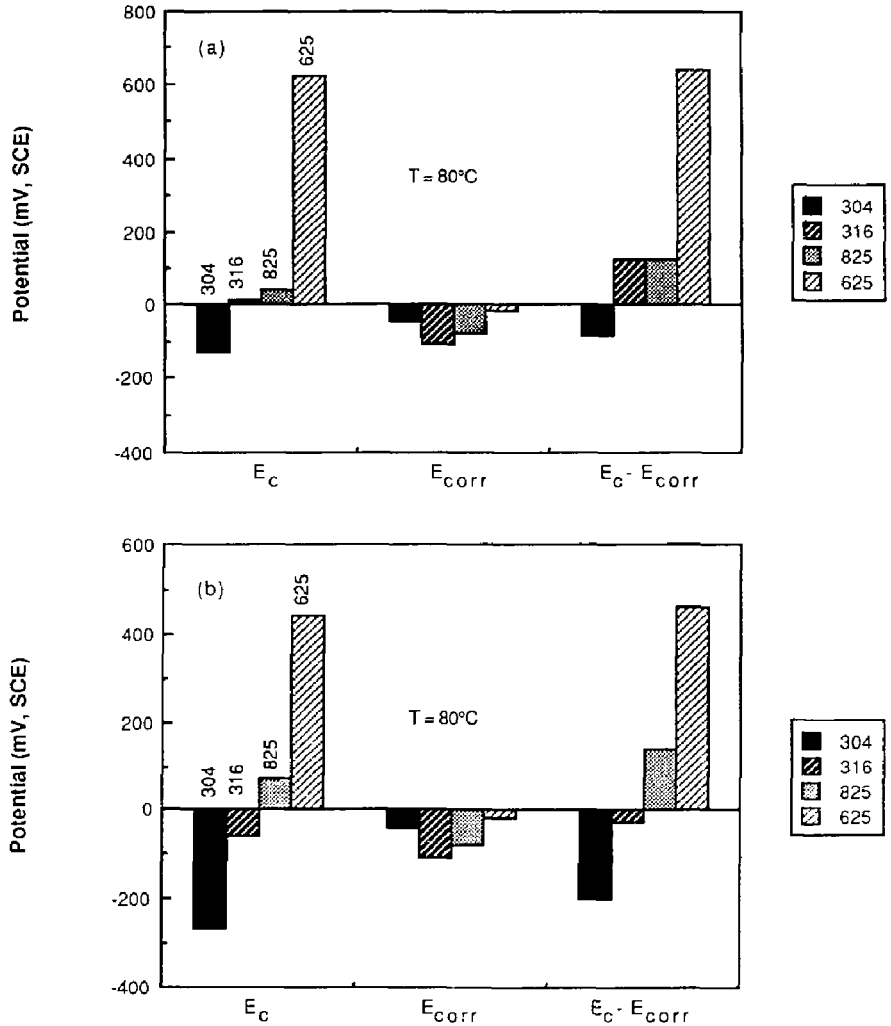


*Figure 20. Pitting potential ($E_c$) and corrosion potential ($E_{corr}$) of candidate materials for (a) fast, and (b) slow scan tests in $SO_2$-saturated, substitute ocean water [34].*

tower, and shutdown conditions in a steam transmission pipeline. The composition of the drip fluid included 200–1400 ppm $CO_2$, 50–200 ppm $HCO_3$, 10–75 ppm $H_2S$, 1–10 ppm HS, 30–40 ppm $NH_4$, 0.2 ppm Fe, 1–20 ppm $SO_4$, <1 ppm $SiO_2$, and 30–70 ppm Cl. This solution was maintained at pH 5–6 and 10–20°C. For the austenitic alloys tested, resistance to pitting corrosion improved with increasing molybdenum content. Iron-nickel based alloys of low molybdenum

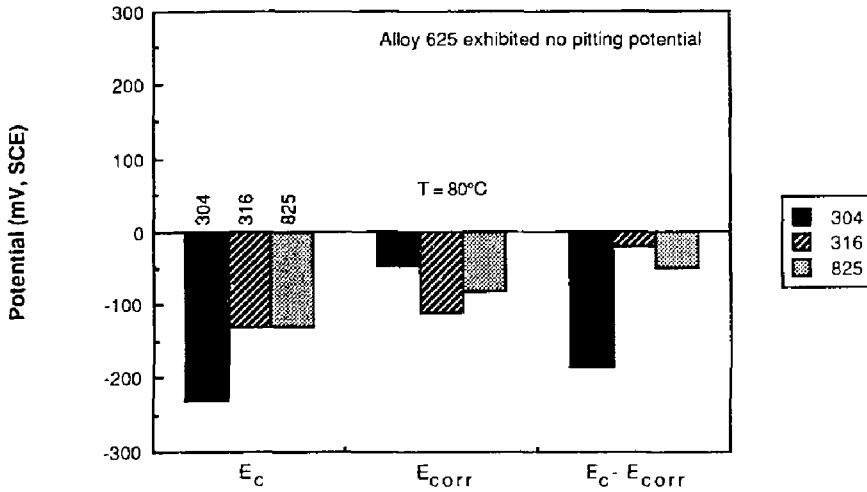


Figure 21. Pitting potential ($E_c$) and corrosion potential ($E_{corr}$) of candidate materials for scratch tests in $SO_2$-saturated, substitute ocean water [34].

Table 3. Corrosion and pitting potentials (mV, SCE) for Type 316L stainless steel in 3.5% NaCl.

| Medium | Surface | $E_{corr}$ (mV) | $E_c$ (mV) | $E_c - E_{corr}$ (mV) |
|---|---|---|---|---|
| Aerated | Passivated only | 138 | 319 | 181 |
| Deaerated | Passivated only | –128 | 309 | 437 |
| Aerated | With emery polish | –135 | 50 | 185 |
| Deaerated | With emery polish | –240 | 232 | 472 |

Table 4. Average pitting potentials of several materials.

| Alloy | Heat | $E_c$ (mV, SCE) 0 V/hr | 0.36 V/hr | 50 V/hr |
|---|---|---|---|---|
| 316 | 1 | –100 to –80 | –94 ± 28 | –147 ± 71 |
| 825 | 1 | 160 to 180 | 209 ± 36 | 1 ± 30 |
| 825 | 2 | 140 to 160 | 178 ± 43 | None |
| 20-Mod | 1 | 180 to 200 | 236 ± 36 | 276 ± 33 |
| 20-Mod | 2 | 260 to 280 | 321 ± 32 | None |
| G | 1 | None | None | None |

Table 5. Energy-dispersive x-ray spectroscopy of inclusions responsible for pit initiation.

| Alloy | Elements detected in inclusion |
|---|---|
| 316 | Ti, Mn, S, Cr, Si |
| 825 | Ti, V |
| 20-Mod | Ti, V |

content, which included Alloy 825, were subject to pitting corrosion but did not show cracking. The high-iron-nickel based alloys, which included Alloy C-276, were immune to all types of localized attack in the test environment. Results are summarized in Table 6 and Fig. 22.

The ASM Metals Handbook also gives data on pit depths in Type 304, Type 316L, and Alloy 825 after approximately 6 months of exposure to chloride-containing environments [39]. Results are summarized in Table 7 and Fig. 23. Note that Type 316L and Alloy 825 are slightly better than Type 304; a representative penetration rate for pitting of these alloys is approximately 1 mm/yr (1000 μm/yr).

## 5.3 Effect of Molybdenum Content on Pitting

Asphahani has conducted an extensive study on the LC of high-performance alloys [40]. The potentiostatic polarization method of testing appears to be the most promising in that it defines the damaging potential range in which localized corrosive attack occurs. The dependency of this potential range on temperature, pH, chloride ion concentration, and molybdenum content was examined. The alloys studied included Type 316 stainless steel (bench mark), Alloy 825, Alloy 625, Alloy G, and Alloy C-276.

Immersion tests were conducted on flat specimens prepared from mill-annealed stock. Smooth specimens had dimensions of approximately 5 × 2.5 × 0.3 cm. Specimens with artificial crevices had dimensions of approximately 7.5 × 2.5 × 0.3 cm. The specimens had saw-cut edges and were dry-polished with fast-cut resin cloth prior to testing. Electrochemical tests were conducted on cylindrical specimens (1.3 × 1.3 cm) that were saw-cut from annealed rods, wet-polished with 120-grit silicon carbide paper, and degreased in acetone. Immersion tests were performed in different environments at ambient and elevated temperatures.

The corrosion rates of the smooth and the creviced specimens were negligible after a 96-hr exposure in a neutral 4% NaCl environment. No localized corrosive attacks were seen, not even on the creviced specimens exposed at 70°C. However, in an acidic-oxidizing solution consisting of 7% by volume $H_2SO_4$, 3% by volume HCl, 1% $CuCl_2$, and 1% $FeCl_3$, the Type 316 and Alloy 825 specimens suffered pitting attack within less than 1 day of exposure at ambient temperature without the need of an artificial crevice to initiate the attack.

The susceptibilities of Alloy G and Alloy 625 alloys to LC in this solution were temperature-dependent. Alloy G performed well up to about 70°C. Localized corrosive attack was induced on Alloy 625 at about 102°C within the 24-hr exposure. At moderate temperatures, the resistance was a function of cold work; as low as 10% cold work rendered this alloy susceptible to LC at 70°C. Finally, alloy C-276 showed excellent resistance regardless of the testing environment, the temperature, and the amount of cold work.

Constant-potential tests were conducted in 4% NaCl and in 3.8% $FeCl_3$ solutions at room temperature and at 70°C. The results are summarized in Fig. 24. Clearly, the potential required for localized attack becomes more positive with increasing molybdenum content. From these experiments, it is obvious that there is a direct correlation between the molybdenum content of an alloy and its resistance to localized attack. A ranking of these alloys for resistance to pitting corrosion at the conditions described is: Type 316 stainless steel (worst) < Alloy 825 < Alloy G < Alloy 625 < Alloy C-276.

Clearly, the molybdenum content of stainless steels enhances their resistance to LC. Yu et al. studied the structure and chemical composition of the oxide film, before and after SCC, on Types 316 and 321 stainless steels corroded in high-temperature and high-pressure water containing 2000 ppm $Cl^-$ and 8 ppm dissolved oxygen [41]. The methods used were CEMS (conversion

Table 6. Pitting and SCC in heated U-bends.

| Alloy | Exposure (wk) | Max. pit depth (μm) | Comment on cracking |
|---|---|---|---|
| 304 | 3 | 290 | Branched cracking in all samples |
| | 6 | 140 | |
| | 8 | 216 | |
| 316L | 3 | 161 | Branched cracking in all samples |
| | 6 | 123 | |
| | 9 | 145 | |
| 825 | 1 | 147 | Not detected |
| | 9 | 137 | |
| | 15 | 208 | |
| 625 | 9 | None | Not detected |
| C-276 | 9 | None | Not detected |

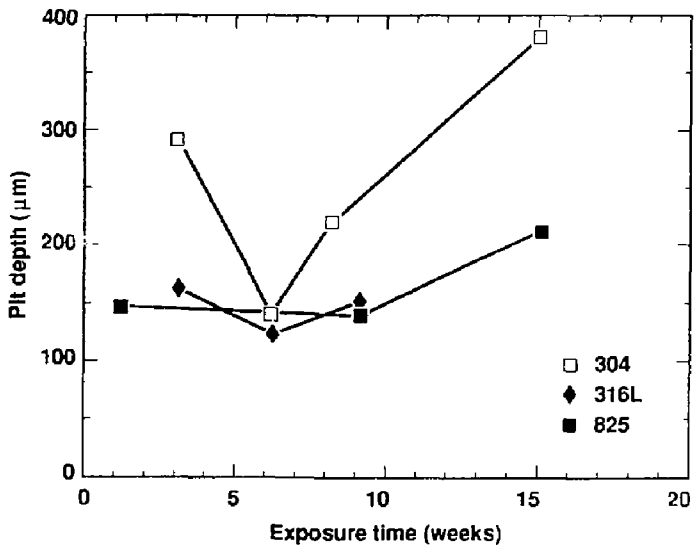


Figure 22. Pit depth for heated U-bends exposed to a geothermal condensate [38].

electron Mossbauer spectroscopy), AES (Auger electron spectroscopy), and XPS (x-ray photoelectron spectroscopy). In this study, a correlation was established between the structure and chemical composition of the oxide film and SCC resistance. Experimental results showed that the alloying element molybdenum reacted with the corrosive medium to form the $Fe_2(MoO_4)_3$

Table 7. Depth of pits on stainless steel spool test specimens in a flue-gas desulfurization system after 6 months of exposure (39 days on bypass).

| Alloy | Environment | pH | Temp (°C) | $Cl^-$ (ppm) | Pit depth (mm) | Density |
|---|---|---|---|---|---|---|
| 304 | [a] | 4.4 | 60 | 100 | 1.19 | Profuse |
| 316L | | | | | 0.58 | Profuse |
| 825 | | | | | 0.66 | Profuse |
| 304 | [b] | 1–2 | 60–170 | 7000 | 1.24 | Profuse |
| 316L | | | | | 0.91 | Profuse |
| 825 | | | | | 0.74 | Profuse |

[a] Quencher spray header above a 7000-ppm $Cl^-$ slurry.
[b] Wet/dry inlet duct.

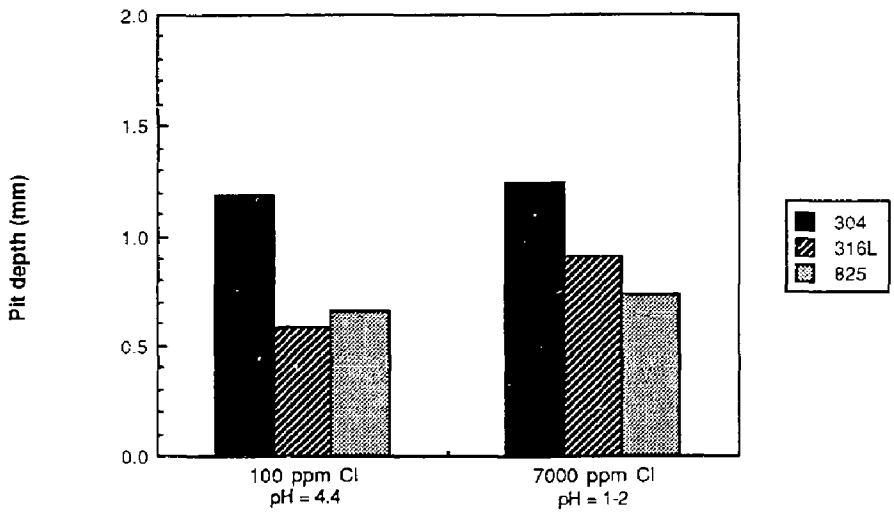


Figure 23. Pit depths in Types 304 and 316L stainless steels and in Alloy 825 after approximately 6 months of exposure to chloride-containing environments [39].

phase. Molybdenum in Type 316 alloy affected the composition and growth rate of iron oxides, decreased the dissolution rate of chromium in the transpassive region, and inhibited $Cl^-$ in its penetration through the oxide film. Therefore, molybdenum played an important role in prolonging the incubation period of SCC. The results showed that molybdenum-bearing Type 316 alloy has better SCC resistance than 321 alloy. The role of molybdenum in SCC resistance was also discussed from the point of view of alloy thermodynamics.

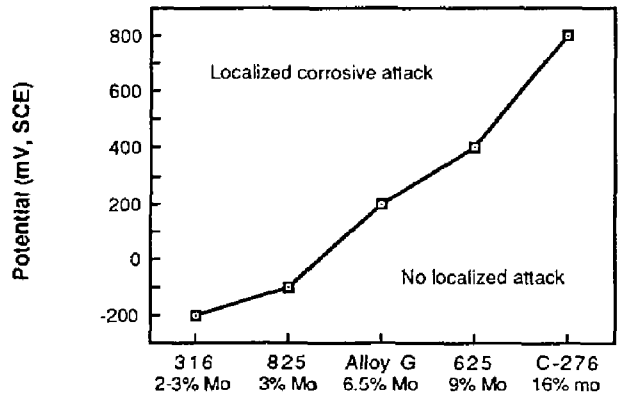


**Figure 24. Effect of molybdenum alloy additions on the localized corrosion potential for a constant applied potential, 24-hr exposure in 3.8% $FeCl_3$ at 70°C [40].**

# 6. Experimental Data on SCC and Other Forms of LC

## 6.1 Tests for SCC

SCC experiments can be classified into three categories: (i) tests on statically loaded smooth samples; (ii) tests on statically loaded precracked samples; and (iii) tests using slowly strained samples. Tests on statically loaded smooth samples are usually conducted at various fixed stress levels, and the time to failure of the sample in the environment is measured.

Tests on statically loaded precracked samples are usually conducted with either a constant applied load or with a fixed crack opening displacement, and the actual rate or velocity of crack propagation, $da/dt$, is measured. As a result, $da/dt$ is plotted vs the stress intensity, $K$.

Much of the data for transgranular stress corrosion cracking (TGSCC) and intergranular stress corrosion cracking (IGSCC) found in the literature was obtained from classic U-bend and bent beam experiments [42, 43]. The stress of principal interest in the U-bend specimen is circumferential. It is nonuniform because (1) there is a stress gradient through the thickness varying from a maximum tension on the outer surface to a maximum compression on the inner surface, (2) the stress varies from zero at the ends of the specimen to a maximum at the center of the bend, and (3) the stress may vary across the width of the bend.

When a U-bend specimen is stressed, the material in the outer fibers of the bend is strained into the plastic portion of the true stress-true strain curve. As discussed in ASTM Standard Procedure G30 [44], the total strain $\varepsilon$ on the outside of the bend can be closely approximated to the equation:

$$\varepsilon = T/2R \quad \text{when } T << R \tag{24a}$$

where:

$T$ = specimen thickness, and
$R$ = radius of the bend curvature.

Stressing is usually achieved by either a one- or a two-stage operation. Single-stage stressing is accomplished by bending the specimen into shape and maintaining it in that shape without allowing relaxation of the tensile elastic strain. Two-stage stressing involves first forming the approximate U-shape, then allowing the elastic strain to relax completely before the second stage of applying the test stress.

In two-stage U-bend experiments such as those conducted by Warren, the applied flexural stress, $\sigma$, is proportional to the deflection, $d$, as shown in Fig. 25 [42]. The deflection, $d$, and applied stress are related by Eq. (24b).

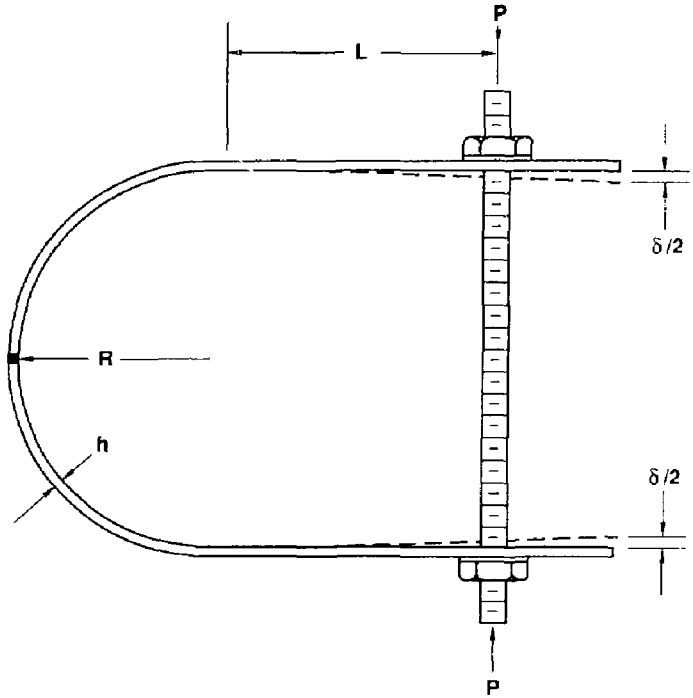


Figure 25. Schematic showing parameters in a U-bend experiment [42].

$$d = \{[12\sigma(2R + h)]/[(L + R)(8R + h)hE]\}$$

$$\times [L^3/3 + R(\pi L^2/2 + \pi R^2/4 + 2LR)] \quad (24b)$$

where $E$ is the modulus of elasticity, $R$ is the radius of the specimen bend, $h$ is the specimen thickness, and $L$ is the length of the specimen straight section.

Four-point, bent-beam tests are also used to determine susceptibility to SCC [43]. The specimen is supported at the ends and by forcing two inner supports against it in a fashion shown in Fig. 26. The two inner supports are usually located symmetrically around the midpoint between the outer supports. As discussed in ASTM Standard Procedure G39 [45], the elastic stress for the midportion of the specimen (between contact points of the inner support) in the outer fibers of four-point-loaded specimens can be calculated from the following relationship:

$$\sigma = 12Ety/(3H^2 - 4A^2) \quad (25)$$

where:

$\sigma$ = maximum tensile stress,
$E$ = modulus of elasticity,
$t$ = thickness of specimen,
$y$ = maximum deflection (between outer supports),
$H$ = distance between outer supports, and
$A$ = distance between inner and outer supports.

The dimensions are often chosen so that $A = H/4$.

Either of these techniques can be used to determine a threshold stress, $\sigma_{th}$. The threshold stress is illustrated in Figs. 27 and 28 and is defined as the stress at which the time to failure approaches infinity [46, 47].

More recently, corrosion scientists have begun to use slow strain rate testing (SSRT) in electrochemical environments [48]. Usually, a tensile machine pulls a smooth sample that is exposed to the corrosive environment at a low crosshead speed ($10^{-5}$ to $10^{-9}$ m/s). The strain to failure in

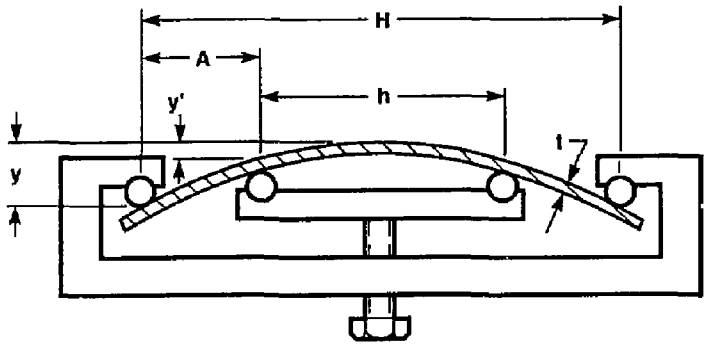


Figure 26. Configuration for a four-point loaded specimen [43].

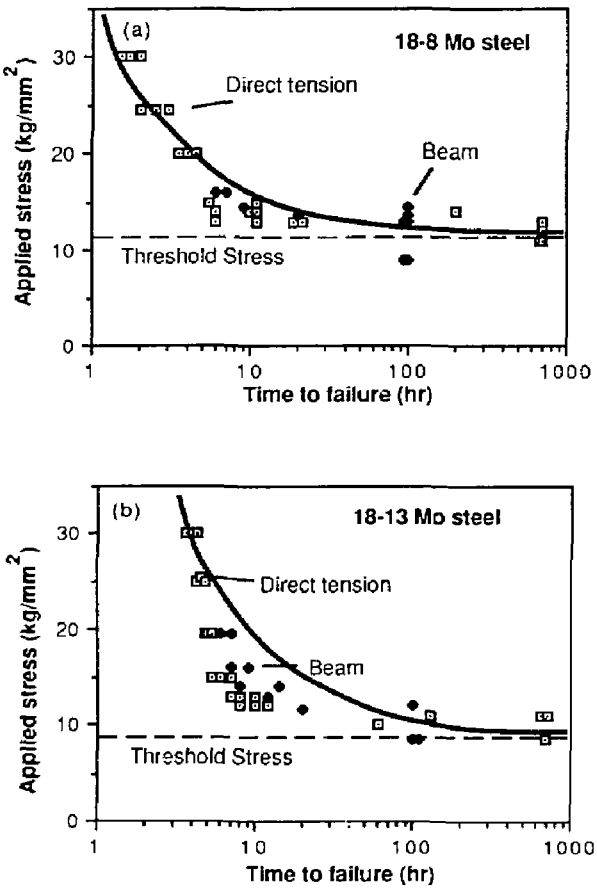


Figure 27. Results of SCC tests on 18-8 and 18-13 molybdenum steels in boiling $MgCl_2$ solution [47].

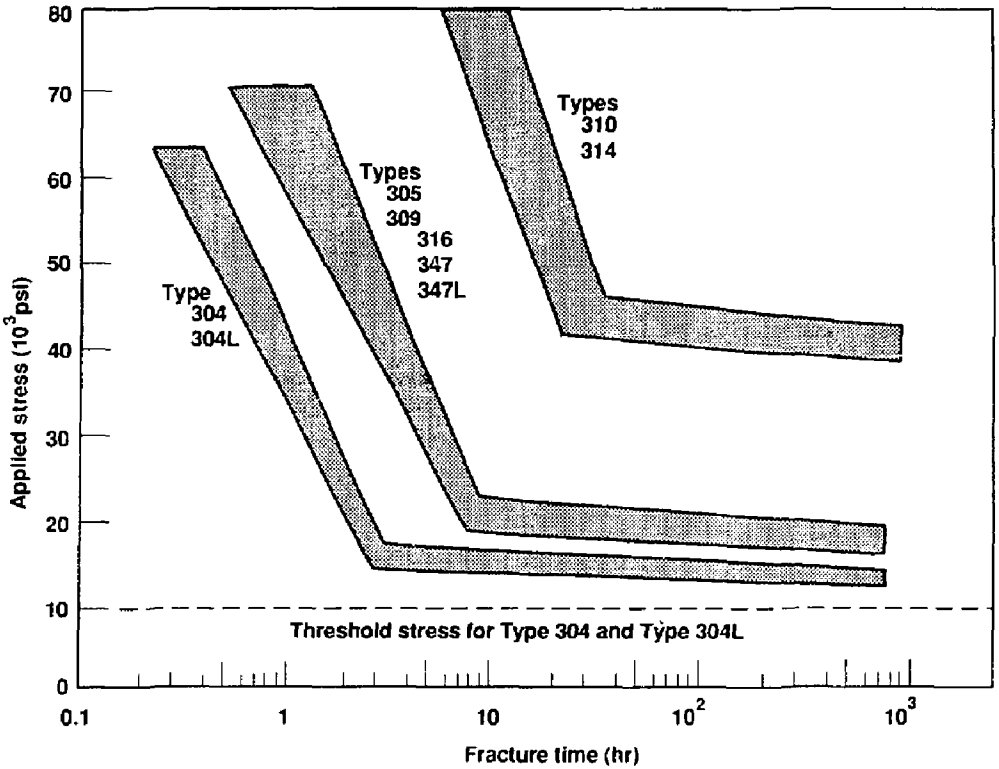


Figure 28. Composite curves illustrating the relative SCC resistance for commercial stainless steels in boiling 42% $MgCl_2$ [3].

the corrosive environment can then be plotted against the strain rate. In the future, it may be possible to use both acoustic emission and electrochemical noise measurements to better determine model parameters from precise analysis of individual steps in the rupture/repassivation process [49].

Solomon has used SSRT to study SCC in Type 304 stainless steel in oxygenated 288°C water [50]. In this work, Solomon found that the type of cracking was determined by the degree of sensitization (DOS), defined as the percentage of grain-boundary attack, and the strain rate, $d\varepsilon/dt$. This is illustrated in Fig. 29. In the case of unsensitized samples (DOS < 26), ductile failure was observed at values of $d\varepsilon/dt > 2 \times 10^{-4}$ min$^{-1}$; TGSCC was observed at values of $d\varepsilon/dt < 2 \times 10^{-4}$ min$^{-1}$. In the case of sensitized samples (DOS > 91), ductile failure was observed at values of $d\varepsilon/dt > 6 \times 10^{-3}$ min$^{-1}$; IGSCC was observed at values of $d\varepsilon/dt < 6 \times 10^{-3}$ min$^{-1}$. At intermediate values of DOS, "granulated" attack was observed.

From Solomon's work, it is clear that when SSRT is used to study SCC phenomena, the experimentalist has to be very careful to select a sufficiently slow strain rate, $d\varepsilon/dt$, so that fracture can occur by corrosion-assisted processes (film rupture and repassivation).

## 6.2 Types of Test Environments for SCC

Type 304 stainless steel in boiling 42% $MgCl_2$ has become the model system for SCC studies. In fact, boiling 42% $MgCl_2$ is specified for SCC tests by ASTM Standard G-36 [19]. $MgCl_2$ solutions are probably the most aggressive SCC agent for

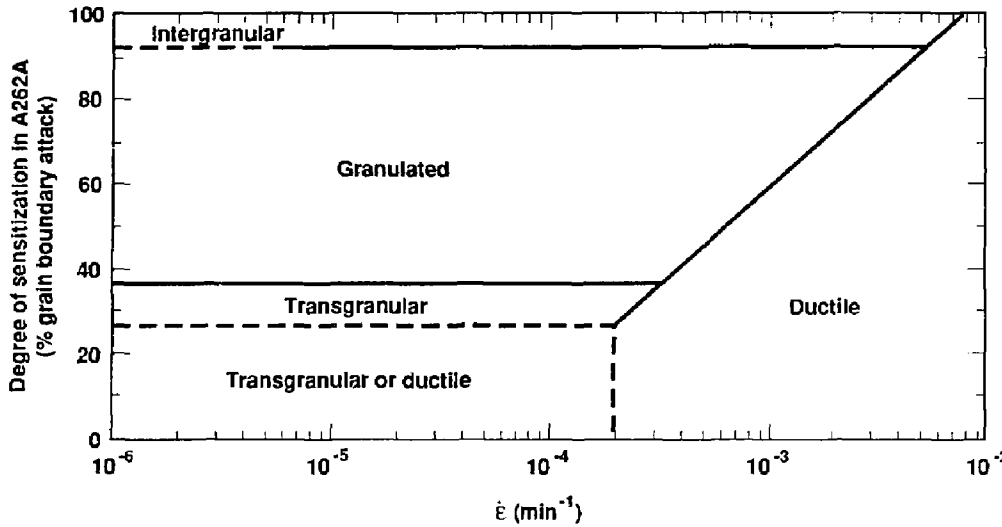


Figure 29. Fracture map showing the mode of fracture as a function of the degree of sensitization of the test specimen and the strain rate employed in the slow strain rate test [50].

the 300-series stainless steels. This was demonstrated by Warren [42]. He exposed 18-8 steel U-bend samples to several chloride solutions, each having a different cation. The cations investigated included $Na^+$, $Ca^{2+}$, $Fe^{3+}$, and $Mg^{2+}$; the $Mg^{2+}$ cation proved to be the most aggressive (Fig. 30). Warren also demonstrated the detrimental effect of pH suppression on Type 304 stainless steel in $MgCl_2$ solutions (Fig. 31). For this reason, an abundance of literature has been published on SCC studies in $MgCl_2$ solutions. Furthermore, many of these publications have focused on Type 304 stainless steel because this alloy is of great industrial importance and is relatively susceptible to TGSCC in the annealed state and IGSCC in the sensitized state [51–70].

Harsh-boiling $MgCl_2$ solutions enable the experimentalist to perform screening tests of alloys. However, other test environments are of more practical importance. For example, a 3.5% NaCl solution approximates conditions in seawater. Note that many articles have also been published on the SCC of Type 304 stainless steel in chloride and sulfate electrolytes [71–109]. High-temperature, high-pressure water with very low levels of dissolved oxygen (DO) and chloride is encountered in boiling-water reactors (BWRs) [110–122]. These reactors, originally fabricated with Type 304 stainless steel, have water systems that are maintained at 289°C (551°F) and 1040 psi. The chloride concentrations are usually a few ppm; the DO is less than 200 ppb (with hydrogen-water chemistry). Note that the DO can be almost 200 ppb without hydrogen-water chemistry [123]. Finally, articles have appeared on the effects of various species, including borates [124, 125], miscellaneous impurities [126], nitrates and DO [127], organic acids [128], and thiosulfate [129, 130].

## 6.3 Effects of the Environment on SCC

Several environmental parameters are known to influence the rate of crack growth in aqueous solutions. These include, but are not limited to, temperature, pressure, solute species, solute concentration and activity, pH, electrochemical potential, solution viscosity, and electrolyte agitation.

Congleton et al. studied the effects of chloride and oxygen concentration on SCC in high-temperature water [131]. SSRTs were performed on Type 316 stainless steel in 265°C water containing from 0 to 45 ppm oxygen and from less than 0.1 to 1000 ppm chloride. They found that time to failure, total elongation, maximum load, and reduction in area were all useful

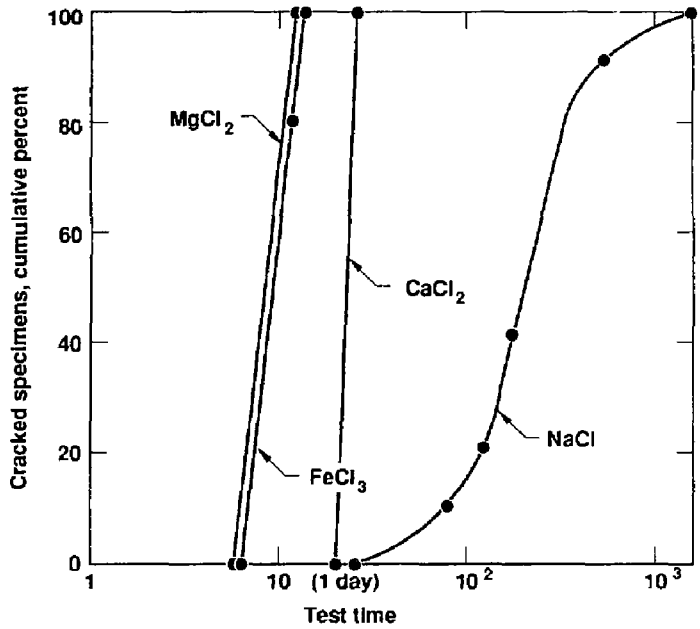


Figure 30. Effect of metallic cation on the time-for-cracking of Type 304 stainless steel specimens exposed at 100°C to water containing 100 ppm chloride. $Mg^{2+}$ is the most aggressive cation [42].

numerical parameters for quantifying cracking propensity, but they all tended to be less sensitive than metallographic and fractographic examination for identifying small changes in susceptibility or for highlighting differences in the mechanism of cracking. Consequently, metallographic and fractographic studies were extensively used in their present work, and the results were primarily discussed in those terms.

Specimens used by Congleton et al. were fabricated from 4.76-mm-diam rods, had threaded ends and a 2.54-mm-diam × 12.7-mm-long gauge length, and were strained in moderately stiff machines, most frequently at an initial strain rate of $2 \times 10^{-6}$ $s^{-1}$. For each experiment, the time to failure, percentage elongation, and percent reduction in area were recorded. In addition, one-half of the fractured specimen was sectioned at midplane through the longest observable surface crack and prepared for metallographic examination, the remaining part being examined by scanning electron microscopy where considered necessary. All potentials were measured relative to the Ag-AgCl external reference electrode.

Tests were performed on both annealed and sensitized Type 316 stainless steel. For the specimens sectioned at midplane, the maximum crack lengths in the necked region, $a_n$, and in the uniformly deformed gauge length, $a_u$, were measured. An examination of the number and distribution of cracks in the section indicated three somewhat different types of cracking. Type A denotes the situation in which the cracks had similar lengths in both the necked and unnecked regions, implying that the crack growth rate is relatively independent of stress level (once the threshold is exceeded) and that crack initiation occurred well before the onset of necking. In contrast, Type B refers to a case in which cracks in the necked region were somewhat longer than in the uniformly deformed gauge length. This difference is due to the dependence of crack propagation rate on stress intensity. Finally, Type C refers to a case in which cracking occurred almost exclusively in the necked region at stresses well

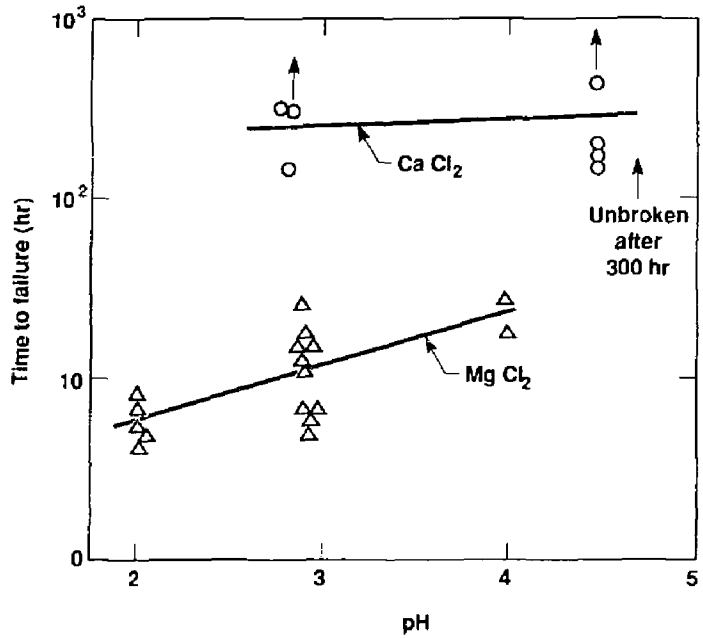


Figure 31. Effect of pH on the time to failure of Type 304 stainless steel at 50,000 psi in $MgCl_2$ and $CaCl_2$ solutions at 125°C [42].

above the yield stress (YS) and approaching the ultimate tensile stress (UTS).

One parameter that can be useful in assessing susceptibility to SCC from SSRTs is the crack growth rate, although there are various ways in which this can be calculated. An average crack growth rate can be obtained by dividing the maximum length by the total test time. This average crack growth rate can conveniently separate susceptible material from unsusceptible material but takes no account of differences in the time for crack initiation that occur from specimen to specimen.

There are thus three methods that can be used for obtaining a crack growth rate: (i) $V_m = a_{max}/$(total time); (ii) $V_L = a_s/$(time to maximum load); and (iii) $V_H = (a_n - a_s)/$(total time – time to maximum load). Clearly, $V_m$ neglects any initiation time and is likely to be more applicable to Types A and B cracking, which also are relevant to $V_L$, where crack initiation and growth occur at low stresses. On the other hand, $V_H$ appears to be most relevant for cracks that initiate and grow at high stresses, as with Type C cracking. The differences between $V_L$ and $V_m$ are small, whereas $V_H$ is usually the largest, presumably because of an increase in velocity as $K_{ISCC}$ is approached. The velocities $V_m$ or $V_L$ are probably the more realistic for practical considerations, and $V_H$ is only likely to be relevant in the later stages of a failure, where stress intensification is high and total failure imminent.

The available data have been plotted using an interpolation procedure. $V_m$ is described as a function of oxygen and chloride contents for the annealed condition (Fig. 32) and for the sensitized state (Fig. 33). In the case of annealed material, maximum crack velocities were observed at high and low oxygen or chloride concentrations. In contrast, the sensitized material shows high crack velocities extending from intermediate oxygen contents and very low chloride levels to wider oxygen limits as the chloride increases. The implication would appear to be that in components that contain regions of sensitization but are otherwise in the annealed state, cracking may

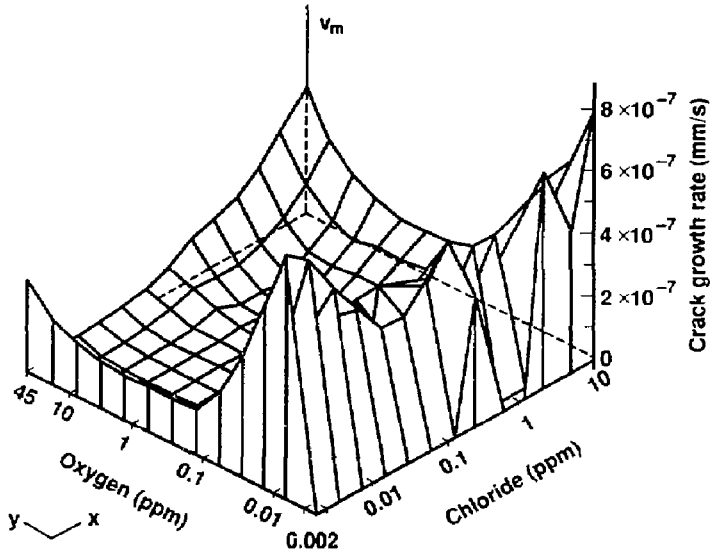


Figure 32. The effects of oxygen and chloride contents of waters on mean crack growth rates in annealed Type 316 stainless steel [131].

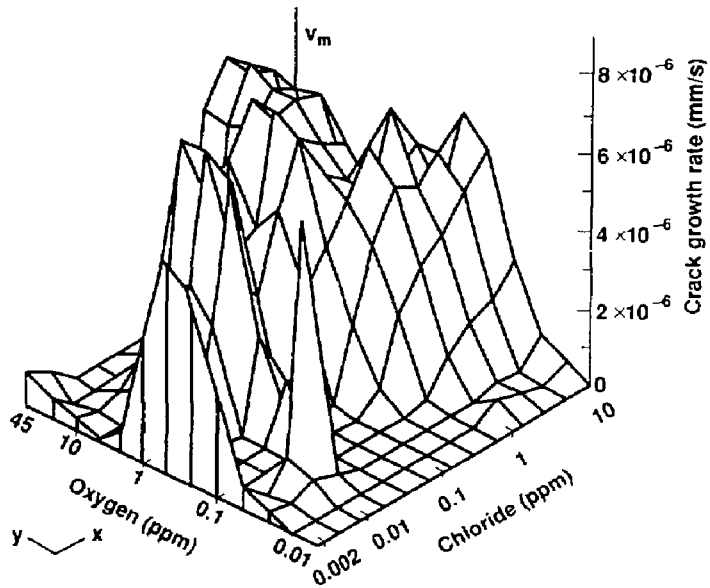


Figure 33. The effects of oxygen and chloride contents of waters on mean crack growth rates in sensitized Type 316 stainless steel [131].

occur over virtually the whole range of oxygen and chloride contents studied.

Figure 34 shows plots of $V_L$ and $V_H$ against chloride content for the annealed steel and reinforces the point that any definition of susceptibility to SCC should take stress into account. Figure 35(a) shows the mean crack growth rate for annealed stainless steel plotted against potential inferred from the appropriate water conditions, using the potential map given in Fig. 35(b). It is clear that a no-cracking regime exists for annealed material in the potential range from about -200 to +150 mV, SHE. Such data clearly confirm the two potential ranges in which cracking occurs for annealed material. Above about 150 mV, SHE, isolated cracks form and grow to relatively large depths, whereas at low potentials, a multitude of short cracks form close to one another, and these readily link together to give a shallow annulus of transgranular cracking.

The review by Gordon of the susceptibility of Type 304 stainless steels in oxygenated and chlorinated high-temperature waters used the data of Williams, as well as those of many other investigators, to obtain a revised diagram showing the domains of water composition within which cracking occurred [132, 133]. Williams' original data are shown in Fig. 36, and Congleton's data are shown in Figs. 37 and 38. Figures 39 and 40 show the results of experiments by Congleton et al. together with those produced by earlier workers in the form of the plots used by Gordon. The upper line in Fig. 39, due to Williams, indicates that transgranular cracking only occurs in annealed stainless steels for the high-chloride and high-oxygen region of the diagram.

The following conclusions are drawn from the work of Congleton et al. First, the predominant cracking modes for annealed and sensitized Type 316 stainless steel in high-temperature waters are transgranular and intergranular, respectively. In very-low-oxygen waters containing 210 ppm chloride, sensitized material displayed transgranular cracking. The extent of the cracking depended upon the water composition, the severity of the cracking generally increasing with increasing oxygen and chloride contents of the water. Crack growth rates at low or high stresses are functions of oxygen content in particular, but also of chloride content of the waters to some extent. For annealed material, the highest crack growth rates occurred at low oxygen contents, but for sensitized material, intermediate oxygen contents, between 0.1 and 10 ppm, gave the highest crack velocities.

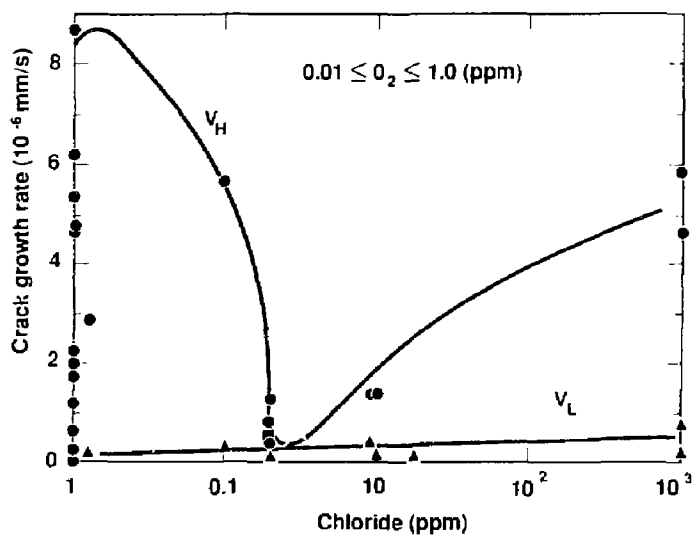


**Figure 34. Crack growth rates, $V_L$ and $V_H$, for annealed Type 316 stainless steel as a function of chloride contents of waters [131].**

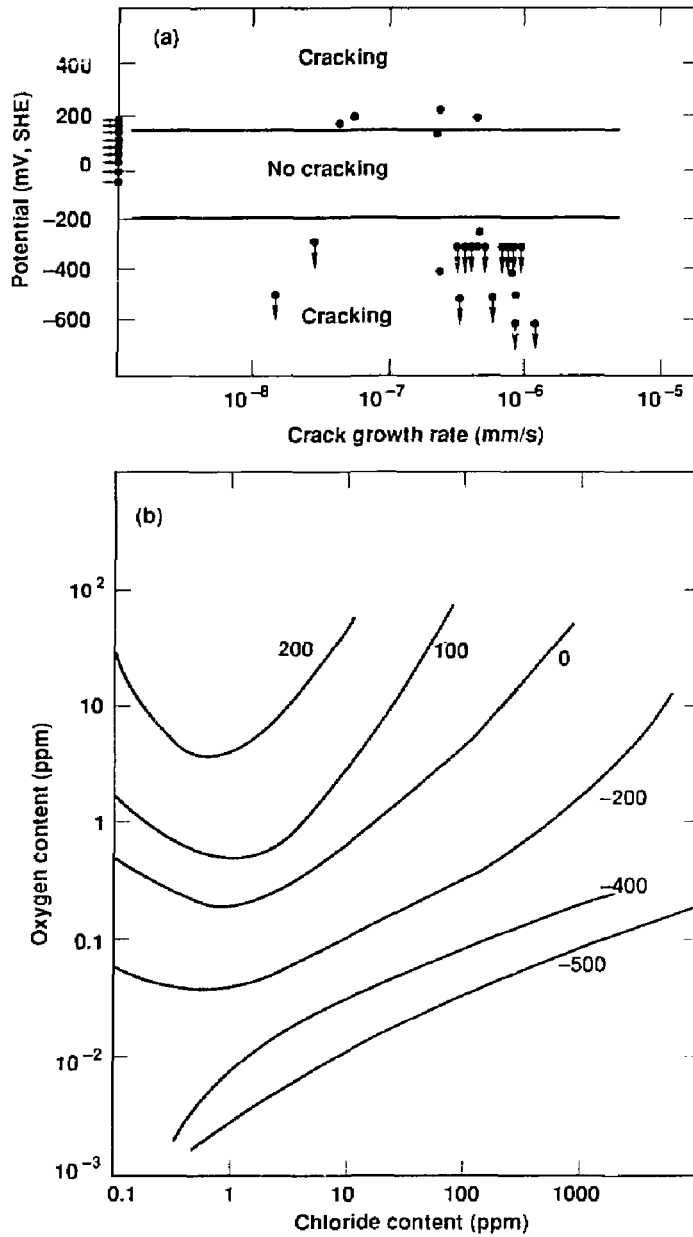


Figure 35. (a) Graph of mean crack growth rate for annealed stainless steel plotted against potential inferred from the appropriate water conditions using the potential map given in (b). (b) Potential-oxygen-chloride content map for Type 316 stainless steel in 265°C water. Equipotential lines are plotted, the numbers associated with each line indicating the equilibrium potential achieved under those water conditions expressed as mV, SHE [131].

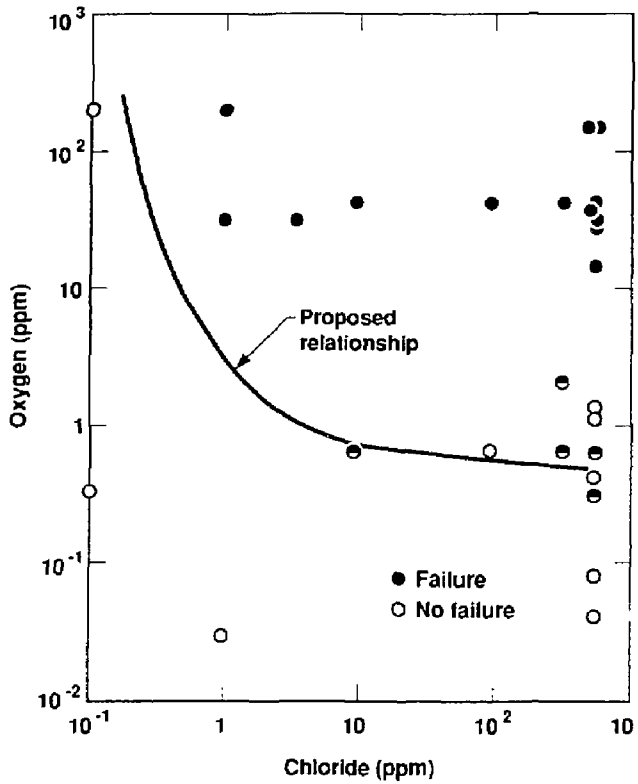


**Figure 36. Proposed relationship between chloride and oxygen content of alkaline-phosphate-treated boiler water, and susceptibility to SCC of austenitic stainless steel exposed to the steam phase with intermittent wetting [133].**

The data presented by Congleton et al. significantly affect the positions of the "cracking-no-cracking" domains on the $O_2$-Cl diagram by reducing the size of the "no-cracking" domain below that previously assumed. This change is due to the occurrence of transgranular cracking in annealed Type 316 steel at very low oxygen contents even when the chloride is less than 0.1 ppm. Potential-oxygen-chloride maps for annealed Type 316 steel have been obtained that allow the effects of oxygen and chloride contents of waters upon the incidence of cracking to be explained in terms of potential. By appropriate potentiostatic control, cracking may be prevented in waters that promote cracking at open circuit potential, or it may be promoted in waters that prevent cracking at the free corrosion potential. The reasons for the dependence of cracking on potential, and hence water composition, in Type 316 stainless steel will remain obscure until more electrochemical and other data are available.

## 6.4 Effects of Alloy Composition on SCC

First, the general effects of alloy composition (nickel content) are considered. The most well-known curve summarizing the data for the effect of nickel on the chloride SCC of Fe-18Cr alloys is that shown in Fig. 41, as originally reported by Copson [134] and discussed by Wu [135].

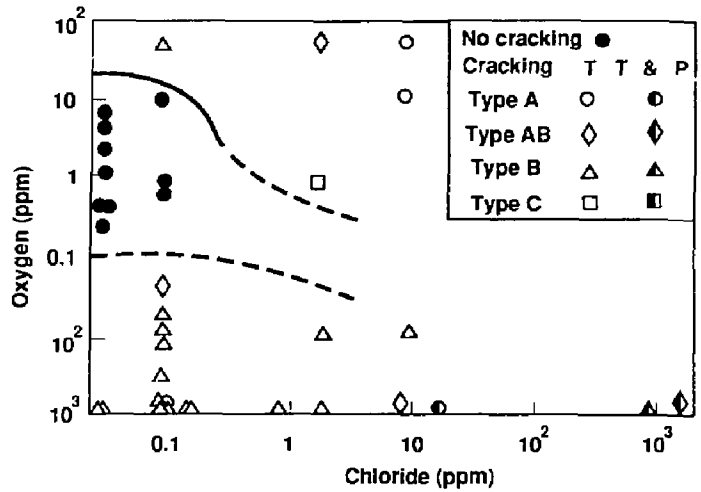


Figure 37. Types of SCC observed in annealed Type 316 stainless steel as a function of oxygen and chloride contents of waters [131]. T, transgranular; P, pitting. Type A, $a_n/a_s = 1$; Type B, $a_n/a_s \geq 2$; Type C, $a_s = 0$; where $a_n$ is the crack length in the necked region, and $a_s$ is the crack length over the uniform gauge length.

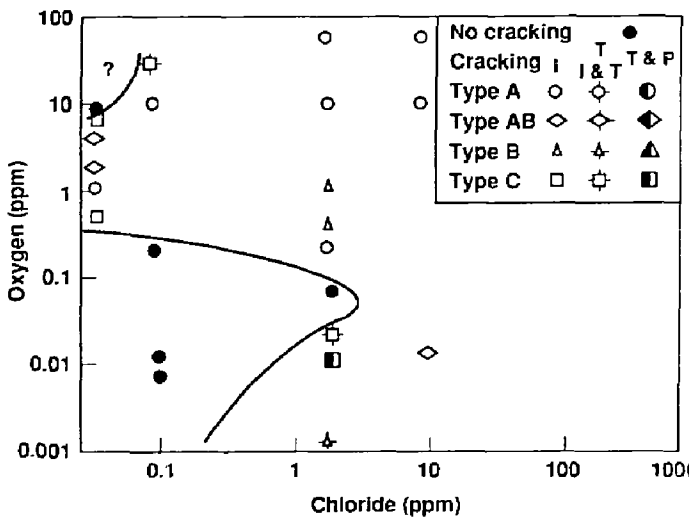


Figure 38. Types of SCC observed in sensitized Type 316 stainless steel as a function of oxygen and chloride contents of waters [131]. I, intergranular; T, transgranular; P, pitting. (See Fig. 37 for meanings of A, B, and C.)

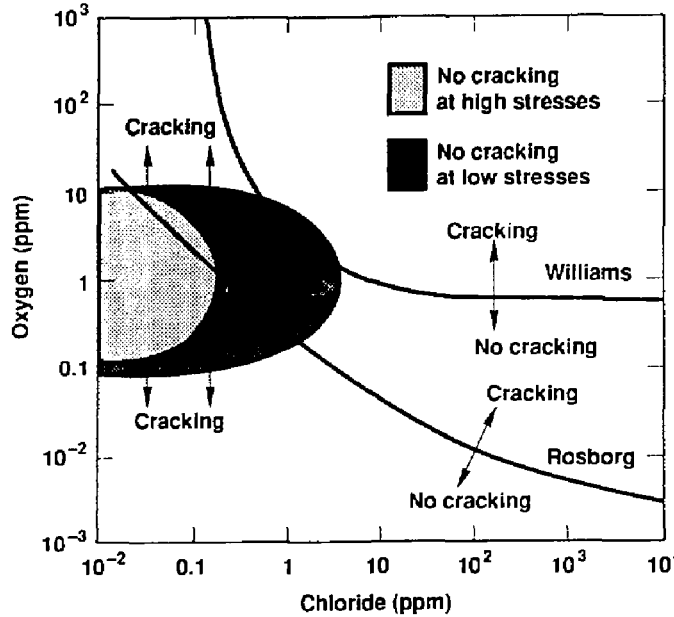


Figure 39. Cracking and no-cracking regimes for annealed Type 316 stainless steel as a function of oxygen and chloride contents of waters [131].

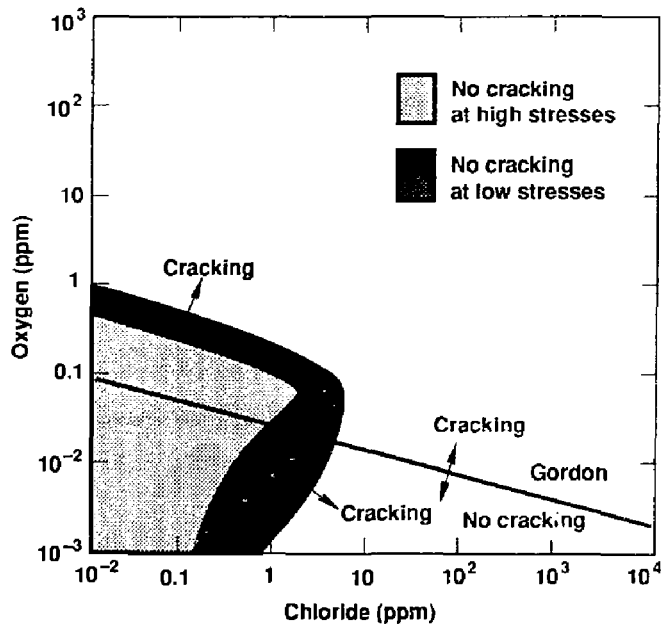


Figure 40. Cracking and no-cracking regimes for sensitized Type 316 stainless steel as a function of oxygen and chloride contents of waters [131].

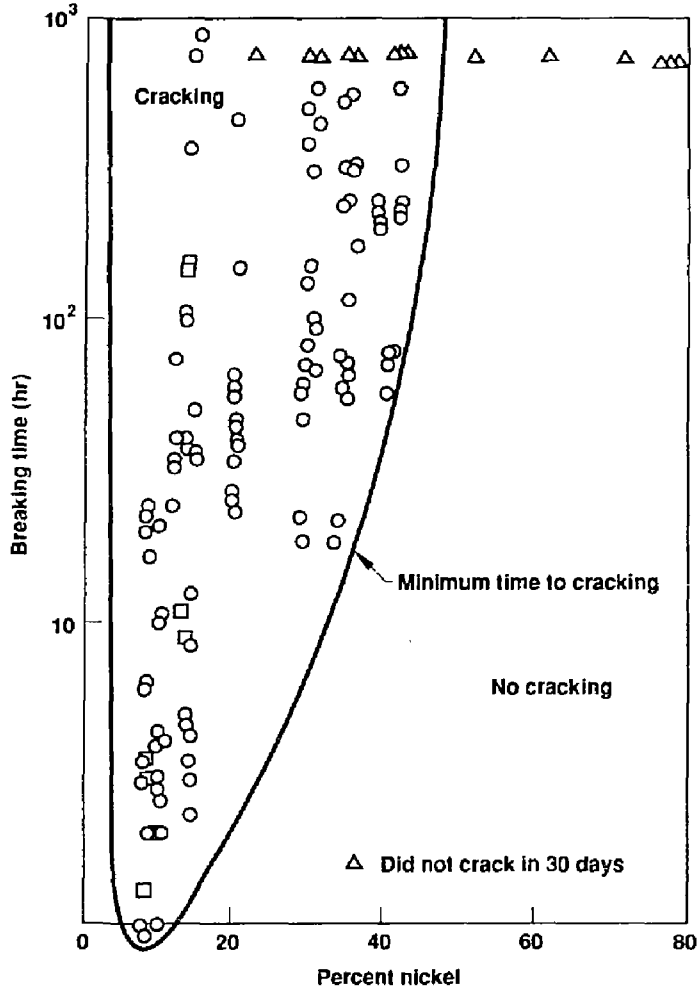


**Figure 41. Effect of increasing the nickel content on the susceptibility of iron-chromium-nickel wires in boiling 42% $MgCl_2$ [134].**

On the basis of the results shown in the figure, it is reasonable to conclude that alloys with more than 45 to 50% nickel should be resistant to chloride cracking. In the case of 12% chromium martensitic steels, the cracking resistance in a chloride environment is dependent upon the final tempering temperature [136]. For example, Type 410 stainless steel tempered at approximately 565°C and above is resistant to cracking in chlorides, and when tempered in the region of 455°C it is very susceptible to cracking in chlorides. However, this could be due to the structural changes brought about by tempering. The second conclusion, that higher-nickel alloys are immune to cracking in chlorides, should be modified, because high-nickel alloys such as Alloy 600 (Inconel) have been reported to crack, even in high-purity water [137]. Staehle reported that Alloy 718 (Inconel), which contains 50–55% nickel, is still susceptible to cracking in chlorides [138]. This may be due to the precipitation of a gamma double-prime phase, $Ni_3(Al,Ti)$, which

leads to reduction of the nickel content of the alloy matrix.

Kowaka et al. conducted studies to develop a SCC-resistant stainless steel as one of the countermeasures against SCC in the piping systems of BWRs [139]. It was found that molybdenum in Type 316 stainless steel has the beneficial effect of increasing SCC resistance by retardation of chromium carbide precipitation at grain boundaries, thereby reducing the tendency toward sensitization. Kowaka et al. believe that molybdenum also promotes the formation of a molybdenum-containing passive film, which is also rich in chromium.

Duckworth et al. performed electrochemical polarization and exposure tests and found that the pitting/crevice corrosion of chemical-plant materials is related to the water content of the hydrochloride salt [140]. Corrosion resistance of Alloys C-276 and 825 is superior to that of Type 316 stainless steel because of increasing amounts of chromium and molybdenum. Kyrolainen [141], Carter et al. [142], Fujii [143], and Maiya [144] have also observed that increased molybdenum content enhances resistance to localized corrosion of 300-series austenitic stainless steels.

Oltra and Colson studied the effect of chromium, nickel, and molybdenum additions on the SCC of austenitic stainless steels in chloride solutions [145]. Using the constant strain rate (CSR) method, various criteria allowed evaluation of these compositional effects on mechanical depassivation, localized dissolution, and repassivation. The investigation was conducted in boiling 44% $MgCl_2$ solution. This study found that nickel decreases the critical elongation rate required for localized depassivation. The density of cracks formed at a given elongation rate was decreased by the addition of molybdenum. Chromium increased the density of crack initiation.

## 6.5 Carbon Content and Sensitization

IGSCC of austenitic stainless steels occurs when these materials are subjected to a sufficiently severe combination of stress, corrosive environment, and sensitization, a term denoting increased susceptibility to attack following a thermal exposure that causes chromium-rich $M_{23}C_6$ carbides to precipitate at grain boundaries.

The phenomenon of sensitization has been the subject of extensive investigation [146–171]. Chromium carbide precipitation in stainless steels occurs in the temperature range from 500 to 850°C (930 to 1560°F), with the rate of precipitation controlled by chromium diffusion [24]. A variety of metallurgical changes have been suggested as mechanisms for sensitization, but it is generally accepted that the principal feature responsible is a narrow chromium-depleted zone adjacent to the carbides. This mechanism was suggested in 1933 by Bain et al. [146] and was further developed by Stawstrom and Hillert [147] and Tedmon et al. [148]. Tedmon et al. suggest that susceptibility to intergranular attack occurs when there is an essentially continuous zone in which the local chromium concentration is below about 13 at.%. Chromium is the element responsible for the formation of stable passive films in stainless steels, and localized depletion of this element adjacent to grain boundaries results in the establishment of an active path (one which does not repassivate) into the bulk material.

The austenite chromium concentration in equilibrium with the $Cr_{23}C_6$ carbide depends most sensitively on the activity coefficient of chromium and on the activity of carbon, as expected from thermodynamic arguments. It is assumed that the diffusing chromium atom reacts with a coordinated carbon atom, which is represented by (6/23)C.

$$Cr + (6/23)C \leftrightarrow CrC_{6/23} \tag{26}$$

The equilibrium constant for this reaction, $K_{CrC}$, is related to the standard free energy of formation for this reaction, $\Delta G^{\circ}_{CrC}$ by Eq. (27).

$$K_{CrC} = \exp(-\Delta G^{\circ}_{CrC}/RT) \tag{27}$$

where $R$ is the universal gas constant and $T$ is the absolute temperature. The equilibrium constant can also be written in terms of the activities of the two reactants, $a_{Cr}$ and $a_C$.

$$K_{CrC} = 1/[a_{Cr} \cdot (a_C)^{6/23}] \tag{28}$$

From Eq. (28), an expression can be derived for the mole fraction of chromium in the depleted region adjacent to the carbide precipitates, $X_{Cr,eq}$:

$$X_{Cr,eq} = 1/K_{CrC}\gamma_{Cr}(a_C)^{6/23} \tag{29}$$

This expression clearly shows that by decreasing the activity of carbon, $a_C$, in the bulk alloy, the mole fraction of chromium in the depleted region is increased, thereby decreasing the tendency of an alloy to undergo sensitization. Of course, this

is why Type 304L is less prone to sensitization than Type 304.

In addition to lowering the carbon content of an austenitic alloy such as Type 304 or 316, it is also possible to add stabilizing elements (strong carbide formers such as titanium and niobium). Note that the above development is an idealization which neglects the possible formation of carbides from iron, nickel, or stabilizing elements. A thermodynamic model has been developed by Fullman that accounts for these effects through the incorporation of chromium equivalency parameters, $\varepsilon_j$ [149]. Sufficient parameters have been included in Fullman's computational model to predict the effects of aluminum, cobalt, copper, manganese, silicon, titanium, vanadium, and tungsten on sensitization. The parameter $\varepsilon_j$ is defined as the change in chromium content with respect to a change in element $j$, $-(\partial P_{Cr}/\partial P_j)_{XCr}$.

Takaku et al. have used constant extension rate tests (CERTs), constant load tests, and cyclic tension tests to study the susceptibility to IGSCC of high-nitrogen, forged stainless steel pipe in 288°C water [150]. Specifically, this study investigated Types 304LN and 316LN stainless steels as alternate materials for BWRs. In general, grain refining is relatively difficult in the processing of forged seamless pipe compared with extruded and rolled pipe, in which a high working ratio can be obtained. Therefore, the decrease in strength due to coarse grains and low carbon content was compensated for by the solid solution strengthening afforded by the addition of nitrogen. As a result, good ductility and toughness as well as strength were obtained by the addition of 0.10 to 0.133% nitrogen, for the forged Types 304LN and 316LN steels.

Takaku et al. also studied low-temperature sensitization and determined that nitrogen addition up to approximately 0.14% was not detrimental to intergranular corrosion resistance. Sensitization could not be induced, provided the carbon content was maintained below 0.02%. This study concluded that Types 316LN and 304LN stainless steel pipes, containing approximately 0.14% nitrogen (maximum), have excellent overall properties, including high SCC resistance in 288°C water, and are suitable for application in BWRs.

The stress corrosion susceptibility and crack growth rate of austenitic stainless steel can be described by the degree of sensitization (DOS) as measured by corrosion tests such as the Strauss or electrochemical potentiokinetic reactivation (EPR) tests [151–153]. EPR was developed by the nuclear power industry for determining degree of sensitization in Types 304, 304L, 316, and 316L austenitic stainless steels. The method is nondestructive and was developed to permit the degree of sensitization to be related to susceptibility to IGSCC in high-purity water environments.

The report by Arey and Lyle [152] describes a test program conducted to evaluate the EPR test as a method for use in chemical plants to determine whether installed austenitic stainless steel components are sensitized. Results from EPR tests on Types 304 and 316 stainless steel samples were compared with results from standard ASTM tests. It was concluded that the EPR test is equivalent to the standard electrolytic oxalic acid etch (EOAE) test (ASTM A 262-81, Practice A) for determining whether a component is or is not sensitized. However, the EPR test provides a quantitative measure of the degree of sensitization of stainless steels, which the EOAE test does not. In this regard, it is to be noted that ASTM Committee G1 is in the process of standardizing the EPR test.

Majidi and Streicher have compared three different electrochemical reactivation tests with etch structures produced in the EOAE test [151]. These nondestructive tests are needed to evaluate welded stainless steel (Types 304, 304L) pipes and other plant equipment for susceptibility to intergranular attack. Sensitization associated with precipitates of chromium carbides at grain boundaries can make these materials subject to intergranular attack in acids and, in particular, to IGSCC in high-temperature water (289°C) in boiling-water nuclear reactor power plants.

In the first of the two older reactivation tests investigated by Majidi and Streicher [151], sensitization is detected by the electrical charge generated during reactivation. In the second, sensitization is measured by the ratio of maximum currents generated by a prior anodic loop and the reactivation loop. A third, simpler reactivation method based on a measurement of the maximum current generated during reactivation is proposed. If the objective of the field tests, which are to be carried out with portable equipment, is to distinguish between nonsensitized and sensitized material, this can be accomplished most simply, most rapidly, and at lowest cost by an evaluation of oxalic acid etch structures.

Clark has extended the EPR technique to characterize weld heat-affected zones (HAZs) and to correlate degree of sensitization with IGSCC

resistance [153]. Current studies are directed toward establishing procedures for, and qualifying, a technique to obtain EPR measurements in situ on reactor components.

In addition to EPR, constant extension rate testing (CERT) has been used to study sensitization effects in 300-series stainless steels. Note that CERT is also known as SSRT. For example, Povich and Broecker have used CERT in an attempt to study SCC in high-temperature (288°C), high-pressure (1500 psi) water that contained 8 ppm oxygen [154]. The alloys evaluated included Types 304, 304L, 316, 316L, 347, and XM-19 (Nitronic 50). Attempts were made to determine the effects of solution annealing (SA), furnace sensitization (FS), and shot peening (SP). SA was done at 1100°C for 30 min in argon; samples were quenched in water. FS was done at 600°C for 24 hr in argon; samples were quenched in argon. The strain rate used in the CERT tests was approximately $1.33 \times 10^{-4}$ $min^{-1}$. The work required for fracture was then determined by integrating the area under stress-strain curves (Figs. 42 and 43). From this quantity, a CERT index (CI) is defined: CI = the work required to fracture a sample divided by the work required to fracture a reference sample. Since SA samples failed in a ductile mode and never by SCC, SA samples were used as the reference. Thus, a CI of unity indicates no SCC tendency and a CI of less than unity indicates that some SCC has occurred.

These investigators concluded that in the SA condition, only Type 304 exhibited SCC. The mode of cracking was transgranular (TG). The fracture surface was about 15% TG and 85% ductile. In the FS condition, Type 304 exhibited

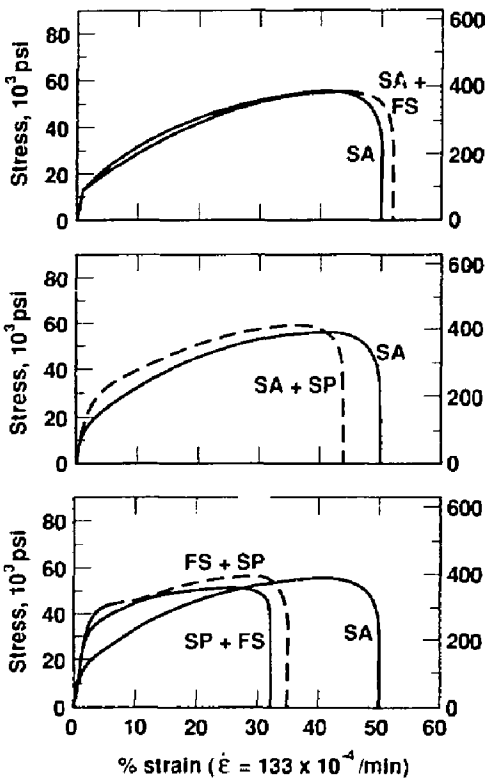


Figure 42. CERT stress-strain results for Type 304L stainless steel in air-saturated water at 288°C [154]. SA, solution annealed; FS, furnace-sensitized; SP, shot peened.

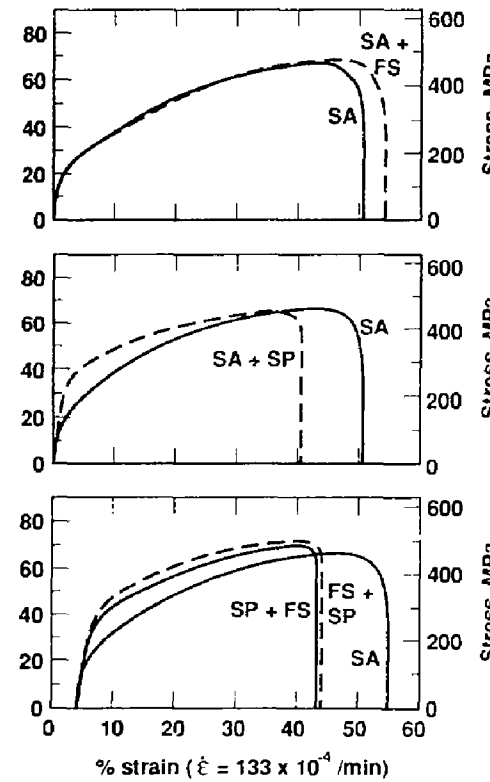


Figure 43. CERT stress-strain results for Type 316L stainless steel in air-saturated water at 288°C [154].

significant intergranular (IG) SCC. There were also signs of TG cracking near the surface. This suggests a TG crack initiation mechanism followed by IG crack propagation. The fracture surface was about 45% IG, 5% TG, and 50% ductile. Other alloys (Types 304L, 316, 316L, 347, and XM-19) exhibited only ductile fracture in the SA and FS conditions (no IGSCC or TGSCC was observed). The CIs for alloys in the FS condition are shown in Fig. 44 and range from approximately 1.1 for Type XM-19 to 0.6 for Type 304.

In the SP condition, all alloys exhibited SCC. Significant TGSCC was exhibited in the case of Type 304; the fracture surface was about 50% TG and 50% ductile. Some degree of TGSCC was also observed in Types 304L, 316, 316L, and 347. Type XM-19 exhibited only secondary surface cracking; however, the cracks did not propagate. The CIs for alloys in the SP condition are shown in Fig. 45 and range from approximately 0.95 for Type XM-19 to 0.7 for Type 304.

For the FS + SP condition, the FS heat treatment preceded the SP. Both TGSCC and IGSCC were observed for Type 304 in the FS + SP condition. In contrast, significant TGSCC and no IGSCC were observed in Types 304L and 347. The absence of IGSCC suggests that there was no grain-boundary sensitization in either Type 304L or 347. No SCC was observed in Types 316, 316L, and XM-19. The CIs for alloys in the FS + SP condition are shown in Fig. 46 and range from approximately 0.95 for Type XM-19 to 0.6 for Type 304.

For the SP + FS condition, SP preceded the FS heat treatment. TGSCC seemed to initiate IGSCC in Type 304. TGSCC and IGSCC were both observed in Types 304L and 316. Only TGSCC was observed in Type 347. There was very little indication of SCC in Types 316L and XM-19. The CIs for alloys in the SP + FS condition are shown in Fig. 47 and range from approximately 0.9 for Type XM-19 to 0.4 for Type 304. Clearly, SCC effects were most severe for alloys in the SP + FS condition.

Sensitization effects have been observed and reported in Types 304 and 316 stainless steels by numerous investigators. For example, Kowaka et al. also found that a decrease in the carbon markedly reduces the SCC susceptibility of Type 316 stainless steel in high-temperature water [155]. A carbon content of less than 0.02% is particularly preferable from the viewpoint of superior SCC resistance. This group also found that additions of nitrogen of less than 0.02% are preferable from the viewpoint of superior SCC resistance. Additions of nitrogen of less than 0.12% or the presence of phosphorus and sulfur at impurity levels have no detrimental effect on SCC in high-temperature water.

Kudo et al. have studied the corrosion resistance of as-rolled Types 304 and 316 stainless steels for cladding [156]. The effect of several

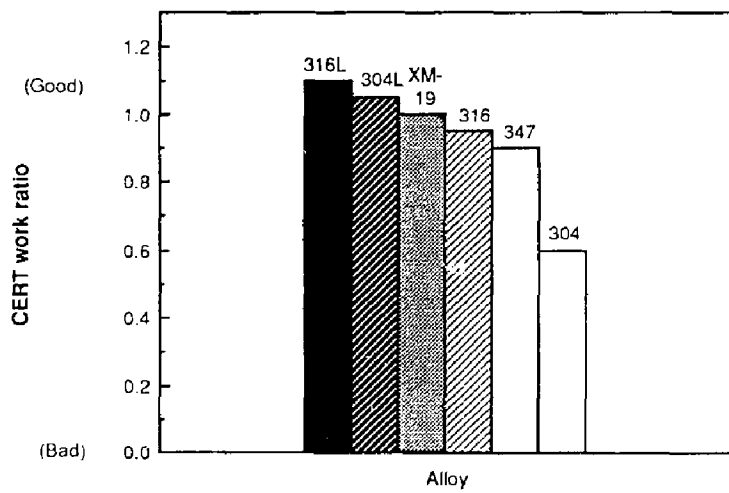


**Figure 44. Effect of furnace sensitization on CERT work ratios for various alloys in air-saturated water at 288°C [154].**

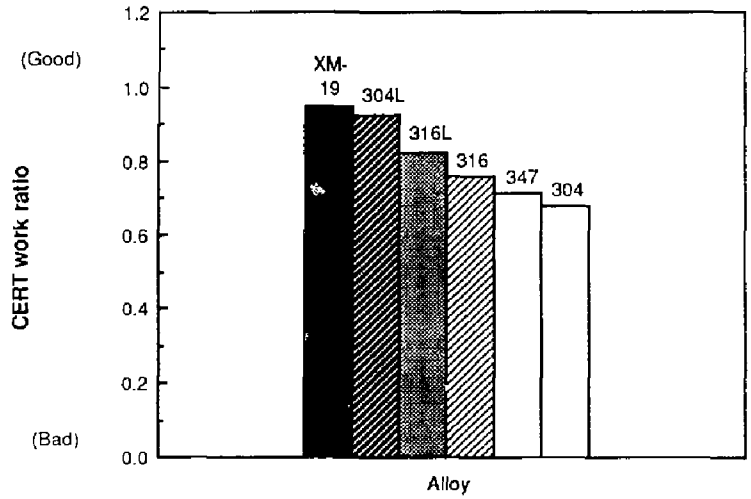


**Figure 45. Effect of shot peening on CERT work ratios for various alloys in air-saturated water at 288°C [154].**

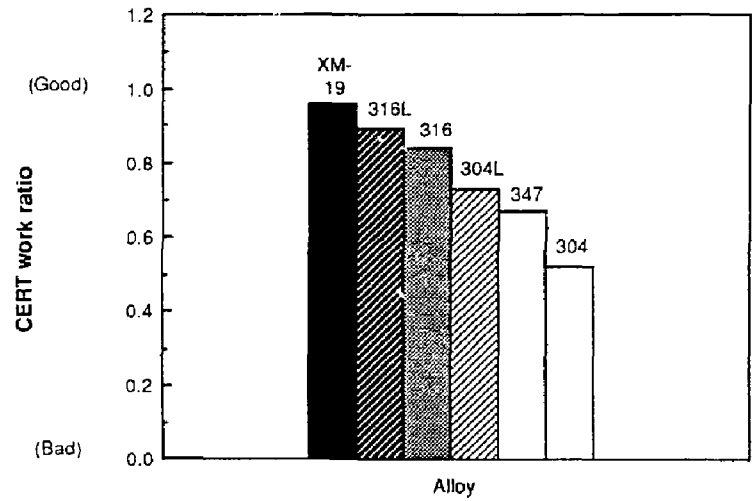


**Figure 46. Effect of furnace sensitization followed by shot peening on CERT work ratios for various alloys in air-saturated water at 288°C [154].**

factors on the corrosion resistance of as-rolled Types 304 and 316 stainless steels for clad use was investigated. No intergranular corrosion occurred on steel with a carbon content below 0.02%. However, long-time heat treatment for stress relief around 650°C caused deterioration of the general corrosion resistance of the steel in acids. In order to maintain the resistance of the alloy to general corrosion, Kudo et al. found that it is desirable to reduce the carbon content below 0.01%. The finishing temperature for hot rolling had no significant effect on the corrosion

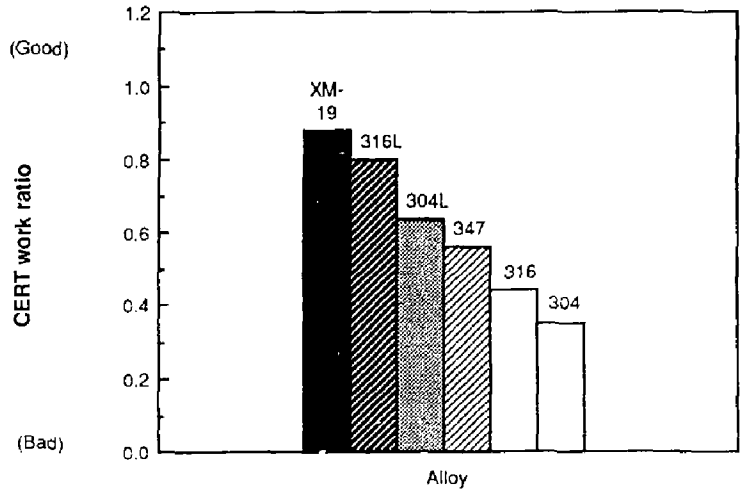


**Figure 47. Effect of shot peening followed by furnace sensitization on CERT work ratios for various alloys in air-saturated water at 288°C [154].**

resistance of steel with carbon content below 0.02%, and the crevice corrosion and SCC resistance of the steel are not inferior to those of solution-treated steels. Carbide precipitation of as-rolled steels was accelerated as compared with that of solution-treated steels.

Kass et al. studied the SCC of welded Type 304 stainless steel under cyclic loading [157]. This study found that decreasing the carbon content of welded Type 304 stainless steel results in a marked resistance to IGSCC in cyclic loading tests. Type 304L is superior to Type 304 in regard to IGSCC.

Davison et al. reviewed the literature on stainless steels used in heat exchanger applications [158]. They found that the opportunity for intergranular attack is readily eliminated by the selection of low-carbon or stabilized grades. Although it is always recommended that design eliminate crevices, it is unlikely that crevices can be completely avoided. In all cases, it is prudent to select a grade of stainless steel that will show crevice corrosion resistance for all reasonably anticipated regimes of operation. SCC can be avoided by the selection of ferritic, duplex, or highly alloyed austenitic grades. Alternatively, grades especially sensitive to SCC, such as Types 304 and 316L, may be used when precautions are taken to eliminate one or more of the factors of SCC, namely stress, chloride, and temperature. Davison et al. found that for high temperature, the microalloyed austenitic stainless steel Type 253MA provided creep resistance and oxidation resistance superior to those of Type 310. These properties are achieved at a lower total alloy content, thereby reducing cost and suppressing undesirable reactions.

Finally, it is important to note that alloys such as Alloys 825, 625, and 600 have actually shown improved corrosion resistance at grain-boundaries after cold working and heat treatment [159]. For example, samples of these mater-ials were cold-drawn to 47% reduction, then heat-treated at 850°C for 1 hr and 650°C for 1 hr. The depth of grain-boundary penetration into heat-treated specimens was approximately 3 μm after 120 hr of exposure to boiling $HNO_3$, compared with 390 μm of penetration without the heat treatment. These data indicate that Alloy 825 does not undergo sensitization.

## 6.6 Effect of Grain-Boundary Segregation on SCC

Grain-boundary segregation of various impurities, including phosphorus, sulfur, carbon, silicon, and nitrogen, has been reported in austenitic stainless steels and can produce a grain boundary that is composed of up to 50% impurity

within a 1- to 2-mm thick region [16, 172]. Phosphorus segregation has been shown to cause intergranular corrosion in highly oxidizing solutions, and impurity segregation of phosphorus and perhaps silicon has been suggested as a primary factor in irradiation-assisted SCC, which occurs in the oxidizing in-core environment of light-water reactors [173].

## 6.7 Direct Comparison of SCC and Crevice Corrosion Susceptibilities of the Austenitic Candidates

Asphahani [174] has studied the chloride SCC of all of the austenitic candidate materials in acidic sodium chloride solutions. Chloride SCC of Types 304, 304L, 316, and 316L was observed in dilute NaCl solutions (0.8 to 4%) containing either $H_3PO_4$ (0.2 to 1%) or $CH_3OOH$ (0.5%). For example, SCC of these austenitic stainless steels could be induced by 10 days of exposure to a solution containing 0.8% NaCl and 0.2% $H_3PO_4$ at a temperature of 141°C. Pitting and crevice corrosion were predominant in solutions containing acetic acid.

In sharp contrast to the 300-series stainless steels, Asphahani found that the austenitic stainless alloys with higher nickel content, including Alloy 20Cb-3 (Carpenter), Alloy 825, and Alloy 20-Mod (Haynes), are very resistant to chloride stress cracking. However, some pitting and crevice corrosion of these materials were observed, with the exception of Alloy 20-Mod. Asphahani found that the high-performance nickel-based alloys, Alloys G and C-276, show excellent resistance to chloride stress cracking and to localized corrosive attack. The compositions of the alloys investigated by Asphahani are summarized in Table 8. Figure 48 is a graphic comparison of the compositions of Type 304L, Type 316L, and Alloy 825 extracted from Table 8.

The SCC tests were conducted on U-bend specimens approximately 133 × 13 × 3 mm in size. Each specimen was deformed around a 25-mm mandrel and then further stressed by straining its ends (tightening a nut and bolt) to a final span of 12 mm. The imposed stress depended on the yield strength of the material, and no effort was made to calculate the exact value of the applied stress. Samples were exposed to the acidic sodium chloride solutions at 141°C in sealed Alloy C-276 autoclaves.

The following results were obtained after a 1-month exposure to a solution containing 4% NaCl and 1% $H_3PO_4$ [Table 9(a)]. The SCC observed in the 300-series specimens (Types 304, 304L, 316, and 316L) was of the branching, transgranular type (TGSCC). Furthermore, severe crevice corrosion was observed under the nut and the head of the bolt used for stressing these samples. Alloy 20Cb-3 suffered severe pitting and crevice corrosion but no SCC. Alloy 825 showed only slight crevice corrosion and was completely resistant to SCC. Alloys 20-Mod, G, and C-276 all demonstrated outstanding resistance to both localized attack and SCC. In fact, it is interesting to note that Alloy C-276 had been selected as the autoclave material. Similar results were observed in more dilute solutions of sodium chloride and phosphoric acid, except that

Table 8. Nominal compositions of alloys tested (wt%).

| Alloy | Fe | Ni | Cr | Mo | Mn | Si | Cu | C |
|---|---|---|---|---|---|---|---|---|
| 304 | Bal | 9 | 19 | — | 2[a] | 1[a] | — | 0.05 |
| 304L | Bal | 9 | 19 | — | 2[a] | 1[a] | — | 0.05 |
| 304L | Bal | 9 | 19 | — | 2[a] | 1[a] | — | 0.03[a] |
| 316 | Bal | 12 | 17 | 2.5 | 2[a] | 1[a] | — | 0.05 |
| 316L | Bal | 12 | 17 | 2.5 | 2[a] | 1[a] | — | 0.03[a] |
| 20Cb-3 | Bal | 33 | 20 | 2.5 | 2[a] | 1[a] | 3 | 0.04 |
| 825 | 30 | Bal | 21 | 3 | 1[a] | 0.5[a] | 2 | 0.04 |
| 20-Mod | Bal | 26 | 22 | 5 | 2.5[a] | 1[a] | — | 0.05[a] |
| G | 20 | Bal | 22 | 7 | 1.5 | 1 | 2 | 0.05[a] |
| C-276 | 5 | Bal | 16 | 16 | 1[a] | 0.8[a] | — | 0.02[a] |

[a] Maximum concentration.

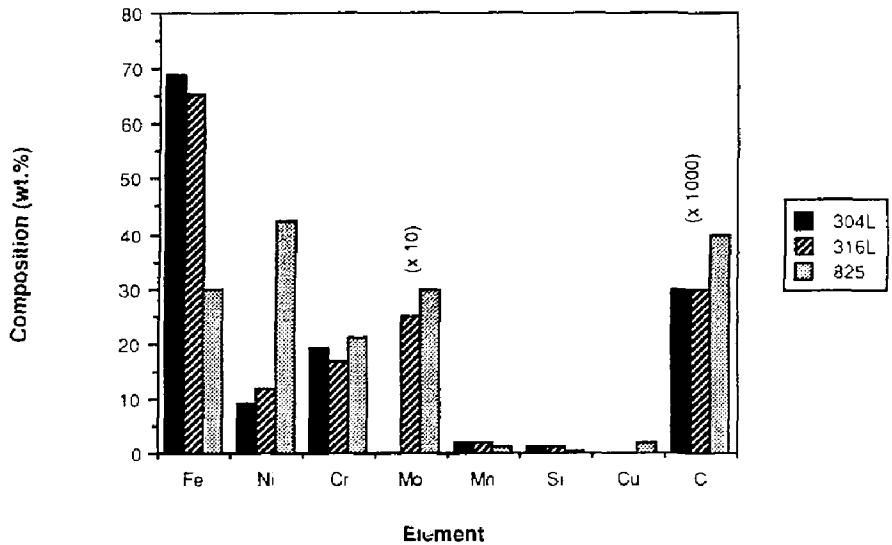


**Figure 48. Nominal compositions for the austenitic candidate materials [174].**

the attack of the Alloy 825 was slightly worse [Table 9(b)].

Asphahani also conducted experiments in a solution of 0.8% NaCl + 0.5% $CH_3COOH$ [Table 9(c)]. Again, branching TGSCC was observed for the 300-series alloys. Acetic acid tended to increase the pitting and crevice corrosion of the specimens. The results of this series of tests indicated that SCC of the Types 304, 304L, 316, and 316L stainless steels was not limited only to the chloride solutions containing $H_3PO_4$.

Finally, Asphahani's results for a solution of NaCl and HCl are presented [Table 9(d)]. SCC was observed in the 300-series alloys after 30 days of exposure; no SCC was observed in Alloy 825 or the alloys with higher nickel content. All specimens with no cracking after the 10-day exposure were further tested for an additional 20-day exposure [Table 9(d)]. The temperature of the container was maintained at 285°C. The container developed a leak at the seal, and the test solution evaporated some time near the end of the testing period.

Table 9(a). U-bend specimens after 1 month in 4% NaCl and 1% $H_3PO_4$ at 141°C.

| Alloy | Corrosion rate (mm/yr) | Localized corrosion | SCC |
|---|---|---|---|
| 304 | 0.15 | Crevice corrosion | Yes |
| 304L | 0.13 | Crevice corrosion | Yes |
| 316 | 0.11 | Crevice corrosion | Yes |
| 316L | 0.04 | Slight attack | Yes |
| 20Cb-3 | 0.07 | Crevice corrosion and pitting | No |
| 825 | <0.01 | Slight attack | No |
| 20-Mod | <0.01 | No attack | No |
| G | <0.01 | No attack | No |
| C-276 | <0.01 | No attack | No |

Table 9(b). U-bends after 1 month in 0.8% NaCl and 0.2% $H_3PO_4$ at 141°C.

| Alloy | Corrosion rate (mm/yr) | Localized corrosion | SCC |
|---|---|---|---|
| 304 | 0.14[a] | Crevice corrosion | Yes |
| 304L | 0.03[a] | Crevice corrosion | Yes |
| 316 | 0.02[a] | Crevice corrosion | Yes |
| 316L | 0.01[a] | Slight attack | Yes |
| 20Cb-3 | 0.07 | Crevice corrosion and pitting | No |
| 825 | 0.03 | Crevice corrosion and pitting | No |
| 20-Mod | <0.01 | No attack | No |
| G | <0.01 | No attack | No |
| C-276 | <0.01 | No attack | No |

[a] Specimen removed after 10 days.

Table 9(c). U-bend specimens after 1 month in 0.8% NaCl and 0.5% $CH_3COOH$ AT 141°C.

| Alloy | Corrosion rate (mm/yr) | Localized corrosion | SCC |
|---|---|---|---|
| 304 | 0.03 | Severe pitting | Yes |
| 304L | 0.02 | Severe pitting | Yes |
| 316 | 0.01 | Severe pitting | Yes |
| 316L | <0.01 | Pitting | Yes[a] |
| 20Cb-3 | <0.01 | No attack | No |
| 825 | <0.01 | No attack | No |
| 20-Mod | <0.01 | No attack | No |
| G | <0.01 | No attack | No |
| C-276 | <0.01 | No attack | No |

[a] One specimen out of two cracked.

Table 9(d). U-bend specimens in 0.8% NaCl and HCl (pH 2.2) at 141°C.

| Alloy | 10-day exposure | 30-day exposure |
|---|---|---|
| 304 | No cracking | Cracking |
| 304L | No cracking | Cracking |
| 316 | No cracking | Cracking |
| 316L | No cracking | Cracking |
| 20Cb-3 | No cracking | No cracking |
| 825 | No cracking | No cracking |
| 20-Mod | No cracking | No cracking |
| G | No cracking | No cracking |
| C-276 | No cracking | No cracking |

As Asphahani noted, it is surprising that phosphoric or acetic acids cause localized corrosion and SCC of stainless steels in dilute chloride solutions. Phosphates and acetates have been known to inhibit corrosion and SCC. For example, $NaH_2PO_4$ additions to NaCl solutions inhibit the SCC of high-strength, low-alloy steels [175]. Similarly, $CH_3COOH$ additions to boiling $MgCl_2$ solutions have proven effective in inhibiting the SCC of 18-8 stainless steel [176].

Asphahani also performed experiments in which Type 316L specimens were galvanically coupled to other alloys close in performance or more noble (Types 304L and 316, Alloys 20Cb-3 and G, etc.). The corrosion potential, $E_{corr}$, of Type 316L was shifted to more noble values above the critical pitting potential, $E_c$, and within the susceptible potential range for cracking.

The exceptional corrosion resistance of the high-performance nickel-based alloys is believed to be due to both their high nickel and high molybdenum contents. For example, not only are Alloy G and C-276 immune to SCC in the acidic sodium chloride solutions discussed here, they are also immune to SCC in boiling 42% $MgCl_2$ solutions. While carbon content and molybdenum addition do not improve the performance of the 300-series stainless steels, increasing the molybdenum content of the high-chromium, high-nickel stainless alloys, such as 20Cb-3, Alloy 825, and 20-Mod plays a definite role in improving their resistance to localized attack and SCC. This finding is consistent with the discussion above.

# 7. Unusual Environmental Effects in the Repository: Gamma Irradiation and Biological Corrosion

The metal barriers used for high-level nuclear wastes will be exposed to high fluxes of gamma radiation. Therefore, the effect of gamma radiation on SCC must be considered. Furthermore, the barriers will have to remain intact for several thousand years. Consequently, it is also necessary to consider other corrosion scenarios that may arise over extended periods of time, such as *microbiologically induced corrosion (MIC)*.

## 7.1 General Effects of Gamma Irradiation

It has been known for many years that the irradiation of liquid water by gamma rays produces ionic, free radical, and molecular products. Because of the fast reaction of ionic species, the "primary products" of water radiolysis are considered to be $H^+$, $OH^-$, $e^-_{aq}$, $HO_2$, $H_2O_2$, and $H_2$, where the first four are called the radical products, and the last two are the molecular products. The radical products are very chemically reactive with the molecular products or with dissolved solutes in the water, if present. If oxygen is dissolved in the water, both H and $e^-_{aq}$ react with it rapidly to form $HO_2$ and $O_2^-$, respectively. At pH near neutral, the $HO_2$ ionizes rapidly to form $H^+$ and $O_2^-$. The result of all these reactions is that in irradiated oxygenated water, one has steady-state concentrations of the oxidizing species OH, $O_2^-$, and $H_2O_2$. One also has a low steady-state concentration of $H_2$ (which is effectively inert to stainless steel at temperatures at which water is liquid).

When one inserts an electrode into such an irradiated solution, one observes a corrosion potential, $E_{corr}$, which reflects the composite of the reactions of all the reactive species in the solution with the material of the electrode. Several research groups, including Glass et al. [177, 178], Marsh et al. [179], Kim and Oriani [180, 181], Clarke and Jacobs [182], and Ruther et al. [183] have observed that $E_{corr}$ of stainless steel shifts to more positive (noble) values in the presence of gamma irradiation.

The initial understanding of this radiolytic effect on corrosion potential is attributed to Glass et al. of the Nevada Nuclear Waste Storage Investigations Project. This study found that the positive shift in $E_{corr}$ was composed of three parts. The major part was found to persist after the irradiation was terminated, but most of it was removed if the irradiated solution was replaced by a new solution. This part was attributed to hydrogen peroxide, $H_2O_2$. The part that remained after the solution was changed was attributed to permanent changes in the oxide layer on the stainless steel. The third part was only present during irradiation and was attributed to the transient radical species.

According to Glass et al., the following anodic and cathodic reactions are believed to be of major importance in determining the corrosion potentials of austenitic stainless steels under gamma irradiation [177]. First, the cathodic reactions are:

$$H_2O_2 \rightarrow 2(\cdot OH)_{ADS} \quad (30)$$

$$(\cdot OH)_{ADS} + e^- \leftrightarrow OH^- \quad (31)$$

$$O_2 + 2H_2O + 4e^- \rightarrow 4OH^- \quad (32)$$

$$O_2^- + H_2O + e^- \rightarrow HO_2^- + OH^- \quad (33)$$

$$HO_2^- + H_2O + 2e^- \rightarrow 3OH^- \quad (34)$$

where ADS denotes adsorbed species. Equation (30), not given explicitly by Glass et al., has been included for completeness. The reactions represented by Eqs. (33) and (34) are believed to be relatively less important than reactions represented by Eqs. (31) and (32). The cathodic reactions are:

$$Fe \rightarrow Fe^{2+} + 2e^- \quad (35)$$

$$Cr \rightarrow Cr^{3+} + 3e^- \quad (36)$$

$$Ni \rightarrow Ni^{2+} + 2e^- \quad (37)$$

The coupling of the cathodic processes with metal dissolution reactions results in the observed mixed corrosion potential, $E_{corr}$. The effect of a single radiolysis product such as hydrogen peroxide on the corrosion potential can be understood by comparing its reduction potential with that of the usual depolarizer, dissolved oxygen (DO) [184].

$$H_2O_2 + 2H^+ + 2e^- \rightarrow 2H_2O \text{ (1535 mV, SCE)} \quad (38)$$

$$O_2 + 4H^+ + 4e^- \rightarrow 2H_2O \text{ (988 mV, SCE)} \quad (39)$$

Preferential reduction of hydrogen peroxide would shift the corrosion potential to more positive values; it is evident that hydrogen peroxide is a more effective depolarizer than oxygen. Such changes in the corrosion potential tend to decrease the difference $E_c - E_{corr}$, thereby decreasing the material's resistance to pitting and SCC. Note that Glass et al. found that gamma irradiation had little effect on the pitting potential [177].

Marsh et al. found increases in $E_{corr}$ for both oxygenated and de-oxygenated solutions, but the de-oxygenated solutions responded more slowly [179]. This study concluded that the increase was caused by oxidizing radicals and molecular species, and that the presence of oxygen enhances the production of oxidizing products. Furthermore, this study found that irradiation inhibits the initiation of localized corrosion at relatively low electrode potentials. It was tentatively suggested that this inhibition occurs because the adsorption of oxidizing radiolysis products enhances the protective properties of the passivate oxide film.

The primary effect of gamma irradiation is probably to form the free radicals $H^+$ and $OH^-$ [180, 181]. These free radicals also react with one another to some extent to form $H_2$, $O_2$, and $H_2O_2$. Some of the radicals escape from the radiolysis zone and react with dissolved $H_2$, $O_2$, and $H_2O_2$ molecules in the solution to lead to the reformation of water. This concept is not original with Kim and Oriani. Radiation chemistry is discussed in detail by Spinks and Wood's [185].

## 7.2 Effects of Gamma Irradiation on SCC of Stainless Steels

Intergranular stress corrosion cracking (IGSCC) was observed in 1967 in the heat-affected zone (HAZ) of Type 304 stainless steel piping used in the recirculation circuit of a BWR [186]. Since then, the problem has been found in many reactors of this type.

It is widely recognized that IGSCC occurs in stainless steels when three conditions are simultaneously present: (1) the material must be sensitized, i.e., the concentration of dissolved chromium in the grain boundaries must be depleted to less than 12 wt% by the formation of chromium carbide precipitates, (2) the material must be placed under sufficient tensile stress, and (3) the environment must be sufficiently corrosive to attack the material in the grain boundaries. Since gamma irradiation of aqueous solutions produces several oxidizing and reducing species by radiolysis, it might be expected to affect SCC.

Fujita et al. performed constant extension rate tests (CERTs) on sensitized Type 304 stainless steel with and without exposure to gamma rays in high-temperature water that had been purified by an ion exchanger [186]. The CERT results are shown in Table 10. Two different DO concentrations were investigated: DO < 20 ppb and DO = 8 ppm. The chloride concentrations were

Table 10. Results obtained from CERT tests of Type 304 stainless steel under gamma irradiation.

| Gamma irradiation | DO | Lead time (days) | At fracture | | | |
|---|---|---|---|---|---|---|
| | | | Time (hr) | Elong. (mm) | Strain (%) | Stress ($kg/mm^2$) |
| No | ≤20 ppb | 0 | 109 | 6.54 | 32.7 | 39.9 |
| Yes | ≤20 ppb | 0 | 110 | 6.60 | 33.0 | 39.2 |
| No | ≤20 ppb | 5 | 112 | 6.72 | 33.6 | 39.4 |
| Yes | ≤20 ppb | 5 | 120 | 7.20 | 36.0 | 39.8 |
| No | 8 ppm | 0 | 55 | 3.30 | 16.5 | 30.6 |
| Yes | 8 ppm | 0 | 36 | 2.16 | 10.8 | 22.3 |
| No | 8 ppm | 5 | 112 | 6.72 | 33.6 | 39.7 |
| Yes | 8 ppm | 5 | 119 | 7.14 | 35.7 | 39.0 |

Note: the test environment was highly purified water at 250°C and 50 MPa; the extension rate was $1 \times 10^{-3}$ mm/min.

not reported. The gamma-ray dose rate was $4.5 \times 10^4$ R/hr, the temperature was 250°C, and the flow rate was $2 \times 10^4$ $cm^3$/min, with an autoclave volume of 550 $cm^3$. The samples had been solution heat-treated at 1050°C for 30 min and sensitized at 650°C for 2 hr in vacuum. The strain rates during the tests ranged between $4 \times 10^{-7}$ $s^{-1}$ and $4 \times 10^{-6}$ $s^{-1}$.

Fujita et al. found that under the low-oxygen conditions (< 20 ppb), the specimens failed ductilely whether or not they were gamma-irradiated. The strain at fracture was slightly higher under irradiation, while the maximum stress was about the same. It was therefore concluded that under these conditions the gamma irradiation actually had a slight protective effect. Under the higher-oxygen conditions (8 ppm), Fujita et al. found that specimens that had been pre-oxidized in the test environment for 5 to 10 days without applied load also exhibited ductile failure during subsequent CERT testing, whether or not they were irradiated. In this case, gamma irradiation again gave some increase in the strain at fracture. However, specimens that were not pre-oxidized showed IGSCC both with and without irradiation under the high-DO conditions and had greatly reduced fracture strains. Moreover, in this case, gamma irradiation was deleterious, giving 25 to 34% lower fracture strains.

In 1985 Ishigure et al. reported on an extension of this work to include intermediate values of the oxygen concentration [187]. This study found that the failures were ductile for concentrations up to 200 ppb of oxygen. At 500 ppb and above, IGSCC was observed. The effect of gamma irradiation was slightly beneficial (i.e., higher fracture strains were found) for oxygen concentrations up to and including 500 ppb, but the irradiation produced lower fracture strain at 8 ppm oxygen, as mentioned above. Ishigure et al. also observed that the addition of $H_2O_2$ with irradiation increased the fracture strain. Addition of $H_2$ improved (increased) the fracture strain without irradiation, and was even more beneficial with irradiation.

Kuribayashi and Okabayashi conducted experiments to examine the influence of gamma irradiation on SCC of sensitized austenitic stainless steel [188]. The SCC tests were conducted with gamma irradiation in boiling 12% NaCl solution, pH adjusted to 3 with HCl, and a high-temperature pure water (230°C). In this study, it was found that gamma irradiation increased IGSCC susceptibility of sensitized Type 304 stainless steel in the acidic NaCl environment. Ferric ions ($Fe^{3+}$) are radiolytically formed by gamma irradiation from ferrous ions ($Fe^{2+}$) in acid solution, and this phenomenon is the widely known principle of the Fricke dosimeter. The ferric ions may act as a strong oxidizing agent and may increase the susceptibility to IGSCC in the boiling acid chloride solution. Furthermore, gamma radiation also increased IGSCC susceptibility of sensitized Type 304 steel in high-temperature oxygenated pure water.

Furuya et al. reported experiments on the effects of gamma irradiation on SCC in boiling deionized water [46]. The alloys studied were Types 304, 304L, 304EL, and 309S stainless steels, Alloys 825, 600, and 625, and SMA 50 (a low-alloy steel containing small amounts of manganese and copper). The materials were sensitized by heat

treatments at 700°C for 100 min and then at 500°C for 24 hr. The samples were formed into double U-bends, some with V-notches. All the materials were included in the first test series, which lasted 180 days. Furuya et al. found that the samples made of Types 304, 304L, and 309S exhibited SCC, while the others (Type 304EL, Alloys 825, 600, and 625, and SMA 50) did not. This was found to be the case both with and without gamma irradiation, but the number of failures with Type 304, particularly at V-notches, was much greater for the irradiated samples. The chloride concentrations in the first series were between 0.2 and 3.8 ppm.

Furuya et al. performed a second series of tests on Type 304 only, in which care was taken to keep the chloride and DO at lower concentrations by using a closed refluxing system rather than a flowing system. In this series, which ran for 60 days, IGSCC was observed on the irradiated samples but not on the unirradiated ones. The chloride concentrations were less than 0.7 ppm in this series. The oxygen concentrations were not reported. Figure 49 illustrates the effects of gamma irradiation on SCC observed by Furuya et al.

It is difficult to harmonize the results of Fujita et al. and Ishigure et al. with those of Furuya et al. Fujita et al. found a slight beneficial effect of gamma irradiation on IGSCC in sensitized Type 304 stainless steel when the oxygen concentration was minimized, while Furuya et al. found a strong deleterious effect under conditions that presumably minimized the oxygen concentration. However, the first group used liquid water at 250°C, while the second group used boiling water, presumably at 100°C. Also, since the first group did not specify the chloride concentration, it is difficult to ascertain that the same chemical conditions prevailed in the two sets of experiments. It can be concluded though, that both groups observed effects of gamma irradiation on IGSCC in sensitized Type 304 stainless steel under some conditions. Note that Kuribayashi and Okabayashi also observed an enhancement of SCC by gamma irradiation in acidic NaCl solutions and in oxygenated water. In contrast to the deleterious effects of gamma irradiation on Type 304 stainless steel, Furuya et al. found that gamma irradiation had little effect on Alloy 825.

Kikuchi et al. performed SCC experiments using solutions of $O_2$ and $H_2O_2$ without irradiation [189].

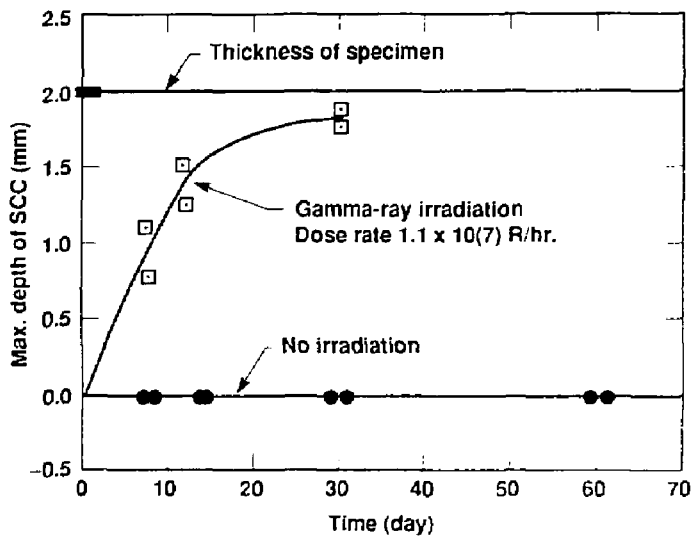


**Figure 49. Effects of gamma-ray irradiation on SCC failures of sensitized Type 304 stainless steel [47].**

In this study, it was found that $H_2O_2$ can effectively inhibit the formation of IGSCC caused by DO, and that the threshold concentration of $H_2O_2$ needed to inhibit IGSCC increases with increased concentration of dissolved $O_2$.

It should be noted that nuclear-waste containers will not be subjected to significant fluences of neutrons. However, it is of interest that a program has been conducted by Clarke and Jacobs to study the effects of prior neutron irradiation on the effects of gamma irradiation on the SCC behavior of Type 304 stainless steel in high-temperature water [182]. A series of CERT tests were completed at 288°C in oxygenated water on annealed materials machined from neutron-irradiated reactor components. These tests confirmed that high fluences of prior neutron irradiation promote IGSCC in Type 304 stainless steel, and that a threshold fluence exists for high plastic-strain levels at about $5 \times 10^{20}$ n/cm$^2$ ($E > 1$ MeV). An experiment was also conducted to measure the electrochemical potential (ECP) of stainless steel in oxygenated 288°C water as a radiation source was moved closer to the electrode surface.

On the basis of the results developed during this study, the following generalized conclusions were made. First, the results of the CERT testing of annealed and irradiated Type 304 stainless steel material reveal an irradiation effect on IGSCC resistance. A sample irradiated to $3 \times 10^{21}$ n/cm$^2$ ($E > 1$ MeV) and then CERT-tested in 288°C water with 32 to 36 mg/l DO failed entirely by IGSCC. A companion specimen irradiated to $1 \times 10^{18}$ n/cm$^2$ and tested identically to the above failed in a ductile mode. This result is highly significant, as similar testing of nonirradiated, annealed Type 304 stainless steel in high-temperature oxygenated water had never produced IGSCC in this material. Second, testing of reactor-irradiated tube material, after high in-reactor fluence accumulation, confirmed the irradiation-assisted SCC effect noted for the plate material. In addition, CERT tests conducted on the absorber-tube samples indicated a threshold neutron fluence of about $5 \times 10^{20}$ n/cm$^2$ for irradiation-assisted SCC at high strain levels. Third, a 25-fold increase in strain rate, from $4 \times 10^{-6}$/min to $1 \times 10^{-4}$/min, can reduce the amount of IGSCC in high-fluence specimens from 100 to 40%. James [190] discussed the effects of gamma irradiation on various candidate materials for high-level radioactive waste storage and found that irradiation had very little influence on SCC resistance.

Finally, it was found that the ECP of stainless steel became more noble (150 mV) over the steady-state potential as a gamma-radiation source was moved very close to the electrode. This finding is consistent with the work of Glass et al. [177, 178]. The significance of this finding is that the effect of gamma irradiation on the water close to the electrode surface is to move the ECP into a region where IGSCC is more likely to occur. However, this high gamma-radiation level cannot be the sole contributor to IGSCC initiation and propagation since a sample exposed to a low neutron fluence ($1 \times 10^{18}$ n/cm$^2$) failed ductilely when CERT-tested in a manner that produces IGSCC in high-fluence material (>$5 \times 10^{20}$ n/cm$^2$). It is apparently necessary that the material's microstructure be made susceptible to intergranular attack, whether by thermal treatment (sensitization), or by high levels of neutron irradiation. The effect of neutron irradiation is to cause displacement of atoms and radiation-enhanced diffusion. These processes have been found to change the chemical composition at the grain boundaries.

## 7.3 Effects of Biological Growth on Pitting and LC

Microbiologically induced (or influenced) corrosion (MIC) has been observed and studied since the 1800s [191]. Observations of MIC on stainless steels have been reported several times since the 1970s [Kobrin, 1976; Tatnall, 1981a; Tatnall, 1981b; Pope et al., 1982; Puckorius, 1983; Gorelov and Talybly, 1983; Pope et al., 1984; Das and Mishra, 1986; Silva et al., 1986; Kobrin 1986; Thorpe, 1986 and 1987; Pope, 1984; and Hayner et al., 1984] [192–205]. The possibility of the occurrence of MIC in deep geological repositories for high-level nuclear waste has been discussed by West and McKinley [206].

It is clear from the literature that a variety of microbes are capable of inducing corrosion in stainless steels under appropriate conditions. Microbial crevice, pitting, and "gouging" types of corrosion have been seen, as well as SCC. Sometimes small pits are found to lead to large subsurface cavities in the metal. MIC has been found on Types 304, 304L, E308, 316, and 316L stainless steels, especially on welds. Also, Kobrin blamed MIC for some corrosion failures on nickel and Alloy B (Hastelloy) [192]. Pope [207], in reviewing the work up to 1984, stated: "No cases

could be made for MIC of these materials [higher nickel-chromium alloys and titanium] from the available literature. All are resistant to the types of MIC familiar to the scientific and engineering communities at the present time."

Most observed cases of MIC on stainless steels have occurred in warm water containing an abundance of organic material, sulfur compounds, or both. Examples are often reported from the paper industry, the oil and chemical industries, and from sewage systems. Cooling systems using river water or seawater have also experienced MIC problems, as have hydrotesting operations using well water.

In cases in which MIC has been observed on stainless steel in relatively pure water, the most common culprits have been the bacteria *Gallionella* and *Sphaerotilis*. These aerobic bacteria are able to oxidize ferrous to ferric ions or manganous to manganic ions. They co-accumulate chloride ions from the water to achieve charge neutralization, and the resulting solutions are corrosive to stainless steel, particularly to the delta-ferrite phase in the weld metal.

In assessing the likelihood of the occurrence of MIC in a high-level nuclear-waste repository in tuff, it must be noted that the conditions there are expected to be unfavorable for the survival of bacteria. These conditions include high temperature; dryness; lack of light; scarcity of electron donor materials such as organics, molecular hydrogen, ammonia, nitrate, or ferrous iron in the natural tuff environment; and the simultaneous presence of oxygen and high gamma-ray dose rates near the waste containers.

Temperatures near the containers may range as high as 250°C, although some may be below the boiling point of water. Most bacteria cannot survive heating above the boiling point, although some have been found to survive at above 250°C ("black smoker" bacteria living in hot sulfurous water vents on the midocean ridges) [208]. Dryness is not favorable for the growth of bacteria, although some can survive it for long periods. Lack of light precludes the growth of photosynthetic species. Without light there must be a chemical energy source, including an electron donor. While the tuff environment lacks a significant source, the metal in the packages could serve as one.

The simultaneous presence of oxygen and high gamma-ray dose rates is very deleterious to bacteria. Oxygen is expected to be present at near the concentration in the atmosphere. Dose rates at the package surfaces will range up to $10^4$ rad/hr. In comparison, the commercial radiation "sterilization" of medical devices and pharmaceuticals is performed with $2.5 \times 10^6$ rad. Hall has found that the sterilization of food for long-term storage requires doses up to $6 \times 10^6$ rad [209]. Christensen has found that even the most resistant known bacterial spores (such as those of Micrococcus radiodurans) can be sterilized with doses of no more than a factor of 2 times this [210]. It must be noted that high dose rates will be present only near the surfaces of the packages, and that they will eventually decay. This decay means that the packages will be objects of concern for corrosion. The predominant gamma emitter is $^{137}Cs$, which has a 30-yr half-life.

In summary, though biological corrosion cannot be totally ruled out, it appears to be very unlikely that a species of bacteria will be found that possesses all the qualities necessary to survive and grow in this environment and also have the capability of corroding stainless steels [197, 211]. No reports of MIC on Alloy 825 have been found for any environment.

## 8. Results and Conclusions

From the survey of degradation modes on uniform corrosion, pitting, crevice corrosion, and SCC in austenitic steels, it is obvious that Alloy 825 is the best austenitic candidate among the three being evaluated. From this survey, it is clear that other materials such as Alloys C-276 and 625 have superior resistance to localized corrosion. However, they are also significantly more expensive than the best candidate material, Alloy 825. Materials such as Alloys C-276 and 625 are being considered by the Alternate Materials Task Group.

The results of the survey can be summarized as follows:

1. All three austenitic candidates (Types 304L and 316L stainless steels and Alloy 825) demonstrated pitting and crevice corrosion in chloride-containing environments.

2. Alloy 825 has greater resistance to pitting and crevice corrosion than either Types 304L or 316L stainless steels.

3. In acidic chloride media, SCC was always observed in Types 304L and 316L.

4. SCC was not reported in the literature for Alloy 825. This does not mean that SCC will not occur in Alloy 825 under other circumstances.

5. Heat treatment at 600°C leads to sensitization of Type 304. This heat treatment does not lead to sensitization of low-carbon alloys such as Types 304L and 316L. Shot peening followed by heat treatment at 600°C does increase SCC in Types 304L and 316L. However, the mode of failure is transgranular, not the intergranular mode that would be expected if the samples were sensitized. No data have been found to indicate sensitization in Alloy 825.

6. Gamma irradiation enhances SCC of Types 304 and 316L under some conditions. However, Alloy 825 shows no change in its resistance to SCC in the presence of gamma irradiation.

7. Though microbiologically induced (or influenced) corrosion, and possible SCC, have been observed for 300-series stainless steels, the nickel-based alloys such as Alloy 825 seem to be immune to such problems.

8. On the basis of the data from the literature on susceptibility to SCC, the candidates are ranked as follows: Alloy 825 (best) > Type 316L > Type 304L (worst).

## 9. Acknowledgments

This work was performed under the auspices of the U.S. Department of Energy by Lawrence Livermore National Laboratory under contract No. W-7405-Eng-48, and was supported by the Yucca Mountain Project. The authors thank Jay C. Cherniak for his editorial assistance.

# 10. References


1. "Disposal of High-Level Radioactive Wastes in Geologic Repositories," Technical Criteria, 10 CFR Part 60, Nuclear Regulatory Agency, Federal Register, Rules and Regulations, Vol. 48, No. 120, Tuesday, June 21, 1983, pp. 28194–28229. HQ2.870302.3019
2. "Environmental Standards for the Management and Disposal of Spent Nuclear Fuel, High-Level and Transuranic Radioactive Wastes," 40 CFR Part 191, Environmental Protection Agency, Federal Register, Rules and Regulations, Vol. 50, No. 192, Thursday, September 19, 1985, pp. 38066–38089. HQ2.870301.5394
3. M. G. Fontana, N. D. Greene, *Corrosion Engineering*, 2nd ed., McGraw-Hill Book Co., New York, 1978. NNA.891018.0176
4. H. H. Uhlig, *Corrosion and Corrosion Control: An Introduction to Corrosion Science and Engineering*, 2nd ed., John Wiley and Sons, New York, 1971. NNA.891018.0177
5. T. Okada, "Halide Nuclei Theory of Pit Initiation in Passive Metals," *Journal of the Electrochemical Society*, Vol. 131, No. 2, 1984, pp. 241–247. NNA.891005.0087
6. T. Okada, "A Theory of Perturbation-Initiated Pitting," *Proceedings of an International Symposium Honoring Professor Marcel Pourbaix on His Eightieth Birthday: Equilibrium Diagrams and Localized Corrosion*, Vol. 84-9, Robert P. Frankenthal, Jerome Kruger, Eds., The Electrochemical Society, Pennington, New Jersey, 1984, pp. 402–431. NNA.891005.0088
7. H. W. Pickering, R. P. Frankenthal, "On the Mechanism of Localized Corrosion of Iron and Stainless Steel: I. Electrochemical Studies," *Journal of the Electrochemical Society*, Vol. 119, No. 10, October 1972, pp. 1297–1304. NNA.891005.0089
8. T. Shibata, T. Takeyama, "Stochastic Theory of Pitting Corrosion," *Corrosion*, Vol. 33, No. 7, July 1977, pp. 243–251. NNA.891005.0090
9. H. J. Engell, N. D. Stolica, "Die Kinetik der Entstehung und des Wachstums von Lochfraßstellen auf passiven Eisenelektroden," *Zeitschrift für Physikalische Chemie N. F.*, Vol. 20, 1959, pp. 113–120. NNA.891005.0091
10. M. Janik-Czachor, "An Assessment of the Processes Leading to Pit Nucleation on Iron," Reviews and News, *Journal of the Electrochemical Society*, Vol. 128, No. 12, December 1981, pp. 513C–519C. NNA.891005.0092
11. G. Matamala R. [sic], "Correlation Model of the AISI 316 Stainless Steel Pitting Potential with Cellulose Bleach Process Variables," *Corrosion*, Vol. 43, No. 2, February 1987, pp. 97–100. NNA.890831.0063
12. C. Y. Chao, L. F. Lin, D. D. McDonald, "A Point Defect Model for Anodic Passive Films, II. Chemical Breakdown and Pit Initiation," *Journal of the Electrochemical Society*, Vol. 128, Vol. 6, June 1981, pp. 1194–1198. NNA.891005.0093
13. P. E. Manning, D. J. Duquette, W. F. Savage, "The Role of Sulfide Inclusion Morphology in Pit Initiation of Several Type 300 Series Stainless Steels," *Corrosion*, Vol. 36, No. 6, June 1980, pp. 313–319. NNA.891005.0094
14. L. Hagn, "Lifetime Prediction for Parts in Corrosion Environments," in *Corrosion in Power Generating Equipment*, Plenum Press, 1983. NNA.891005.0095
15. O. Buck, R. Ranjan, "Evaluation of a Crack-Tip-Opening Displacement Model Under Stress-Corrosion Conditions," in *Modeling Environmental Effects on Crack Growth Processes*, R. H. Jones, W. W. Gerberich, Eds., The Metallurgical Society, 1986, p. 209. NNA.891005.0096
16. R. H. Jones, "Stress Corrosion Cracking," *Metals Handbook*, 9th ed., Vol. 13, L. J. Korb and D. L. Olson, Co-Chairmen, ASM International, Metals Park, Ohio, September 1987, pp. 145–163. NNA.891005.0097
17. M. Pourbaix, *Atlas of Electrochemical Equilibria in Aqueous Solutions*, Pergamon Press, New York, New York, 1966. NNA.891005.0098
18. D. Cubicciotti, L. Ljungberg, "The Pourbaix Diagram of Chromium With Iron and the Stress Corrosion Cracking of Stainless Steel," *Journal of the Electrochemical Society*, Vol. 132, No. 4, April 1985, pp. 987–988. NNA.891005.0099

19. *1987 Annual Book of ASTM Standards*, Section 3, Metals Test Methods and Analytical Procedures, Volume 3.02, Wear and Erosion; Metal Corrosion, pp. 209–217, ASTM Standard Procedure G36, "Standard Practice for Performing Stress-Corrosion Cracking Tests in a Boiling Magnesium Chloride Solution," American Society for Testing and Materials, Philadelphia, Pennsylvania, 1987. NNA.891005.0100
20. M. Da Cunha Belo, J. Bergner, B. Rondot, "Relationships Between the Critical Potential for Stress Corrosion Cracking of Stainless Steels and the Chemical Composition of the Films Formed in Boiling $MgCl_2$ Solutions," *Corrosion Science*, Vol. 21, No. 4, 1981, pp. 273–277. NNA.891005.0101
21. G. Cragnolino, "The Significance of a Critical Potential in the Intergranular Stress Corrosion Cracking of Stainless Steel Piping in BWR Environments," *Predictive Capabilities in Environmentally Assisted Cracking, Miami Beach, Florida, USA, November 17-22, 1985*, American Society of Mechanical Engineers, New York, New York, 1985, pp. 293–318.
22. F. Mancia, A. Tamba, "Electrochemical Prevention and Control of Localized Corrosion and SCC of AISI 304 Stainless Steels in NaCl Solutions," *Electrochemical Methods in Corrosion Research, Toulouse, France, July 9–12, 1985*, Materials Science Forum, Vol. 8, 1986, pp. 189–199.
23. F. P. Ford, "Current Understanding of the Mechanisms of Stress Corrosion and Corrosion Fatigue," *Symposium on Environment-Sensitive Fracture: Evaluation and Comparison of Test Methods, Gaithersburg, Maryland, April 26–28, 1982*, ASTM Special Technical Publication 821, ASTM Publication Code Number (PCN) 04-821000-27, S. W. Dean, E. N. Pugh, G. M. Ugiansky, Eds., American Society for Testing and Materials, Philadelphia, Pennsylvania, 1982, pp. 32–51. NNA.891005.0102
24. R. L. Fullman, "Modeling of Composition Effects on the SCC of Stainless Steels," Paper No. 6, *Proceedings: Seminar on Countermeasures for Pipe Cracking in BWRs, Palo Alto, California*, Vol. 1, May 1980, 8 pages. NNA.891005.0103
25. G. P. Cherepanov, "On the Theory of Crack Growth Due to Hydrogen Embrittlement," *Corrosion*, Vol. 29, No. 8, August 1973, pp. 305–309. NNA.891005.0104
26. J. F. Newman, "The Stress Corrosion of Steel in Sodium Hydroxide Solution: A Film Rupture Model," *Corrosion Science*, Vol. 21, No. 7, 1981, pp. 487–503. NNA.891005.0105
27. R. H. Jones, M. J. Danielson, C. A. Oster, "Modeling Environmental Effects on Crack Growth," Symposium Proceedings, *Metallurgical Society, Warrendale, Pennsylvania, 1986*, pp. 41–53. NNA.891005.0106
28. J. Newman, *Electrochemical Systems*, Prentice Hall, Englewood Cliffs, New Jersey, 1973.
29. T. Nakayama, M. Takano, "Application of Slip Dissolution-Repassivation Model for Stress Corrosion Cracking of AISI 304 Stainless Steel in a Boiling 42% $MgCl_2$ Solution," *Corrosion*, Vol. 42, No. 1, January 1986, pp. 10–14. NNA.891005.0194
30. P. L. Andresen, "Modeling of Water and Material Chemistry Effects on Crack Tip Chemistry and Resulting Crack Growth Kinetics," *3rd International Conference, Degradation of Materials in Nuclear Power Industry, Traverse City, Michigan, August 31–September 4, 1987*. NNA.891005.0107
31. I. Maier, J. R. Galvele, "Straining Metal Electrode Technique as a SCC Test, Type 304 Stainless Steel in NaCl + $H_2SO_4$ Solutions," *Corrosion*, Vol. 36, No. 2, February 1980, pp. 60–66. NNA.891005.0108
32. P. I. Marshall, G. T. Burstein, "Repassivation of Stainless Steels," *International Congress on Metallic Corrosion, Toronto, June 3–7, 1984*, Vol. 2, National Research Council of Canada, pp. 121–128. NNA.891005.0109
33. T. Hodgkiess, S. Rigas, "A Comparison of the Corrosion Resistance of Some Higher-Alloy Stainless Steels in Seawater at 20–100°C," *Desalination*, Vol. 44, 1983, pp. 283–294. NNA.891018.0178
34. R. C. Scarberry, E. L. Hibner, J. R. Crum, "Assessment of Pitting-Potential Measurements in Severely Corrosive Environments," Paper Number 245, *Corrosion '79, Atlanta, Georgia, March 12–16, 1979*, National Association of Corrosion Engineers, Katy, Texas. NNA.890831.0064
35. R. Fratesi, "Statistical Estimate of the Pitting Potential of AISI 316L Stainless Steel in 3.5% NaCl Measured by Means of Two Electrochemical Methods," *Corrosion*, Vol. 41, No. 2, February 1985, pp. 114–117. NNA.891005.0110
36. R. C. Newman, E. M. Franz, "The Protection Potential for Pitting Corrosion of Stainless Steel," *International Congress on Metallic Corrosion, Toronto, June 3–7, 1984*, National Research Council of Canada, Vol. 4, pp. 373–377. NNA.891005.0111

37. F. Mancia, A. Tamba, "Slow Strain Rate Stress Corrosion Cracking of AISI 304 Stainless Steel in NaCl Solution and its Prevention by Controlled Cathodic Protection," *Corrosion*, Vol. 42, No. 6, June 1986, pp. 362–367. NNA.891005.0112
38. K. A. Lichti, H. Bijnen, P. G. McIlhone, "A Comparison of Pitting Corrosion and Stress Corrosion Cracking Characteristics of Some Engineering Alloys," *Metals Australasia*, June–July 1984, pp. 4–6. NNA.891005.0113
39. *ASM Metals Handbook*, 9th ed., Vol. 13, L. J. Korb and D. L. Olson, Co-Chairmen, ASM International, Metals Park, Ohio, September 1987, pp. 555–559. NNA.890921.0078
40. A. I. Asphahani, "Localized Corrosion of High Performance Alloys," *Materials Performance*, Vol. 19, No. 8, August 1980, pp. 9–21. NNA.890831.0071
41. F. H. Yu, C. M. Chen, F. Zhou, W. X. Hu, J. M. Chen, "CEMS, AES and XPS Study of the Role of Molybdenum in 316 Stainless Steel SCC Resistance in High Temperature and High Pressure Water," *Journal of the Chinese Society for Corrosion Protection*, Vol. 5, No. 3, September 1985, pp. 176–188.
42. D. Warren, "Chloride-Bearing Cooling Water and the Stress-Corrosion Cracking of Austenitic Stainless Steel," *Proceedings of the Fifteenth Industrial Waste Conference, May 3–5, 1960*, Engineering Bulletin of Purdue University, Engineering Extension Series, Series No. 106, pp. 420–438. NNA.891005.0115
43. T. Shimose, A. Takamura, K. Mori, K. Shimogori, "Stress Corrosion Cracking of Austenitic Stainless Steels in Chloride Solutions," *Transactions of the Japan Institute of Metals*, Vol. 6, No. 2, 1965, pp. 83–87. NNA.891005.0116
44. *1987 Annual Book of ASTM Standards*, Section 3, Metals Test Methods and Analytical Procedures, Volume 3.02, Wear and Erosion; Metal Corrosion, p. 169, ASTM Standard Procedure G30, PCN: 01-030287-27, American Society for Testing and Materials, Philadelphia, Pennsylvania, 1987. NNA.891005.0117
45. *1987 Annual Book of ASTM Standards*, Section 3, Metals Test Methods and Analytical Procedures, Volume 3.02, Wear and Erosion; Metal Corrosion, p. 236, ASTM Standard Procedure G39, PCN: 01-030287-27, American Society for Testing and Materials, Philadelphia, Pennsylvania, 1987. NNA.891005.0117
46. F. Mancia, A. Tamba, "Slow Strain Rate Stress Corrosion Cracking of AISI 304 Stainless Steel in NaCl Solution and Its Prevention by Controlled Cathodic Protection," *Corrosion*, Vol. 42, No. 6, June 1986, pp. 362–367. NNA.891005.0112
47. T. Furuya, T. Fukuzuka, K. Fujiwara, H. Tomari, "Gamma-Ray Irradiation Effects on Stress Corrosion Cracking of Alloys for a High Level Liquid Waste Package," *R-D Kobe Sielosho Gijutsu Hokoku*, Vol. 33, No. 1, January 1985, pp. 43–46. NNA.890831.0067
48. M. J. Povich, D. E. Broecker, "The Stress Corrosion Cracking of Austenitic Stainless Steel Alloys in High Temperature Air Saturated Water," *Materials Performance*, October 1979, pp. 41–48. NNA.891005.0118
49. W. E. Wood, W. W. Gerberich, "Mechanical Nature of Stress-Corrosion Cracking in Al-Zn-Mg Alloys. 2. Electrochemical-Mechanical Model," *Metallurgical Transactions*, Vol. 5, No. 6, June 1974, p. 1285. NNA.891005.0119
50. H. D. Solomon, "Transgranular, Granulated and Intergranular Stress Corrosion Cracking in AISI 304 Stainless Steel," *Corrosion*, Vol. 40, No. 9, September 1984, pp. 493–506. NNA.891005.0120
51. T. Shibata, K. Furusaki, J. Nakata, "Probability Distribution of Crack Initiation and Propagation Times for Stress Corrosion Cracking of Type 304 Stainless Steel," *Boshoku Gijutsu*, Vol. 33, No. 4, 1984, pp. 223–231.
52. T. Nakayama, M. Takano, "Stress Corrosion Behavior of AISI 304 Stainless Steel in a Boiling 42% $MgCl_2$ Solution Under a Cyclic Slow Strain Rate Technique," *Corrosion*, Vol. 42, No. 10, October 1985, pp. 592–597. NNA.891005.0121
53. P. Muraleedharan, H. S. Khatak, J. B. Gnanamoorthy, P. Rodriguez, "Effect of Cold Work on Stress Corrosion Cracking Behavior of Types 304 and 316 Stainless Steels," *Metallurgical Transactions, [Section] A, Physical Metallurgy and Materials Science*, Vol. 16A, No. 2, February 1985, pp. 285–289.
54. D. Itzhak, D. Eliezer, "The Influence of NaI Additions on the Stress Corrosion Cracking of Austenitic Stainless Steel in $MgCl_2$ Solution," *Materials Engineering Conference, Haifa, Israel, December 20-22, 1981*, Freund Publishing House, P.O. Box 35010, Tel Aviv, Israel, 1981, pp. 252–256.

55. W. Y. Chu, J. Yao, C. M. Hsiao, "Stress Corrosion Cracking of Stainless Steel Under Compressive Stress," *Corrosion*, Vol. 40, No. 6, June 1984, pp. 302–306. NNA.891005.0214
56. H. Uchida, K. Yamamoto, K. Koterazawa, I. Yamada, H. Kawabe, "Effects of Cold Working and Heat Treatment on Stress Corrosion Cracking Susceptibility of SUS 304 Stainless Steel," *Journal of the Society of Materials Science, Japan*, Vol. 30, No. 337, October 1981, pp. 988–994.
57. I. A. Maier, E. L. Perez, J. R. Galvele, "Straining Metal Electrode as a SCC Test. Type 304 Stainless Steel in $MgCl_2$, $CaCl_2$, and LiCl Solutions," *Corrosion Science*, Vol. 22, No. 6, 1982, pp. 537–550. NNA.891101.0023
58. K. Teramoto, M. Takano, "Crack Growth Rate in Stress Corrosion Cracking of Type 304 Stainless Steel in Boiling 42% $MgCl_2$ in the CERT Method," *Journal of the Japan Institute of Metals, Sendai*, Vol. 43, No. 8, August 1979, pp. 744–752.
59. M. Takano, K. Teramoto, T. Nakayama, H. Yamaguchi, "Extremely Slow Strain Rate Stress-Corrosion Testing Machine and Some Experimental Results," *Tetsu-to-Hagane*, Vol. 65, No. 2, February 1979, pp. 212–218.
60. H. Kwon, C. H. Kim, "The Effect of Temperature on the Stress Corrosion Cracking of Austenitic Stainless Steel," *Journal of the Korean Institute of Metals*, Vol. 17, No. 6, 1979, pp. 484-490.
61. W. A. Baeslack, III, W. F. Savage, D. J. Duquette, "Effect of Strain Rate on Stress Corrosion Cracking in Duplex Type 304 Stainless Steel Weld Metal," *Metallurgical Transactions A—Physical Metallurgy and Materials Science*, Vol. 10A, No. 10, October 1979, pp. 1429–1435. NNA.891005.0122
62. A. J. A. Mom, R. T. Dencher, C. J. v. d. Wekken, W. A. Schultze, "Some Aspects of the Stress Corrosion Testing of Austenitic, Martensitic, Ferritic-Austenitic and Ferritic Types of Stainless Steel by Means of the Slow Strain-Rate Method," *Conference on the Stress Corrosion Cracking Slow Strain Rate Technique, Toronto, Canada, May 2–4, 1977*, American Society for Testing and Materials, Philadelphia, Pennsylvania, pp. 305–319.
63. W. J. Daniels, "Comparative Findings Using the Slow Strain-Rate, Constant Flow Stress and U-Bend Stress Corrosion Cracking Techniques," *Conference on the Stress Corrosion Cracking Slow Strain Rate Technique, Toronto, Canada, May 2–4, 1977*, American Society for Testing and Materials, Philadelphia, Pennsylvania, 1979, pp. 347–361.
64. M. J. Robinson, J. C. Scully, "Stress Corrosion Crack Propagation in Austenitic Stainless Steels," *Conference on Stress Corrosion Cracking and Hydrogen Embrittlement of Iron Base Alloys, Unieux-Firminy, France, June 12–16, 1973*, National Association of Corrosion Engineers, Katy, Texas, 1977, pp. 1095–1103.
65. T. Shibata, T. Takeyama, "Analysis of Stress Corrosion Cracking Failure Times of Type 316 Stainless Steel by the Weibull Distribution," *Boshoku Gijutsu*, Vol. 30, No. 1, January 1981, pp. 47–53.
66. K. J. Bundy, V. H. Desai, "Studies of Stress-Corrosion Cracking Behavior of Surgical Implant Materials Using a Fracture Mechanics Approach," *Conference on Corrosion and Degradation of Implant Materials, Second Symposium, Louisville, Kentucky, May 9–10, 1983*, American Society for Testing and Materials, Philadelphia, Pennsylvania, 1979, pp. 73–90.
67. V. Desai, "Stress Corrosion Cracking Studies of Surgical Implant Alloys," Johns Hopkins University, *Dissertation Abstracts International*, Vol. 45, No. 11, May 1985.
68. M. C. Belo, J. Bernger, B. Rondot, "Relationships Between the Critical Potential for Stress Corrosion Cracking of Stainless Steels and the Chemical Composition of the Films Formed in Boiling $MgCl_2$ Solutions," *Corrosion Science*, Vol. 21, No. 4, 1981, pp. 273–277. NNA.891005.0123
69. T. Misawa, "The Use of Recrystallization to Study the Plastic Zone Associated with Stress Corrosion Cracking in Type 304 Stainless Steel," *Corrosion*, Vol. 37, No. 7, July 1981, pp. 427–428. NNA.891005.0124
70. I. A. Ward, H. Masuda, K. R. L. Thompson, L. H. Keys, "The Effects of Environmental Factors on the Mechanical Behavior of Fe-Ni-Cr Alloys and Their Weldments," *Conference on Metals and Energy, Auckland, New Zealand, May 19–23, 1980*, Australasian Institute of Metals, 191 Royal Parade, Parkville 3052, Victoria, Australia, 1980, pp. 126–129.
71. K. Tanno, Y. Yuasa, H. Yashiro, "Stress Corrosion Cracking of Sensitized AISI 304 Stainless Steel in Oxygenated $Na_2SO_4$ Solution at High Temperature," *Corrosion*, Vol. 43, No. 4, April 1987, pp. 248–250. NNA.891005.0329

72. T. Shibata, S. Fujimoto, A. Asada, J. Nakata, "Effect of $CaCl_2$ Concentration on the Probability Distribution of Stress Corrosion Cracking Failure Time of Type 304 Stainless Steel," *Journal of the Society of Materials Science, Japan*, Vol. 36, No. 400, January 1987, pp. 65–71.
73. T. A. Mozhi, W. A. T. Clark, B. E. Wilde, "The Effect of Nitrogen and Carbon on the Stress Corrosion Cracking Performance of Sensitized AISI 304 Stainless Steel in Chloride and Sulfate Solutions at 250°C," *Corrosion Science*, Vol. 27, No. 3, March 1987, pp. 257–273. NNA.891101.0022
74. K. Fujiwara, H. Tomari, K. Shimogori, T. Fukuzuka, "Effects of pH and Applied Potential on the IGSCC Susceptibility of Sensitized 304 Stainless Steel in Dilute $Na_2SO_4$ Solution at High Temperature," *Boshoku Gijutsu*, Vol. 30, No. 5, May 1981, pp. 270–275.
75. J. K. Lee, "Stress Corrosion Cracking and Pitting of Sensitized Type 304 Stainless Steel in Chloride Solutions Containing Sulfur Species at Temperatures from 50–200°C," Ohio State University, *Dissertation Abstracts International*, Vol. 47, No 3, September 1986.
76. T. Oki, M. Okido, H. Kanematsu, "Fractography of Sensitized 304 Stainless Steel in Neutral Aqueous Solution by Means of Potentiostatic SSRT Method," *Boshoku Gijutsu*, Vol. 34, No. 10, 1985, pp. 546–551.
77. J. Congleton, R. N. Parkins, T. Shoji, "SCC of an Austenitic Stainless Steel in High Temperature Aqueous Environments," *Reports of the Research Institute for Strength and Fracture of Materials, Tohoku University*, Vol. 17, No. 1-2, March 1984, pp. 13–28.
78. S. H. Shim, "The Effect of Fluid Flow on the Stress Corrosion Cracking of Sensitized Type 304 Stainless Steel in 0.01 M $Na_2SO_4$ Solution at 250°C," Ohio State University, *Dissertation Abstracts International*, Vol. 46, No. 12, June 1986.
79. F. Mancia, A. Tamba, "Slow Strain Rate Stress Corrosion Cracking of AISI 304 Stainless Steel in NaCl Solution and Its Prevention by Controlled Cathodic Protection," *Corrosion*, Vol. 42, No. 6, June 1985, pp. 362–367. NNA.891005.0112
80. J. Congleton, H. C. Shih, T. Shoji, R. N. Parkins, "The Stress Corrosion Cracking of Type 316 Stainless Steel in Oxygenated and Chlorinated High Temperature Water," *Corrosion Science*, Vol. 25, No. 8-9, 1985, pp. 769–788. NNA.891005.0125
81. A. Tamba, F. Mancia, "Prevention of SCC of AISI 304 Stainless Steel in NaCl Solution by 'Cathanodic' Protection," *Stainless Steel '84, Chalmers University of Technology, Goteborg, Sweden, September 3–4, 1984*, The Institute of Metals, 1 Carlton House Terrace, London SJW1Y 5DB, UK, 1985, pp. 194–197.
82. D. E. Davies, J. P. Dennison, A. A. Odeh, "The Assessment of Stress Corrosion Damage in Austenitic Stainless Steel by Measurements of Cracks Formed During Constant Strain Rate and Constant Load Tests in 1 M HCl," *Corrosion Science*, Vol. 24, No. 11-12, 1984, pp. 953–964. NNA.891101.0020
83. A. Friganani, G. Trabanelli, F. Zicchi, "The Use of Slow Strain Rate Technique for Studying Corrosion Cracking Inhibition," *Corrosion Science*, Vol. 24, No. 11-12, 1984, pp. 917–927. NNA.891101.0021
84. I. A. Maier, V. Mandredi, J. R. Galvele, "The Stress Corrosion Cracking of an Austenitic Stainless Steel in HCl + NaCl Solutions at Room Temperature," *Corrosion Science*, Vol. 25, No. 1, 1985, pp. 15–34. NNA.891005.0126
85. A. Poznansky, D. J. Duquette, "The Effects of Sulfate and Chloride on the Stress Corrosion Cracking of Type 304 Stainless Steel at 290°C," *Materials Engineering Conference, Haifa, Israel, December 20–22, 1981*, Freund Publishing House, P.O. Box 35010, Tel Aviv, Israel, 1981, p. 277.
86. A. Poznansky, D. J. Duquette, "The Effect of Sensitization Heat Treatment on the Stress Corrosion Cracking of AISI 304 Stainless Steel," *Corrosion*, Vol. 40, No. 7, July 1984, pp. 375-381. NNA.891005.0127
87. R. J. L. Meyburg, J. M. Krougman, F. P. Ijsseling, "Constant Strain-Rate Testing of AISI Type 304 Stainless Steel in 0.5 M $H_2SO_4$ + 0.1 M NaCl Solution at Room Temperature with Controlled Potential," *Corrosion Science*, Vol. 23, No. 9, 1983, pp. 943–957. NNA.891101.0019
88. T. Kawakubo, M. Hishida, "Crack Initiation and Growth Analysis by Direct Optical Observation During SSRT in High-Temperature Water," *Corrosion*, Vol. 40, No. 3, March 1984, pp. 120–126. NNA.891005.0128

89. W. E. Ruther, W. K. Soppet, G. Ayrault, T. F. Kassner, "Effect of Sulfuric Acid, Oxygen and Hydrogen in High-Temperature Water on Stress Corrosion Cracking of Sensitized Type 304 Stainless Steel," *Corrosion '83, Anaheim, California, April 18–22, 1983*, pamphlet, National Association of Corrosion Engineers, Katy, Texas, 1983.
90. J. Congleton, R. N. Parkins, T. Shoji, "SCC of an Austenitic Stainless Steel in High-Temperature Aqueous Environments," *Corrosion '83, Anaheim, California, April 18–22, 1983*, pamphlet, National Association of Corrosion Engineers, Katy, Texas, 1983.
91. A. Poznansky, D. J. Duquette, "Stress Corrosion Cracking of Annealed and Sensitized Type 304 Stainless Steel in Deaerated Chloride/Sulfate Solutions at 290°C," *Corrosion*, Vol. 39, No. 11, November 1983, pp. 425–431. NNA.891005.0129
92. A. Poznansky, "Stress Corrosion Cracking of Type 304 Stainless Steel in Chloride/Sulfate Solutions," Rensselaer Polytechnic Institute, *Dissertation Abstracts International*, Vol. 42, No. 12, June 1982.
93. M. Osawa, M. Hasegawa, "Stress Corrosion Cracking of Hydrogen-Containing Austenitic Stainless Steel in $H_2SO_4$-NaCl Solution," *Transactions of the Iron and Steel Institute of Japan*, Vol. 21, No. 7, July 1981, pp. 464-468.
94. D. Eliezer, P. Pinkus, D. Itzhak, "Stress Corrosion of Type 304 Steel in $H_2SO_4$ Alkali Halide Environments," *Conference on Environmental Degradation of Engineering Materials in Aggressive Environments, Virginia Polytechnic Institute and State University, Blacksburg, Virginia, September 21–23, 1981*, pp. 193–199.
95. S. Ahmad, M. L. Mehta, S. K. Saraf, I. P. Saraswat, "Stress Corrosion Cracking of Sensitized Stainless Steel in Sulfurous Acid," *Corrosion*, Vol. 37, No. 7, July 1981, pp. 412–415. NNA.891005.0130
96. G. Cragnolino, L. F. Lin, Z. Szklarska-Smialowska, "Stress Corrosion Cracking of Sensitized Type 304 Stainless Steel in Sulfate and Chloride Solutions at 250 and 100°C," *Corrosion*, Vol. 37, No. 6, June 1981, pp. 312–320. NNA.891005.0131
97. M. Yajima, M. Arii, "Chloride Stress Corrosion Cracking of AISI 304 Stainless Steel in Air," *Materials Performance*, Vol. 19, No. 12, December 1980, pp. 17–19. NNA.891005.0132
98. P. L. Andresen, D. J. Duquette, "The Effect of Chloride Ion Concentration and Applied Potential on the SCC Behavior of Type 304 Stainless Steel in Deaerated High-Temperature Water," *Corrosion*, Vol. 36, No. 2, February 1980, pp. 85–93. NNA.891005.0133
99. I. Maier, J. R. Galvele, "Straining Metal Electrode Technique as a SCC Test, Type 304 Stainless Steel in NaCl + $H_2SO_4$ Solutions," *Corrosion* Vol. 36, No. 2, February 1980, pp. 60–66. NNA.891101.0013
100. H. S. Tong, D. J. Swartz, "Stress Corrosion Cracking and Electrochemical Behavior of AISI 304 Stainless Steel in Chloride Containing Sulfate Solutions," *Journal of the Electrochemical Society*, Vol. 127, No. 1, January 1980, pp. 31–36.
101. P. Norberg, S. Bernhardsson, H. Eriksson, S. Lagerberg, "Corrosion Properties of a Recently Developed Duplex Stainless Steel," *8th European Congress of Corrosion, Nice, France, November 19–21, 1985*, Centre Francais de la Corrosion, Societe de Chimie Industrielle, 28 rue Saint-Dominique, F75007, Paris, France, 1986, Vol. 2.
102. T. Shibata, S. Fujimoto, A. Asada, J. Nakata, "Effect of $CaCl_2$ Concentration on the Probability Distribution of Stress Corrosion Cracking Failure Time of Type 304 Stainless Steel," Journal of the *Society of Materials Science*, Japan, Vol. 36, No. 400, January 1987, pp. 65–71.
103. J. Congleton, R. N. Parkins, J. Shoji, "SCC of Austenitic Stainless Steel in High Temperature Aqueous Environments," *Reports of the Research Institute for Strength and Fracture of Materials, Tohoku University*, Vol. 17, No. 1-2, March 1984, pp. 13–28.
104. J. Congleton, H. C. Shih, T. Shoji, R. N. Parkins, "The Stress Corrosion Cracking of Type 316 Stainless Steel in Oxygenated and Chlorinated High Temperature Water," *Corrosion Science*, Vol. 25, No. 8-9, 1985, pp. 769–788.
105. P. S. Maiya, "Quantitative Description of Strain Rate Effects on Susceptibility to Intergranular Stress Corrosion Cracking," *Fracture '84, Conference on Advances in Fracture Research, New Delhi, India, December 4–10, 1984*, Pergamon Press Ltd., Headington Hill Hall, Oxford OX3 OBW, U.K., 1984, Vol. 4, pp. 2335–2343.

106. J. P. Sheehan, C. R. Morin, K. F. Packer, "Study of Stress Corrosion Cracking Susceptibility of Type 316L Stainless Steel in Vitro," *Conference on the Corrosion and Degradation of Implant Materials, Second Symposium, Louisville, Kentucky, May 9–10, 1983*, American Society for Testing and Materials, Philadelphia, Pennsylvania, 1985, pp. 57–72.
107. J. Congleton, R. N. Parkins, T. Shoji, "SCC of an Austenitic Stainless Steel in High-Temperature Aqueous Environments," *Corrosion '83, Anaheim, California, April 18–22, 1983*, pamphlet, National Association of Corrosion Engineers, Katy, Texas, 1983.
108. T. Oki, H. Kondou, S. Kuwano, "Metal-Electrochemical Study on Stress Corrosion Cracking of Type 316 Austenitic Stainless Steel in 3% NaCl Solution by Potentiostatic CERT Method," *Journal of the Society of Materials Science, Japan*, Vol. 31, No. 345, June 1982, pp. 584–588.
109. J. P. Carter, F. X. McCawley, "Corrosion Tests in Brine and Steam from the Salton Sea KGRA," *Journal of Materials for Energy Systems*, Vol. 3, No. 4, March 1982, pp. 30–38.
110. T. Kawakubo, M. Hishida, "J-Integral Analysis of SCC Growth Rate in High Temperature Water," *Boshoku Gijutsu*, Vol. 31, No. 1, January 1982, pp. 19–26. NNA.891005.008926.
111. G. Buzzanca, E. Caretta, L. Meini, R. Pascali, C. Ronchetti, "A Contribution to the Interpretation of the Strain Rate Effect on Type 304 Stainless Steel Intergranular Stress Corrosion Cracking," *Corrosion Science*, Vol. 25, No. 8-9, 1985, pp. 805–813. NNA.891101.0018
112. D. A. Hale, "The Effect of BWR Startup Environments on Crack Growth in Structural Alloys," *Journal of Engineering Materials and Technology*, Vol. 108, No. 1, January 1986, pp. 44–49.
113. S. M. Bruemmer, R. H. Jones, J. R. Divine, A. B. Johnson, Jr., "Evaluating the Intergranular SCC Resistance of Sensitized Type 304 Stainless Steel in Low-Temperature Water Environments," *Conference on Environment-Sensitive Fracture: Evaluation and Comparison of Test Methods, Gaithersburg, Maryland, April 26–28, 1982*, American Society for Testing and Materials, Philadelphia, Pennsylvania, 1984, pp. 256–270.
114. H. D. Solomon, "Transgranular, Granulated and Intergranular Stress Corrosion Cracking in AISI 304 SS," *Corrosion*, Vol. 40, No. 9, September 1984, pp. 493–506. NNA.891005.0134
115. M. Silverman, D. F. Taylor, "The Influence of Crevice Chemistry on Constant Extension Rate Tensile (CERT) Tests of 304L Stainless Steel in 288°C Water," *Corrosion*, Vol. 37, No. 1, January 1981, pp. 58–60. NNA.891005.0135
116. J. Kuniya, I. Masaoka, R. Sasaki, S. Kirihara, "Effects of Surface Finishing on Stress Corrosion Cracking of Austenitic Stainless Steels in High-Temperature Water," *Journal of Materials for Energy Systems*, Vol. 1, No. 4, March 1980, pp. 30–41.
117. M. J. Povich, D. E. Broecker, "The Stress Corrosion Cracking of Austenitic Stainless Steel Alloys in High-Temperature Air-Saturated Water," *Materials Performance*, Vol. 18, No. 10, October 1979, pp. 41–48. NNA.891005.0118
118. J. Kuniya, S. Hattori, I. Masaoka, R. Sasaki, H. Ito, "Stress Corrosion Cracking Susceptibility of Various Austenitic Stainless Steel Pipe Welds in High Temperature Oxygenated Water," *Boshoku Gijutsu*, Vol. 31, No. 4, April 1982, pp. 261–267.
119. E. Kikuchi, N. Ohnaka, A. Minato, "Statistical Evaluation of IGSCC Resistance of Various Austenitic Stainless Steels in High Temperature Water With Impurities," *Boshoku Gijutsu*, Vol. 33, No. 10, 1984, pp. 566–572.
120. H. Takaku, K. Kuwabara, M. Kusuhashi, "Susceptibility to SCC of High Nitrogen Forged Stainless Steel Pipe," *Materials Performance*, Vol. 21, No. 5, May 1982, pp. 36–42. NNA.891005.0136
121. M. J. Povich, D. E. Broecker, "The Stress Corrosion Cracking of Austenitic Stainless Steel Alloys in High-Temperature Air-Saturated Water," *Materials Performance*, Vol. 18, No. 10, October 1979, pp. 41–48.
122. T. Kawakubo, M. Hishida, "An Analysis of Cracking Behavior During CERTS," *Conference on Predictive Methods for Assessing Corrosion Damage to BWR Piping Steam Generators, Fuji, Japan, May 28–June 2, 1978*, National Association of Corrosion Engineers, Katy, Texas, 1982, pp. 266–270.
123. J. N. Kass, R. L. Cowan, "Hydrogen Water Chemistry Technology for BWR's," *Proceedings of the Second International Symposium on Environmental Degradation of Materials in Nuclear Power Systems—Water Reactors, Monterey, California, September 9–12, 1985*, American Nuclear Society, 1986, pp. 211–218. NNA.891026.0002

124. H. C. Park, G. Cragnolino, D. D. MacDonald, "Stress Corrosion Cracking of Sensitized Type 304 Stainless Steel in Borate Solutions at Elevated Temperatures," *Conference on Environmental Degradation of Materials in Nuclear Power Systems—Water Reactors, Myrtle Beach, South Carolina, August 22–25, 1983*, National Association of Corrosion Engineers, Katy, Texas, 1984, pp. 604–622. NNA.891026.0003
125. H. Tsuge, N. Maruyama, S. Nagata, H. Nagano, "Stress Corrosion Cracking of Austenitic Stainless Steels in Borated Water," *Conference on Environmental Degradation of Materials in Nuclear Power Systems—Water Reactors, Myrtle Beach, South Carolina, August 22–25, 1983*, National Association of Corrosion Engineers, Katy, Texas, 1984, pp. 582–591. NNA.891026.0004
126. R. B. Davis, M. E. Indig, "The Effect of Aqueous Impurities on the Stress Corrosion Cracking of Austenitic Stainless Steel in High-Temperature Water," pamphlet, National Association of Corrosion Engineers, Katy, Texas, 1983.
127. H. Hirano, N. Aoki, T. Kurosawa, "The Effect of Dissolved Oxygen and $NO_3^-$ Anions on the Stress Corrosion Cracking of Type 304 Stainless Steel in Water at 290°C," *Corrosion*, Vol. 39, No. 8, August 1983, pp. 313–322. NNA.891005.0137
128. S. Shmad, M. L. Mehta, S. K. Saraf, I. P. Saraswat, "Stress Corrosion Cracking of Sensitized 304 Austenitic Stainless Steel in Petroleum Refinery Environment," *Corrosion*, Vol. 38, No. 6, June 1982, pp. 347–353. NNA.891005.0138
129. R. C. Newman, K. Sieradzki, H. S. Isaacs, *Fracture Mechanisms of Sensitized Stainless Steels in Sulfur Containing Environments*, Brookhaven National Laboratory, Upton, New York, Report No. DE81026052, 1981.
130. R. C. Newman, K. Sieradzki, H. S. Isaacs, "Fracture Mechanisms of Sensitized Stainless Steels in Sulfur-Containing Environments," *Conference on Environmental Degradation of Engineering Materials in Aggressive Environments, Blacksburg, Virginia, September 21–23, 1981*, Virginia Polytechnic Institute, Blacksburg, Virginia, 1981, pp. 163–171.
131. J. Congleton, H. C. Shih, T. Shoji, R. N. Parkins, "The Stress Corrosion Cracking of Type 316 Stainless Steel in Oxygenated and Chlorinated High Temperature Water," *Corrosion Science*, Vol. 25, No. 8-9, 1985, pp. 769–788.
132. B. M. Gordon, "The Effect of Chloride and Oxygen on the Stress Corrosion Cracking of Stainless Steels: Review of Literature," *Materials Performance*, Vol. 19, No. 4, April 1980, pp. 29–38. NNA.891005.0139
133. W. L. Williams, "Chloride and Caustic Stress Corrosion of Austenitic Stainless Steel in Hot Water and Steam," *Corrosion*, Vol. 13, No. 8, August 1957, p. 539t–545t. NNA.890831.0065
134. H. R. Copson, *Physical Metallurgy of Stress Corrosion Fracture*, Interscience, 1959, p. 247.
135. P. C. S. Wu, *Sensitization, Intergranular Attack, Stress Corrosion Cracking, and Irradiation Effects on the Corrosion of Iron-Chromium-Nickel Alloys*, Westinghouse Electric Corporation, Advanced Reactors Division, Oak Ridge National Laboratory, Oak Ridge, Tennessee, ORNL/TM-6311, April 1978. NNA.891026.0008
136. H. Y. Suss, "Untempered Martensite Affects Stress-Corrosion of Type 410 Stainless," *Metal Progress*, Vol. 82, 1962, p. 89.
137. D. Van Rooyen, "Review of the Stress Corrosion Cracking of Inconel 600," *Corrosion*, Vol. 31, No. 9, September 1975. NNA.891005.0140
138. R. W. Staehle, *A Study of the Mechanism of Stress Corrosion Cracking in the Iron-Nickel-Chromium Alloy System*, Final Report, RF (Research Foundation) Project 1673, The Ohio State University Research Foundation, Columbus, Ohio, Report No. COO-1319-82; U.S. Atomic Energy Commission Contract No. AT(11-1)-1319, February 1970. NNA.891005.0141
139. M. Kowaka et al., "Development of Nuclear Grade Type 316 Stainless Steel for BWR Piping," *Sumitomo Metals*, Vol. 34, No. 1, January 1982, pp. 85–99.
140. A. Duckworth, J. Metcalf, P. J. Moreland, "The Selection and Performance of Materials in Fine Chemicals Plant," *Industrial Corrosion*, Vol. 2, No. 3, March 1984, pp. 12–15.
141. A. Kyrolainen, "Initiation of Pitting at Inclusions in Calcium Treated Stainless Steel," *Stainless Steel '84, Chalmers University of Technology, Goteborg, Sweden, September 3-4, 1984*, The Institute of Metals, 1 Carlton House Terrace, London SW1Y 5DB, U.K., 1985, pp. 173–180.

142. J. P. Carter, S. D. Cramer, R. K. Conrad, "Corrosion of Stainless Steels in the Geothermal Environments of the Salton Sea Known Geothermal Resource Area," *Corrosion '81, Toronto, Canada, April 6–10, 1981*, pamphlet, National Association of Corrosion Engineers, Katy, Texas, 1981.
143. T. Fujii, "Pitting Potentials of Stainless Steel in 0.1 M NaCl Solution at 280°C," *Transactions of National Research Institute for Metals (Japan)*, Vol. 21, No. 1, March 1979, pp. 11–12.
144. P. S. Maiya, "Corrosion Studies on Structural Alloys for Flue Gas Desulfurization Systems," *Corrosion in Flue Gas Desulfurization Systems*, Anaheim, California, New Orleans, Louisiana, USA, April 21, 1983; April 5–6, 1984, National Association of Corrosion Engineers, Katy, Texas, 1984, pp. 93–107.
145. R. Oltra, J. C. Colson, A. Desesatret, "The Electrochemical Effect of Chromium, Nickel, and Molybdenum Additions on the Stress Corrosion Cracking of Austenitic Stainless Steels in a Chloride Solution," *Corrosion*, Vol. 42, No. 1, January 1986, pp. 44–50. NNA.891005.0142
146. E. C. Bain, R. H. Aborn, J. J. B. Rutherford, "The Nature and Prevention of Intergranular Corrosion in Austenitic Steels," *Transactions of the American Society for Steel Treating*, Vol. 21, 1933, p. 481. NNA.891005.0143
147. C. Stawstrom, M. Hillert, "An Improved Depleted-Zone Theory of Intergranular Corrosion of 18-8 Stainless Steel," *Journal of the Iron and Steel Institute*, Vol. 207, 1969, p. 77. NNA.891005.0144
148. C. S. Tedmon, Jr., D. A. Vermilyea, J. H. Rosolowski, "Intergranular Corrosion of Austenitic Stainless Steel," *Journal of the Electrochemical Society*, Vol. 118, 1971, p. 192. NNA.891005.0145
149. R. L. Fullman, "A Thermodynamic Model of the Effects of Composition on the Susceptibility of Austenitic Stainless Steels to Intergranular Stress Corrosion Cracking," *Acta Metallurgica*, Vol. 30, 1982, pp. 1407–1415. NNA.891005.0146
150. H. Takaku, K. Kuwabara, M. Kusuhashi, "Susceptibility to SCC of High Nitrogen Forged Stainless Steel Pipe," *Materials Performance*, Vol. 21, No. 5, May 1982, pp. 36–42. NNA.891005.0147
151. A. P. Majidi, M. A. Streicher, "Four Nondestructive Electrochemical Tests for Detecting Sensitization in Type 304 and 304L Stainless Steels," *Nuclear Technology*, Vol. 75, No. 3, December 1986, pp. 356–369.
152. R. W. Arey, F. F. Lyle, Jr., *Evaluation of the EPR Technique and the WC-5 Metal Sensitization Detector for Determining Susceptibility of Austenitic Stainless Steels to Intergranular Corrosion*, Materials Technology Institute of the Chemical Process Industries, Inc., 1570 Fishinger Rd., Columbus, Ohio 43221, 1983.
153. W. L. Clark, *Reactor Primary Coolant System Pipe Rupture Study Method for Detection of Sensitization in Stainless Steel*, General Electric Company, Report No. NUREG/CR-0834, August 1979.
154. M. J. Povich, D. E. Broecker, "The Stress Corrosion Cracking of Austenitic Stainless Steel Alloys in High-Temperature Air-Saturated Water," *Materials Performance*, Vol. 18, No. 10, October 1979, pp. 41–48. NNA.891005.0118
155. M. Kowaka, H. Nagano, K. Yoshikawa, T. Kobayashi, M. Miura, Y. Sawaragi, K. Ohta, S. Nagata, "Development of Alternative Materials for BWR Piping," *Proceedings on the Conference for Predictive Methods of Assessing Corrosion Damage to BWR Piping and PWR Steam Generators, Fuji Institute of Education and Training, Japan, May 28–June 2, 1978*, published 1982, pp. 193–197. NNA.891005.0148
156. T. Kudo, H. Miyuki, Y. Nakamura, H. Yoshinaga, T. Nakamura, "Corrosion Resistance of As-Rolled Types 304 and 316 Stainless Steels for Clad Steel Use," *Sumitomo Metals*, Vol. 35, No. 1, March 1983, pp. 81–92.
157. J. N. Kass, W. L. Walker, A. J. Giannuzzi, "Stress Corrosion Cracking of Welded Type 304 Stainless Steel Under Cyclic Loading," *Corrosion '79, Atlanta, Georgia, March 12–16, 1979*, National Association of Corrosion Engineers, Katy, Texas, 1979.
158. R. M. Davison, D. W. Rahoi, G. Gemmel, "Stainless Steels for Heat Exchanger Service," *Industrial Heat Exchangers, Pittsburgh, Pennsylvania, USA, November 6–8, 1985*, American Society for Metals, Metals Park, Ohio, 1985, pp. 371–380.
159. Chikazaki, Mitsuo, "Improvement in the Grain Boundary Corrosion Resistance of Nickel-Based Alloys," *Japanese Kokai Tokkyo Koho*, JP 54/69517, June 4, 1979.
160. S. M. Bruemmer, "Composition-Based Correlations to Predict Sensitization Resistance of Austenitic Stainless Steels," *Corrosion*, Vol. 42, No. 1, January 1986, pp. 27–35. NNA.891005.0149

161. T. A. Mozhi, H. S. Betrabet, V. Jagannathan, B. E. Wilde, W. A. T. Clark, "Thermodynamic Modeling of Sensitization of AISI 304 Stainless Steels Containing Nitrogen," *Scripta Metallurgica*, Vol. 20, 1986, pp. 723–728. NNA.891005.0150
162. T. A. Mozhi, W. A. T. Clark, K. Nishimoto, W. B. Johnson, D. D. MacDonald, "The Effect of Nitrogen on the Sensitization of AISI 304 Stainless Steel," *Corrosion*, Vol. 41, No. 10, October 1985, pp. 555–559. NNA.891005.0151
163. T. Kekkonen, P. Aaltonen, H. Hanninen, "Metallurgical Effects on the Corrosion Resistance of a Low Temperature Sensitized Welded AISI Type 304 Stainless Steel," *Corrosion Science*, Vol. 25, No. 89, 1985, pp. 821–836. NNA.891005.0152
164. G. S. Was, R. M. Kruger, "A Thermodynamic and Kinetic Basis for Understanding Chromium Depletion in Ni-Cr-Fe Alloys," *Acta Metallurgica*, Vol. 33, No. 5, 1985, pp. 841–854. NNA.891005.0153
165. R. A. Mulford, E. L. Hall, C. L. Briant, "Sensitization of Austenitic Stainless Steels, II. Commercial Purity Alloys," *Corrosion*, Vol. 39, No. 4, April 1983, pp. 132–143. NNA.891005.0154
166. C. L. Briant, R. A. Mulford, E. L. Hall, "Sensitization of Austenitic Stainless Steels, I. Controlled Purity Alloys," *Corrosion*, Vol. 38, No. 9, September 1982, pp. 468–477. NNA.891005.0155
167. M. Kowaka, "Methods for Determining and Predicting Sensitization of Fe-Cr-Ni Base Alloys in Japan," *Proceedings of the Conference on Predictive Methods for Assessing Corrosion Damage to BWR Piping and PWR Steam Generators, Fuji Institute of Education and Training, Japan, May 28–June 2, 1978*, published 1982, pp. 205–208. NNA.891005.0156
168. Robert L. Fullman, "Predictability of Low Temperature Sensitization in Stainless Steels," *Proceedings: Seminar on Countermeasures for Pipe Cracking in BWRs, Palo Alto, California, May 1980*, Vol. 2, Paper No. 26, 13 pages. NNA.891005.0157
169. J. J. Eckenrod, C. W. Kovach, *Effect of Nitrogen on the Sensitization, Corrosion, and Mechanical Properties of 18Cr-8Ni Stainless Steels*, American Society for Testing and Materials, Philadelphia, Pennsylvania, ASTM Report No. STP-679, 1979, pp. 17–41. NNA.891005.0158
170. M. J. Povich, P. Rao, "Low Temperature Sensitization of Welded Type 304 Stainless Steel," *Corrosion*, Vol. 34, No. 8, August 1978, pp. 269–275. NNA.891005.0159
171. M. J. Povich, "Low Temperature Sensitization of Type 304 Stainless Steel," *Corrosion*, Vol. 34, No. 2, February 1978, pp. 60–65. NNA.891005.0160
172. C. L. Briant, "Grain Boundary Segregation of Phosphorus in 304L Stainless Steel," *Metallurgical Transactions, [Section] A: Physical Metallurgy and Materials Science*, Vol. 16A, No. 11, November 1985, pp. 2061–2062.
173. R. H. Jones, "Some Radiation Damage-Stress Corrosion Synergisms in Austenitic Stainless Steels," in *Proceedings of the Second International Symposium on Environmental Degradation of Materials in Nuclear Power Systems—Water Reactors, American Nuclear Society, September 1985*, p. 173. NNA.891026.0005
174. A. I. Asphahani, "Effect of Acids on the Stress Corrosion Cracking of Stainless Materials in Dilute Chloride Solutions," *Materials Performance*, November 1980, pp. 9–14. NNA.890831.0066
175. A. I. Asphahani, H. H. Uhlig, "Stress Corrosion Cracking of 4140 High Strength Steel in Aqueous Solutions," *Journal of the Electrochemical Society*, Vol. 122, No. 2, 1975, p. 174. NNA.891101.0017
176. H. H. Uhlig, E. W. Cook, Jr., "Mechanism of Inhibiting Stress Corrosion Cracking of 18-8 Stainless Steel in $MgCl_2$ by Acetates and Nitrates," *Journal of the Electrochemical Society*, Vol. 116, No. 2, 1969, p. 173. NNA.891005.0161
177. R. S. Glass, G. E. Overturf, R. A. Van Konynenburg, R. D. McCright, "Gamma Radiation Effects on Corrosion: I. Electrochemical Mechanisms for the Aqueous Corrosion Processes of Austenitic Stainless Steels Relevant to Nuclear Waste Disposal in Tuff," *Corrosion Science*, Vol. 26, No. 8, 1986, pp. 577–590. NNA.891005.0162
178. R. S. Glass, R. A. Van Konynenburg, G. E. Overturf, "Corrosion Processes of Austenitic Stainless Steels and Copper-Based Materials in Gamma-Irradiated Aqueous Environments," *Proceedings of Corrosion 86, The International Forum Devoted Exclusively to the Protection and Performance of Materials, March 17–21, 1986, Albert Thomas Convention Center, Houston, Texas*, Paper No. 258, 11 pages. NNA.891005.0163
179. G. P. Marsh, K. J. Taylor, G. Bryan, S. E. Worthington, "The Influence of Radiation on the Corrosion of Stainless Steel," *Corrosion Science*, Vol. 26, No. 11, 1986, p. 971. NNA.891005.0164

180. Y. J. Kim, R. A. Oriani, "Corrosion Properties of the Oxide Film Formed on Grade 12 Titanium in Brine Under Gamma Radiation," *Corrosion*, Vol. 43, No. 2, February 1987, pp. 85–91. NNA.891005.0165
181. Y. J. Kim, R. A. Oriani, "Brine Radiolysis and its Effect on the Corrosion of Grade 12 Titanium," *Corrosion*, Vol. 43, No. 2, February 1987, pp. 92–96. NNA.891005.0166
182. W. L. Clarke and A. J. Jacobs, "Effect of Radiation Environment on SCC of Austenitic Materials," *Proceedings of the Conference on Environmental Degradation of Materials in Nuclear Power Systems—Water Reactors, Myrtle Beach, South Carolina, August 22–25, 1983*, National Association of Corrosion Engineers, Katy, Texas, 1984, pp. 451–461. NNA.891005.0167
183. W. E. Ruther, W. K. Soppet, T. F. Kassner, "Influence of Gamma Radiation on the ECP of Type 304 SS, Ti, and Pt in 289°C Water," presented at *Meeting of the International Cooperative Group on Irradiation on Stress Corrosion Cracking, Sponsored by the American Nuclear Society, The Metallurgical Society, and the National Association of Corrosion Engineers, Traverse City, Michigan, September 3–4, 1987.* NNA.891005.0168
184. A. J. Bard, L. R. Faulkner, *Electrochemical Systems, Fundamentals and Applications*, John Wiley and Sons, New York, New York, 1980, pp. 699–702.
185. J. W. T. Spinks, R. J. Woods, *An Introduction to Radiation Chemistry*, Second ed., John Wiley and Sons, New York, 1976, p. 261.
186. N. Fujita, M. Akiyama, T. Tamura, "Stress Corrosion Cracking of Sensitized Type 304 Stainless Steel in High Temperature Water Under Gamma Ray Irradiation," *Corrosion*, Vol. 37, No. 6, June 1981, pp. 335–341. NNA.891005.0169
187. K. Ishigure, J. Takagi, Y. Takeuchi, N. Fujiti, M. Muroi, "Effect of Gamma Radiation on Corrosion of Stainless Steel in High-Temperature Water," *Proceedings of the Second International Symposium on Environmental Degradation of Materials in Nuclear Power Systems—Water Reactors, Monterey, California, September 9–12, 1985*, American Nuclear Society, La Grange Park, Illinois, 1986, pp. 181–188. NNA.891018.0179
188. M. Kuribayashi, H. Okabayashi, "Influence of Gamma-Ray Radiation on Stress Corrosion Cracking of Austenitic Stainless Steel," *Journal of the Japan Institute of Metals*, Sendai, Vol. 46, No. 2, 1982, pp. 170–175. NNA.891018.0170
189. E. Kikuchi, N. Ohnaka, A. Minato, "Effect of Hydrogen Peroxide on Stress Corrosion Cracking of Type 304 Stainless Steel (Retroactive Coverage)," *Boshoku Gijutsu*, Vol. 33, 1984, p. 33. NNA.891005.0171
190. L. A. James, *Environmentally-Assisted Cracking Behavior of a Candidate Basalt Repository Container Material in Groundwater Undergoing Gamma Irradiation*, Westinghouse Hanford Company, Richland, Washington, HEDL-SA-3707 FP, April 1987. Also, *Nuclear and Waste Management* (in press). NNA.891018.0180
191. R. L. Starkey, "Anaerobic Corrosion, Perspectives About Causes," *Biologically Induced Corrosion, NACE-8, Proceedings of the International Conference on Biologically Induced Corrosion, Gaithersburg, Maryland, June 10–12, 1985*, S. C. Dexter, Ed., National Association of Corrosion Engineers, Katy, Texas, 1986, pp. 3–7. NNA.891026.0006
192. G. Kobrin, "Corrosion by Microbiological Organisms in Natural Waters," *Materials Performance*, Vol. 15, No. 7, July 1976, pp. 38–43. NNA.891005.0172
193. R. E. Tatnall, "Case Histories: Bacteria Induced Corrosion," *Materials Performance*, Vol. 20, No. 8, August 1981, pp. 41–48. NNA.891005.0173
194. R. E. Tatnall, "Fundamentals of Bacteria Induced Corrosion," *Materials Performance*, Vol. 20, No. 9, September 1981, pp. 32–38. NNA.891005.0174
195. D. H. Pope, R. J. Soracco, E. W. Wilde, "Studies on Biologically Induced Corrosion in Heat Exchanger Systems at the Savannah River Plant, Aiken, SC," *Materials Performance*, Vol. 21, No. 7, July 1982, pp. 43–50. NNA.891005.0175
196. P. R. Puckorius, "Massive Utility Condenser Failure Caused by Sulfide Producing Bacteria," *Materials Performance*, Vol. 22, No. 12, December 1983, pp. 19–22. NNA.891005.0176

197. V. V. Gorelov, A. K. Talybly, "Corrosion Protection of the Equipment in Closed and Reduced-Water Recycling Systems," Pulp and Paper Industry Problems, Vol. 4, *Fourth International Symposium on Corrosion in the Pulp and Paper Industry, Stockholm, Sweden, May 30 to June 2, 1983*, published by the Swedish Corrosion Institute, Stockholm, Sweden, 1983, pp. 113–116.
198. D. H. Pope, D. J. Duquette, A. H. Johannes, P. C. Wayner, "Microbiologically Influenced Corrosion of Industrial Alloys," *Materials Performance*, Vol. 24, No. 4, April 1984, pp. 14–18. NNA.891005.0177
199. C. R. Das, K. G. Mishra, "Biological Corrosion of Welded Steel due to Marine Algae," *Biologically Induced Corrosion, NACE-8, Proceedings of the International Conference on Biologically Induced Corrosion, June 10–12, 1985, Gaithersburg, Maryland*, S. C. Dexter, Ed., National Association of Corrosion Engineers, Katy, Texas, 1986, pp. 114–117. NNA.891005.0178
200. A. J. N. Silva, J. N. Tanis, J. O. Silva, R. A. Silva, "Alcohol Industry Biofilms and their Effect on Corrosion of 304 Stainless Steel," *Biologically Induced Corrosion, NACE-8, Proceedings of the International Conference on Biologically Induced Corrosion, June 10–12, 1985, Gaithersburg, Maryland*, S. C. Dexter, Ed., National Association of Corrosion Engineers, Katy, Texas, 1986, pp. 76–82. NNA.891018.0182
201. G. Kobrin, "Reflections on Microbiologically Induced Corrosion of Stainless Steels," *Biologically Induced Corrosion, NACE-8, Proceedings of the International Conference on Biologically Induced Corrosion, June 10–12, 1985, Gaithersburg, Maryland*, S. C. Dexter, Ed., National Association of Corrosion Engineers, Katy, Texas, 1986, pp. 33–46. NNA.891018.0183
202. P. H. Thorpe, "Microbiological Corrosion of Stainless Steel in Paper Machines and its Causes," *Proceedings of the Fifth International Symposium on Corrosion in the Pulp and Paper Industry*, National Association of Corrosion Engineers, Katy, Texas, pp. 169–173.
203. P. H. Thorpe, "Microbiological Corrosion of Stainless Steel in Paper Machines," *Appita*, Vol. 40, No. 2, 1987, pp. 108–111.
204. D. H. Pope, D. J. Duquette, A. H. Johannes, P. C. Wayner, "Microbiologically Influenced Corrosion of Industrial Alloys," *Materials Performance*, Vol. 24, No. 4, April 1984, pp. 14–18.
205. G. O. Hayner, D. H. Pope, B. E. Crane, "Microbiologically Influenced Corrosion in the Condenser Water Boxes at Crystal River-3," *Materials Performance*, Vol. 24, No. 4, April 1984. NNA.891026.0007
206. J. M. West, I. G. McKinley, "The Geomicrobiology of Nuclear Waste Disposal," *Scientific Basis for Nuclear Waste Management VII, Materials Research Society Symposia Proceedings*, Vol. 26, G. L. McVay, Ed., North-Holland, New York, 1984, pp. 487–494. NNA.891018.0184
207. D. H. Pope, "Microbiologically Influenced Corrosion in the Nuclear Power Industry: Case Histories, Methods of Detection, Control, and Prevention," *Proceedings of the Third International Symposium on Environmental Degradation of Materials in Nuclear Power Systems—Water Reactors, Traverse City, Michigan, August 30 to September 3, 1987*, The Metallurgical Society, 1988 (in press). NNA.891026.0009
208. J. A. Baross, J. W. Deming, "Growth of 'Black Smoker' Bacteria at Temperatures of at Least 250°C," *Nature*, Vol. 303, June 2, 1983, pp. 423–426. NNA.891018.0185
209. E. J. Hall, *Radiation and Life*, 2nd ed., Pergamon Press, New York, 1984, p. 203. NNA.891018.0186
210. E. Christensen, "Report from Denmark," *Radiosterilization of Medical Products, Pharmaceuticals and Bioproducts*, International Atomic Energy Agency, Vienna, Technical Report Series No. 72, 1967, pp. 60–74. NNA.891018.0187
211. J. G. Stoecker, "Guide for the Investigation of Microbiologically Induced Corrosion," *Materials Performance*, Vol. 24, No. 8, August 1984, pp. 48–55. NNA.891018.0181

The following number is for Office of Civilian Radioactive Waste Management Records Management purposes only and should not be used when ordering this document:

Accession Number: NNA.891222.0308